Oligodendrocyte secreted factors shape hippocampal GABAergic neuron transcriptome and physiology

Elisa Mazuir, Louis Richevaux, Merie Nassar, Noémie Robil, Pierre de La Grange, Catherine Lubetzki, Desdemona Fricker, Nathalie Sol-Foulon

OXFORD UNIVERSITY PRESS | Cerebral Cortex

Oligodendrocyte secreted factors shape hippocampal GABAergic neuron transcriptome and physiology

Journal:	*Cerebral Cortex*
Manuscript ID	CerCor-2020-00934.R1
Manuscript Type:	Original Article
Date Submitted by the Author:	n/a
Complete List of Authors:	Mazuir, Elisa; Sorbonne Universite, Neuroscience Richevaux, Louis; Université de Paris, Integrative Neuroscience and Cognition Center Nassar, Merie; Université de Paris, Integrative Neuroscience and Cognition Center Robil, Noemie; Genosplice, GenoSplice technology de la Grange, Pierre; Genosplice, GenoSplice technology Lubetzki, Catherine; Hopital Universitaire Pitie Salpetriere, Department of Neurology Fricker, Desdemona; Université de Paris, CNRS UMR8002 Sol-Foulon, Nathalie; Sorbonne Universite, Neuroscience
Keywords:	GABAergic neurons, neuro-glia interactions, oligodendrocytes, secreted factors, single-cell RNAseq

Oligodendrocyte secreted factors shape hippocampal GABAergic neuron transcriptome and physiology

Running title: Oligodendroglial factors shape GABAergic neurons

Elisa Mazuir[1, ≠] and Louis Richevaux[2, ≠], Merie Nassar[2], Noémie Robil[3], Pierre de la Grange[3], Catherine Lubetzki[1,4], Desdemona Fricker[2, ≠*] and Nathalie Sol-Foulon[1, ≠*]

[1] Sorbonne University, Inserm, CNRS, Paris Brain Institute, ICM, Pitié-Salpêtrière Hospital, F-75013 Paris, France.

[2] CNRS UMR 8002, Integrative Neuroscience and Cognition Center, Université de Paris, Paris, France.

[3] Genosplice, Paris, France

[4] Assistance Publique des Hôpitaux de Paris (APHP), Neurology Department, Pitié-Salpêtrière hospital, Paris, France.

[≠] EM and LR contributed equally to this work as first authors, and DF and NSF as last authors
*Co-Corresponding authors: Desdemona Fricker, desdemona.fricker@parisdescartes.fr, phone number: +33 (0)6 17 59 05 92; Nathalie Sol-Foulon, nathalie.sol-foulon@sorbonne-universite.fr, phone number: +33 (0)1 57 27 44 65.

ABSTRACT

Oligodendrocytes form myelin for central nervous system axons and release factors which signal to neurons during myelination. Here, we ask how oligodendroglial factors influence hippocampal GABAergic neuron physiology. In mixed hippocampal cultures GABAergic neurons fired action potentials of short duration and received high frequencies of excitatory synaptic events. In purified neuronal cultures without glial cells, GABAergic neuron excitability increased and the frequency of synaptic events decreased. These effects were largely reversed by adding oligodendrocyte conditioned medium. We compared the transcriptomic signature with the electrophysiological phenotype of single neurons in these three culture conditions. Genes expressed by single pyramidal or GABAergic neurons largely conformed to expected cell-type specific patterns. Multiple genes of GABAergic neurons were significantly downregulated by the transition from mixed cultures containing glial cells to purified neuronal cultures. Levels of these genes were restored by the addition of oligodendrocyte conditioned medium to purified cultures. Clustering genes with similar changes in expression between different culture conditions revealed processes affected by oligodendroglial factors. Enriched genes are linked to roles in synapse assembly, action potential generation and transmembrane ion transport, including of zinc. These results provide new insight into the molecular targets by which oligodendrocytes influence neuron excitability and synaptic function.

Keywords: GABAergic neurons, neuro-glia interactions, oligodendrocytes, secreted factors, single-cell RNAseq

Communication between oligodendrocytes and neurons is crucial for circuit maturation but still not completely understood. The fast transmission of action potentials relies on insulating properties of myelin sheath which is interrupted at nodes of Ranvier, small axonal domains highly enriched in voltage-gated Na^+ channels (Sherman and Brophy 2005). The profile of myelination and nodes of Ranvier controls the timing of impulse transmission, critical for coincident arrival of synaptic inputs transmitted by multiple axons in sensory systems (Seidl 2014; Freeman et al. 2016; Arancibia-Cárcamo et al. 2017; Monje 2018). Both oligodendrocytes and oligodendrocyte precursor cells (OPCs or NG2 cells) sense neuronal activity, which triggers their differentiation and maturation into myelinating oligodendrocytes (Barres & Raff, 1993; Demerens et al. 1996). Adaptive myelination acts to reinforce selected circuits during learning (McKenzie et al. 2014; Bechler et al. 2018; Monje 2018; Stedehouder et al. 2018). Oligodendrocytes also release lactate to provide metabolic support to axons (Fünfschilling et al. 2012; Lee et al. 2012; Saab et al. 2016).

Factors secreted by oligodendrocytes induce early formation of node-like clusters, termed prenodes, enriched in Nav channels, Nfasc186 and Ankyrin-G, along the axons of retinal ganglion cells and some hippocampal GABAergic neurons (parvalbumin or somatostatin immunopositive) before myelination (Kaplan et al. 1997; Freeman et al. 2015; Bonetto et al. 2019; Dubessy et al. 2019). These early clusters are associated with an increased axonal conduction velocity along GABAergic axons (Freeman et al. 2015). In addition, oligodendrocyte lineage cells close to the soma of pyramidal neurons modulate glutamatergic neurotransmission via secreted factors and restrain high-frequency firing through the rapid uptake of K^+ (Sakry et al. 2014; Birey et al. 2015; Battefeld et al. 2016; Jang et al. 2019; Xin et al. 2019). Moreover, oligodendroglial exosomes and OPC secreted protein NG2 mediate glia signaling to neurons

(Frühbeis et al. 2013; Sakry et al. 2015). The identity of molecular targets by which oligodendrocyte secreted factors affect GABAergic neuron excitability and synaptic interactions remain unknown.

The present study aimed to identify targets of oligodendrocyte mediated regulation of GABAergic hippocampal neurons. Electrophysiological phenotypes of rat hippocampal neurons were compared in mixed cultures, (with glial cells, CTRL) and purified neuron cultures (without glial cells, PUR). We then tested the effects of adding oligodendrocyte conditioned medium (OCM) to purified cultures. OCM tended to reverse changes in GABAergic neuron physiology and anatomy induced by eliminating glial cells from cultures. Single-cell RNA-sequencing of GABAergic neuron cytoplasm collected in patch electrodes let us explore molecular targets of OCM-induced regulation. RNA-seq analysis was validated by the presence of cell-type specific genes, including those for subclasses of GABAergic neurons. Major targets of oligodendrocyte factor signaling to GABAergic neurons included ion channels and transporters contributing to the regulation of membrane potential and action potential generation as well as transmembrane transport of zinc.

MATERIALS AND METHODS

Animals

Care and use of rats in all experiments conformed to institutional policies and guidelines (UPMC, INSERM, and European Community Council Directive 86/609/EEC). The following rat strains were studied: Sprague-Dawley or Wistar rats (Janvier Breeding Center) and VGAT-Venus Wistar rats in which a green fluorescent protein variant is selectively expressed in GABAergic cells (Uemastu et al. 2008). We assume that fluorescent cells in cultures correspond to GABAergic neurons.

Culture Media

We used the following culture media. NM, neurobasal medium (21103ium (2Gibco) supplemented with 0.5 mM L-glutamine, B27 (1×; Invitrogen), and penicillin-streptomycin (100 IU/mL). BS, Bottenstein-Sato medium: DMEM Glutamax supplemented with transferrin (50 µg/mL), albumin (50 µg/mL), insulin (5 µg/mL), progesterone (20 nM), putrescine (16 µg/mL), sodium selenite (5 ng/mL), T3 (40 ng/mL), T4 (40 ng/mL) and PDGF (10 ng/ml).

Preparation of oligodendrocyte conditioned medium

Glial cell cultures were prepared from cerebral cortices of P2 Wistar rats as described previously (Mazuir et al. 2020). After meninges were removed, cortices were incubated for 35 min in papain (30 U/mL; Worthington), supplemented with L-cysteine (0.24 mg/mL) and DNase (50 µg/mL) in DMEM at 37°. They were then mechanically homogenized and passed through a 0.70 µm filter. Cells were re-suspended in DMEM with 10% FCS and 1% penicillin-streptomycin. After 7 to 14 days *in vitro* (DIV), oligodendroglial lineage cells were purified from glial cell cultures which initially contain astrocytes and microglial cells. After cultures were shaken overnight at 230 rpm and 37°C, overlying oligodendroglial and microglial cells could be selectively detached. Microglia were then eliminated by differential adhesion (McCarthy and de Vellis 1980). Collected cells were incubated in dishes for 15 min. Non-adherent cells were retrieved and centrifuged in DMEM for 5 min at 1500 rpm. They were re-suspended and seeded at a density of $1.5x10^5/cm^2$ on Polyethylene-imine (PEI)-coated dishes with BS medium and 0.5% PDGF. Immunostaining showed that 90 ± 4% of cells were positive for the oligodendroglial marker $O4^+$, 7.2 ± 2.5% were $GFAP^+$ astrocytes and 4.6 ± 0.7% were $CD11b^+$ immunopositive microglial cells (Mazuir et al. 2020). Medium from these cultures was collected after 48 hours, filtered (0.22 µm) and stored for use as oligodendrocyte conditioned medium.

Neuronal cultures

Experiments were performed in three different culture conditions (Fig. 1A). Control (CTRL) was mixed hippocampal cultures containing neurons, astrocytes, and oligodendrocyte lineage cells (Sup. Fig1A). They were prepared from E18 rat embryos and were seeded on polyethyleneimine precoated glass coverslips at a density of 50,000 cells/35 mm2 (Freeman et al. 2015). Purified neuron cultures (PUR) were prepared by adding anti-mitotic agents (FdU and U 5µM) for 12 hours, starting at 24 hours after dissection. Immunostaining showed these cultures contained less than 5% astrocytes and virtually no oligodendrocytes. In OCM cultures oligodendrocyte conditioned medium was added to purified neuron cultures. Conditioned medium (500 µl/well) was added at 3 days *in vitro* (DIV). One-third of the medium was replaced with neurobasal medium (NM) at 7 DIV, and then twice a week. Axon initial segments were visualized by 20 min exposure to an anti-Nfasc antibody (clone A12/18, Antibodies Incorporated) coupled to Alexa 594 (using Apex antibody labeling kit, ref A10474, Thermofisher) before recordings (Sup. Fig1B).

Patch-clamp electrophysiological recording and analysis

Electrophysiological recordings were made from cultures at 17 DIV. Dishes were transferred to a recording chamber mounted on a BX51WI microscope (Olympus, France) and superfused with ACSF containing (in mM): 124 NaCl, 2.5 KCl, 26 $NaHCO_3$, 1 NaH_2PO_4, 2 $CaCl_2$, 2 $MgCl_2$, and 11 glucose, bubbled with 5% CO_2 in O_2 (pH 7.3, 305-315 mOsm/L). Temperature was kept at 34° C. Recordings were made with glass pipettes pulled using a Brown–Flaming electrode puller (Sutter Instruments) from borosilicate glass of external diameter 1.5 mm (Clark Capillary Glass, Harvard Apparatus). Pipette resistance was 6 MΩ when filled with a solution containing (in mM): 135 K-gluconate, 1.2 KCl, 10 HEPES, 0.2 ethylene glycol tetraacetic acid (EGTA), 2 $MgCl_2$, 4 MgATP, 0.4 Tris-GTP, 10 Na_2-phosphocreatine and 2.7 biocytin. RNase

inhibitor was added (40U/µl, Thermo Fischer Scientific; 5µl in 1ml) when harvesting cell contents. Pipette solution pH was adjusted to 7.3 with KOH and the osmolarity was 290 mOsm. Whole-cell current-clamp recordings were made using a MultiClamp 700B amplifier and pCLAMP software (Molecular Devices). Potential signals were filtered at 6 kHz and digitized at 20–50 kHz.

Recordings in the whole-cell current clamp configuration were made from fluorescent GABAergic neurons and non-fluorescent pyramidal shaped neurons in cultures prepared from VGAT-Venus Wistar rats. Excitatory postsynaptic potential (EPSP) and action potential (AP) frequencies, membrane potential and input resistance were measured at resting potential. Responses to families of hyperpolarizing and depolarizing current steps of duration 800 ms were recorded from holding potentials near -60 mV. Current intensities were manually adjusted to induce a maximal hyperpolarization close to -100 mV. Incremental positive steps of +1/10 of that value were then applied until the cell was depolarized above rheobase several times. After recording electrical data for ~10 min, neuronal contents were aspirating into the glass electrode tip. They were extracted into a tube containing 3.5 µl of lysis buffer with RNase inhibitor as a first step to prepare a library of neuronal total RNA (Qiu et al., 2012). Electrophysiological signals were analyzed with AxographX and routines written in MATLAB (The Mathwork; Huang et al. 2017). EPSP and AP frequencies were measured from baseline records of duration at least 3000 ms. Sup. Fig2 shows procedures used to measure active and passive membrane parameters.

Reconstruction of neuronal morphology

Pipettes used for patch-clamp recordings included 2.7 mM biocytin. Cultures containing filled cells were fixed at 17 DIV with PFA4% (diluted in PBS 1X; pH 7.2) for 10 min at room temperature (RT). Coverslips were washed three times with PBS 1X and blocked with 5% normal

goat serum containing 0.1% Triton for 15 min at RT. Biocytin-filled cells and their axon initial segments were visualized. Cultures were incubated with anti-Neurofascin (1:100, ab31457, Abcam) for 2 hours at RT. After three PBS rinses, they were incubated with Streptavidine-Alexa 488 (ThermoFisher Scientific) to visualize biocytin-filled neurons and anti-rabbit-Alexa 594 (1:1000, ThermoFisher Scientific) for Neurofascin for 1 hour at RT. Stained cultures were mounted with Fluoromount-G.

Images of stained cells were acquired on a upright spinning disk microscope (Intelligent Imaging Innovations, Inc) using a 20x glycerol immersion objective (NA 1.0), a CSU-W1 spinning disk head (Yokogawa) and a sCMOS ORCA-Flash4.0 camera (Hamamatsu). Multiple tile regions each with Z step series of separation 1.1 µm were acquired for each cell. Tile scans were stitched using Fiji software with BigStitcher plugin. Neuronal arborizations were drawn with the semi-automatic filament tracer tool of IMARIS software (Bitplane). The axon was identified from Neurofascin immunostaining of its initial segment. Axonal and dendritic lengths and data for Sholl analyses were derived by the IMARIS software.

Statistical analysis of electrophysiological properties and morphology

Statistical analyses were performed using GraphPad Prism version 7.0. Experiments for each condition were carried out in at least 3 independent cultures from at least 3 different litters. Electrophysiological parameters in Figs. 1 and 2 were compared using the Mann-Whitney test (for PYR CTRL vs. GABA CTRL) and using Kruskal Wallis and Dunn's multiple comparison *post hoc* test (for GABA CTRL vs. GABA PUR, GABA PUR vs. GABA OCM and GABA CTRL vs. GABA OCM). P-values are given in Table 1.

Axonal and dendritic lengths were compared (Fig. 3) using Kruskal Wallis and Dunn's multiple comparison *post hoc* test (for GABA CTRL vs. GABA PUR and GABA PUR vs. GABA OCM

and GABA CTRL vs. GABA OCM). Dendritic arborizations were assessed with Sholl analysis which measures the number of dendrites which intersect circles of increasing distance from the neuronal soma (20 µm increments were used). They were analyzed using a linear mixed-effects model (LMM) with culture condition and radial distance as fixed effects, and the cell identifier number as a random effect to account for the successive measurements over the concentric rings (Wilson et al. 2017). Significance for the main effects of condition, distance and their interaction was then evaluated using ANOVA Type II Wald chi-square tests. Analyses were made with R (R Development Core Team, ver 3.5.1, 2019) and plots were generated with the ggplot2 package (Wickham et al., 2016). LMM was fitted with the function lmer in the lme4 package (Bates et al., 2015). When a factor had a significant effect or when a significant interaction was found between condition and distance, *post-hoc* pairwise comparisons were completed with Tukey's method. Data were square root transformed before modeling to improve model assumptions of linearity, normality and constant variance of residuals,

Data are given as mean ± SD (*i.e.* standard deviation) in Table 1 and in the text. The level of statistical significance was set at $p < 0.05$ for all tests. Significance is represented as numbers of asterisks: *$p < 0.05$, **$p < 0.01$, ***$p < 0.001$, ****$p < 0.0001$

cDNA synthesis, library preparation and sequencing

mRNA capture, reverse transcription and amplification was achieved using the SMART-Seq v4 ultra low input RNA Kit (Takara, 634891). This kit improves synthesis of the full-length cDNA via a template switching mechanism for synthesis of the second strand cDNA. 5μl of sample was used for hybridization with the 3'smart-seq primer, then poly{T}-primed mRNA was converted to cDNA by reverse transcriptase and PCR amplification was done, according to the kit instructions. Full-length cDNA was then processed with a Nextera XT DNA Library

Preparation Kit (Illumina, FC-131-1096). This kit aims to fragment and add adapter sequences onto template DNA with a single tube Nextera XT tagmentation reaction and so generate multiplex sequencing libraries. The resulting indexed paired-end libraries were sequenced by next-generation sequencing (NGS), using NextSeq500 2x75pb, 33 million of reads per sample (Illumina NextSeq 500 platform) (Sup. Fig3A).

RNA-seq data analysis

RNA-Seq data analysis was performed by GenoSplice technology (www.genosplice.com). Sequencing, data quality, read distribution (to check for ribosomal contamination for instance), and insert size estimation were done with FastQC, Picard-Tools, Samtools and rseqc. Reads were mapped using STARv2.4.0 (Dobin et al. 2013) on the rn6 Rat genome assembly. The regulation of gene expression was studied as in (Noli et al. 2015). For each gene of the Rat FAST DB v2016_1 annotations, reads aligning on constitutive regions (not prone to alternative splicing) were counted. Normalization and differential gene expression was assessed from these reads using DESeq2 running on R (v.3.2.5, Love et al. 2014). FastQC was used for quality control, sequencing quality per base and sequence, per base sequence and GC content, N content, overrepresented sequences, sequence lengths. Sequence coverage of introns and exons was used to ensure that the sequences derived from mRNA rather than genomic DNA.

From 64 samples, 21 passed these control quality steps. Others were discarded due to sample quality (n=32) or contamination detected from marker expression (n=11) based on the following *GFAP*, *Aquaporin 4, Slc1a2, PDGFRa, MOG, Itgam* (Sup. Fig3 B, D, E).

Genes were considered as expressed if their FPKM (*i.e.* Fragments Per Kilobase Million) value was greater than 98% of the background FPKM value from intergenic regions (Sup. Fig4). Data accessibility: GEO access for reviewers (ref: GSE146291) - https://www.ncbi.nlm.nih.gov/geo/query/acc.cgi?acc=GSE146291, (code: cbcfcwamlbmztep).

Clustering and heatmap analyses were performed using dist" and "hclust" functions in R, with Euclidean distance and Ward agglomeration method.

Genes were considered to be differentially expressed when the uncorrected p-value ≤ 0.05 and fold-change ≥ 1.5.

Enriched gene ontology (GO) terms were assessed, from the identity of differentially expressed genes, with the DAVID Functional Annotation Tool (v6.8), (Huang et al. 2007). GO terms were considered enriched when fold enrichment ≥ 2.0 and uncorrected p-value ≤ 0.05 (1.3 value in GO term graph matches with a p value of 0.05), and at least 2 regulated genes in the pathway/term.

A Pearson correlation-based approach was used to compare single-cell RNA values with electrophysiological parameters for neurons (Fig. 6). The procedure was restricted to genes expressed in at least five samples, with coefficients greater than 0.6 and significant p-values ($p<0.05$).

RESULTS

Oligodendrocyte secreted factors control the electrophysiological properties of hippocampal GABAergic neurons

We first asked how the presence of glial cells or oligodendrocyte secreted factors affected GABAergic neuron phenotype. Hippocampal neuron cultures were prepared from VGAT-Venus rat embryos so that GABAergic interneurons could be identified. Spontaneous activity and active and passive membrane properties were recorded in the current clamp mode from fluorescent GABAergic neurons (n=36). These properties were compared with those of unlabeled pyramidal cells (n=11). We further compared the physiology of GABAergic neurons in control cultures (CTRL) with those in purified cultures lacking glial cells (PUR) and with

those in purified cultures supplemented with oligodendrocyte conditioned medium (OCM) (Fig. 1A, B).

Spontaneous synaptic events and spiking activity of recorded cells was quantified at resting potential with no injected current (Fig. 1C-E). In pyramidal cells (PYR), frequencies of excitatory postsynaptic potentials (EPSP) and action potentials (AP) were low in CTRL cultures (PYR CTRL, EPSPs, 7±2 Hz; APs, 0.03±0.01 Hz; n=11). Mean resting potential was -63±9 mV and mean input resistance was 330±218 MΩ (Fig. 1F, G; Table 1). EPSP frequency and AP discharge rate were both higher in GABAergic neurons from the same cultures. Mean EPSP frequency was 70±13 Hz and AP discharge frequency was 0.6±0.5 Hz (GABA CTRL, n=11).

In PUR neuronal cultures, both EPSP frequency and AP discharge by GABAergic neurons were reduced (GABA PUR, EPSPs, 6±2 Hz, n=10; APs, 0.03±0.03 Hz, n=11). This despite a more depolarized mean resting membrane potential (GABA PUR, -49±11 mV vs GABA CTRL, -55±5 mV) and a significantly higher input resistance than in control cultures (GABA PUR, 144±46 MΩ vs GABA CTRL, 74±53 MΩ). Supplementing PUR cultures with oligodendrocyte conditioned medium tended to increase EPSP and AP frequencies towards CTRL levels (GABA OCM, EPSPs, 19±4 Hz, n=13; APs, 0.4±0.03 Hz, n=12). Mean membrane potential and input resistance also reverted towards values in CTRL mixed cultures (GABA OCM, -54±7 mV and 110±104 MΩ). These data suggest that oligodendrocyte secreted factors influence active and passive aspects of the physiological phenotype of GABAergic neurons.

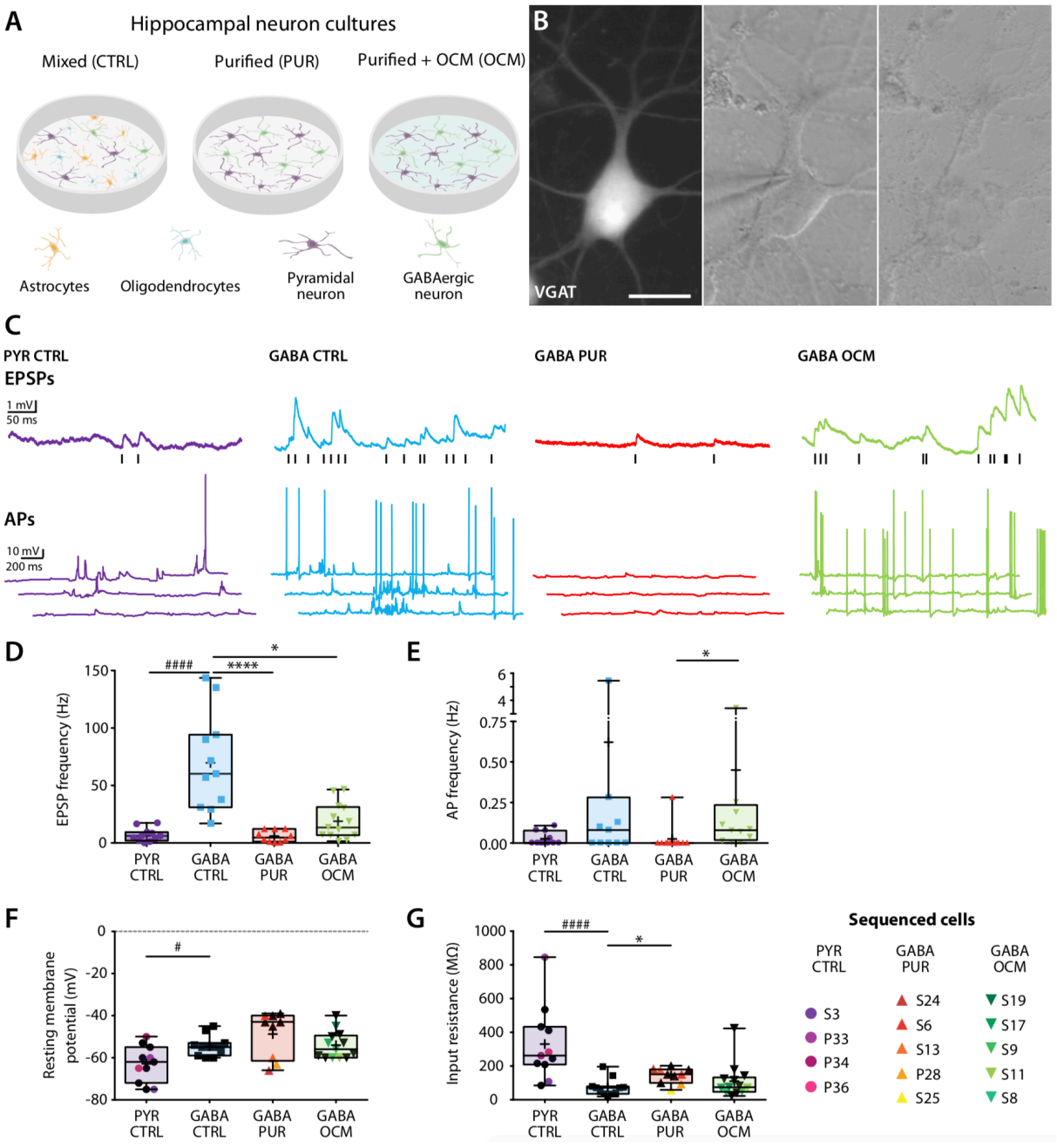

Figure 1: Patch clamp recording and cytosol harvesting of hippocampal neurons. (A) Schematic representation of the culture conditions: neurons from mixed cultures (CTRL), containing hippocampal neurons and glial cells, were compared with those of purified cultures (PUR), which in some cases were treated with oligodendroglia conditioned medium (OCM). (B) Soma and proximal dendrites of a green fluorescent GABAergic neuron (VGAT+ cell; left). Patch pipette sealed to the neuronal membrane for electrical recording (middle). After aspiration of

the cytosolic content (right). Scale bar: 20 µm (C) Representative voltage recordings of pyramidal and GABAergic neurons at 17 DIV in different culture conditions. Top, excitatory postsynaptic potentials (EPSPs), indicated by black lines. Bottom, spontaneous action potential (AP) firing. (D, E) EPSP (D) and AP (E) frequencies measured from neurons in different conditions. EPSP, PYR CTRL vs. GABA CTRL, p<0.0001 (Mann-Whitney test #); GABA CTRL vs. GABA PUR, p < 0.0001; GABA CTRL vs. GABA OCM, p=0.0123. AP, GABA PUR vs. GABA OCM, p=0.0126 (Kruskal-Wallis and Dunn's *post hoc* *). (F, G) Resting membrane potential (F) and input resistance (G) of recorded neurons in different conditions. Color symbols show cells from which sequence data was derived. Mann-Whitney test for PYR CTRL vs. GABA CTRL significance levels indicated with #, Kruskal-Wallis and Dunn's *post hoc* for GABA CTRL vs. PUR vs. OCM indicated by *. P-values are given in Table 1. Boxplots represent the median (middle line), the mean (+ sign), 25th and 75th percentiles (box) and the top and bottom values (whiskers).

	PYR CTRL			GABA CTRL			GABA PUR			GABA OCM		
	Mean	SD	N	Mean	SD	N	Mean	SD	N	Mean	SD	N
Resting membrane potential (mV)	-63	9	11	-55	5	11	-49	11	9	-54	7	13
Neuronal Input Resistance (Mohm)	330	218	11	74	53	11	144	46	10	110	104	13
Tau 1 (ms)	31	16	11	12	10	11	15	7	10	14	6	12
Sag ratio at -100 mV	1.10	0.10	11	1.27	0.10	11	1.17	0.10	10	1.33	0.20	13
Rheobase current	121	83	11	427	284	11	169	121	10	347	276	13
Firing rate at 200 pA (Hz)	26	19	11	3	7	11	21	23	10	7	12	13
Input-output slope (Hz/nA)	225	150	11	99	48	11	188	139	10	113	115	12
AP threshold (at 10V/s)	-30.5	3.3	11	-32.2	3.5	11	-31.8	5.7	10	-35.3	2.9	13
AP width (ms)	1.51	0.80	11	0.50	0.20	11	0.96	0.60	10	0.74	0.50	13
AP AHP (mV)	-19.5	4.4	11	-27.6	3.3	11	-23.8	3.2	10	-29.4	7.3	13
AP rise amplitude	78	7	11	61	9	11	56	13	10	68	8	13
AP maximum depolarization rate (V/s)	325	212	11	294	68	11	192	105	10	327	103	13
AP maximum repolarization rate (V/s)	-61	28	11	-164	82	11	-91	57	10	-119	51	13
Onset latency at rheobase	349	251	11	167	172	11	28	24	10	64	86	13

	PYR CTRL vs GABA CTRL		GABA CTRL vs GABA PUR		GABA PUR vs GABA OCM		GABA CTRL vs GABA OCM	
	p value (MW)	Significance	p value (KW)	Significance	p value (KW)	Significance	p value (KW)	Significance
Resting membrane potential (mV)	0.0175	*	0.6894	ns	0.6360	ns	>0.9999	ns
Neuronal Input Resistance (Mohm)	<0.0001	****	0.0156	*	0.1240	ns	>0.9999	ns
Tau 1 (ms)	0.0041	**	0.2966	ns	>0.9999	ns	0.4235	ns
Sag ratio at -100 mV	0.0005	***	0.1387	ns	0.0317	*	>0.9999	ns
Rheobase current	0.0019	**	0.0464	*	0.1854	ns	>0.9999	ns
Firing rate at 200 pA (Hz)	0.0008	***	0.0523	ns	0.4131	ns	0.9355	ns
Input-output slope (Hz/nA)	0.0336	*	0.3019	ns	0.1416	ns	>0.9999	ns
AP threshold (at 10V/s)	0.1932	ns	0.5216	ns	0.0571	ns	0.9382	ns
AP width (ms)	<0.0001	****	0.1396	ns	0.5170	ns	>0.9999	ns
AP AHP (mV)	0.0003	***	0.1268	ns	0.0075	**	>0.9999	ns
AP rise amplitude	<0.0001	****	>0.9999	ns	0.0480	*	0.2263	ns
AP maximum depolarization rate (V/s)	0.529	ns	0.1148	ns	0.0151	*	>0.9999	ns
AP maximum repolarization rate (V/s)	0.0001	***	0.0815	ns	0.5344	ns	>0.9999	ns
Onset latency at rheobase	0.0281	*	0.1681	ns	>0.9999	ns	0.3630	ns

Table 1: Electrophysiological properties of pyramidal and GABAergic neurons. Top, mean values, SD and number of cells for each parameter and culture condition. Bottom, p-values and significance levels from Mann-Whitney (MW) tests (PYR CTRL vs. GABA CTRL) and from

Kruskal-Wallis (KW) and Dunn's multiple comparison *post-hoc* test (GABA CTRL vs. PUR vs. OCM).

We next asked whether the properties of fluorescent and non-fluorescent cells were consistent with those of GABAergic neurons and pyramidal cells respectively (Pelkey et al. 2017). In control cultures, the mean resting potential of fluorescent neurons was significantly more depolarized (GABA CTRL, -55±5 mV vs. PYR CTRL, -63±9 mV; Fig. 1F), and their input resistance was significantly lower than that of non-fluorescent cells (74±53 MΩ vs. 330±218 MΩ; Fig. 1G). Comparing neuronal responses to depolarizing and hyperpolarizing step current injections (Sup. Fig. 2, Fig. 2) revealed significant differences in the membrane time constant tau (Fig. 2C, GABA CTRL, 12±10 ms vs. PYR CTRL, 31±16 ms), sag ratio, which is linked to the presence of an h-current, (Fig. 2D, 1.27±0.10 vs 1.10±0.10), rheobase current (Fig. 2E, 427±284 pA vs 121±83 pA) and firing rate induced by a 200 pA step current injection (Fig. 2F, 3±7 Hz vs 26±19 Hz). Input-output plots of the number of APs against the injected current had a mean initial slope of 99±48 Hz/pA in fluorescent cells, significantly lower than 224±150 Hz/pA for non-fluorescent cells (Fig. 2G). Action potential width in fluorescent neurons was short, 0.50±0.20 ms (Fig. 2I), as is characteristic of some interneurons, compared to an AP width of 1.51±0.8 ms in non-fluorescent neurons. AP thresholds were similar: -32.2±3.5 mV in fluorescent cells (Fig. 2H) and -30.5±3.3 mV in non-fluorescent cells. AP rising amplitude (Fig. 2K) was 61±9 mV in fluorescent cells, significantly lower than a value of 78±7 mV in non-fluorescent cells. Maximum depolarization and repolarization rates were 294±68 V/s and -164±82 V/s respectively in fluorescent cells, compared to 325±212 V/s (Fig. 2L) and -61±28 V/s (Fig. 2M) in non-fluorescent neurons. Action potential after hyper-polarizations (AHP) were larger in fluorescent cells at -27.6±3.3 mV compared to -19.5±4.4 mV (Fig. 2J). The latency to the first AP at rheobase was significantly shorter, 167±172 ms compared to 349±251 ms (Fig. 2N). Overall these data confirm that fluorescent neurons from VGAT-Venus animals

correspond to GABAergic neurons, and non-fluorescent cells to pyramidal cells. Table 1 summarizes these physiological data and provides statistical support for comparisons.

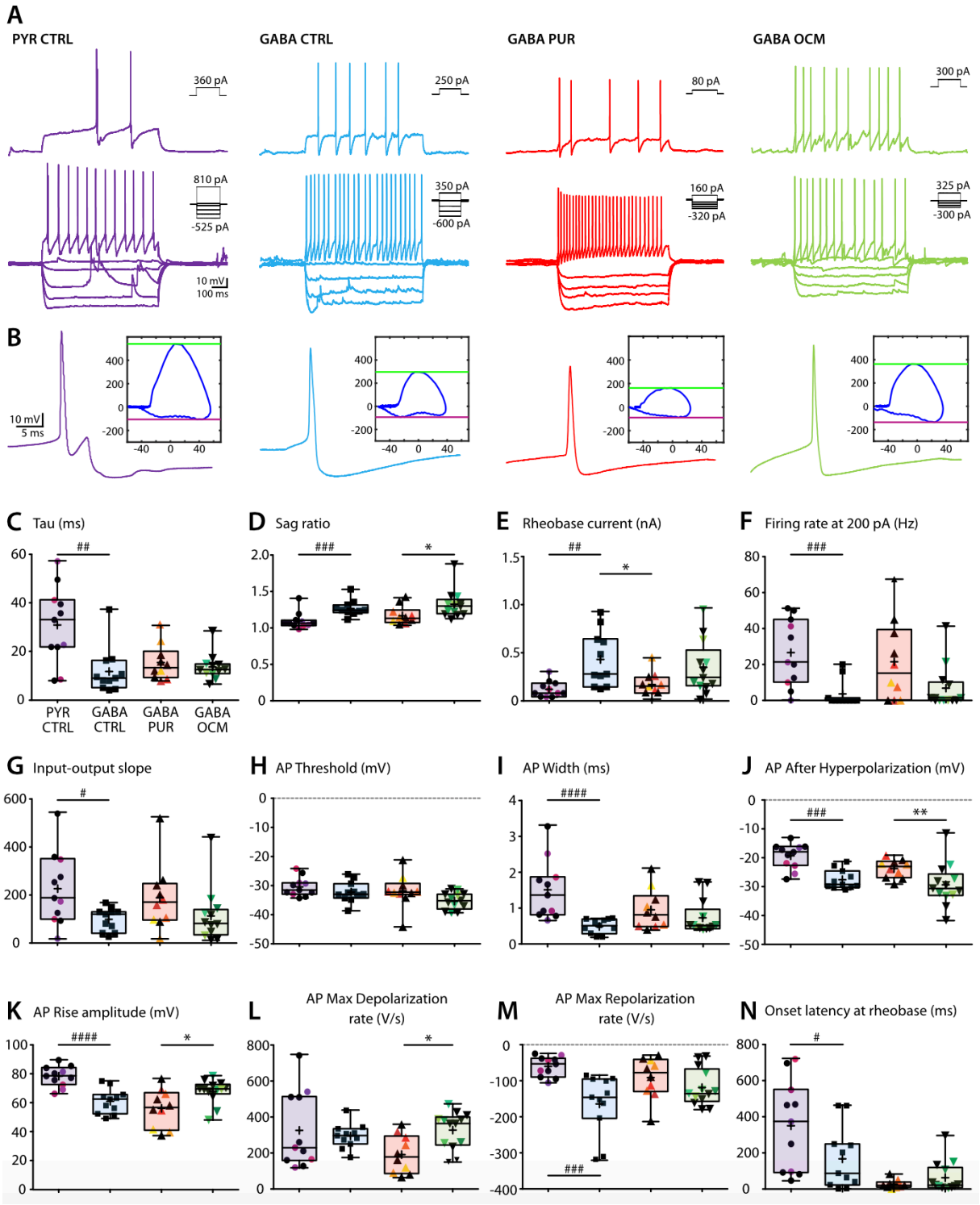

Figure 2: Glial factors affect the electrophysiological properties of GABAergic neurons. (A) Voltage responses to depolarizing and hyperpolarizing current steps recorded from representative neurons at 17 DIV in the different conditions. Top, action potentials initiated at rheobase; bottom, current intensities as shown in insets. (B) Action potential waveforms and phase plots (Y axis, dV/dt (V/s); X axis, membrane potential (mV). Green line, maximum depolarization rate; blue line, maximum repolarization rate. (C) to (N), Effects of culture conditions (PYR CTRL, GABA CRTL, GABA PUR and GABA OCM) on 12 parameters characterizing neuronal intrinsic properties. Each symbol is one neuron. Color symbols correspond to sequenced cells as in Fig. 1 F, G. Significance levels indicated as in Fig. 1, *i.e.* # for Mann-Whitney test and * for Kruskal-Wallis and Dunn's *post hoc* test. Parameters measured as shown in Sup. Fig. 2. P-values given in Table 1. Boxplots represent the median (middle line), the mean (+ sign), 25th and 75th percentiles (box) and the top and bottom values (whiskers).

Our next objective was to compare electrophysiological phenotypes for GABAergic neurons in control conditions (CTRL), in purified cultures (PUR) with no glial cells and in PUR cultures supplemented with oligodendrocyte conditioned medium (OCM). We found nodal proteins were clustered on GABAergic axons in CTRL but not in PUR cultures (Sup. Fig1D). Adding OCM to PUR cultures induced prenode formation as previously shown (Sup. Fig1D; Freeman et al. 2015; Dubessy et al. 2019). We also found some electrophysiological parameters of GABAergic neurons changed when glial cells were absent, and were partially restored by OCM treatment (Fig. 1, 2 and Table 1). The mean resting membrane potential of GABAergic neurons did not change significantly (Fig. 1F, CTRL, -55±5 mV; PUR, -49±11 mV; OCM, -54±7 mV). Input resistance increased in PUR cultures (Fig. 1G, PUR, 144±46 MΩ, GABA CTRL, 74±53 MΩ) and was reduced back towards control values by OCM addition (110±104 MΩ). Tau did not change significantly (Fig. 2C, PUR, 15±7 ms; OCM, 14±6 ms). Sag ratio

decreased significantly in PUR (Fig. 2D, PUR, 1.17±0.10; OCM, 1.33±0.20), as did the rheobase current (2E, PUR, 169±121 pA; OCM, 347±276 pA. Mean firing rate induced by 200 pA step current injection increased in PUR (Fig. 2F, PUR, 21±23 Hz; OCM, 7±12 Hz). The slope of input-output curves did not change (Fig. 2G, PUR, 188±139 Hz/pA; OCM, 113±115 Hz/pA). Mean AP threshold (Fig. 2H) was -31.8±5.7 mV in PUR, and -35.3±2.9 mV in OCM. AP width increased in PUR cultures (Fig. 2I, PUR, 0.96+0.60 ms; OCM, 0.74±0.50 ms), while AHP amplitude decreased (Fig. 2J, PUR, -23.8±3.2 mV; OCM, -29.4±7.3 mV). AP rising amplitude was significantly higher in OCM than in PUR cultures (Fig. 2K, PUR, 56±13 mV; OCM, 68±8 mV). Both the AP depolarization rate (Fig. 2L, PUR, 192±105 V/s; OCM, 327±103 V/s) and maximal repolarization rate were slower (Fig. 2M, PUR, -91±57 V/s; OCM, -119±51 V/s) in PUR culture compared to CTRL and OCM cultures. AP onset latency at rheobase was shorter in PUR conditions than in CTRL (Fig. 2N, PUR, 28±24 ms; OCM, 64±86 ms).

These data show that factors of the OCM have significant effects on the input resistance, rheobase current, and AP and AHP amplitudes of GABAergic neurons. These effects partially reverse changes induced by switching from a mixed culture of neurons, oligodendrocytes, and other glial cells, to a purified neuronal culture.

Impact of OCM on hippocampal GABAergic neuron morphology

We next asked whether factors secreted by oligodendrocyte exert trophic effects on GABAergic neuron anatomy. Biocytin-filled GABAergic neurons from CTRL, PUR, and OCM cultures were reconstructed and axonal and dendritic lengths were measured (Fig. 3A-C). The absence of glial cells had no significant effect on total axonal length (CTRL, 1179 ± 427 µm, n=6; PUR, 1929 ± 1305 µm, n=5; Fig. 3B) or total dendritic length (CTRL, 4405 ± 983 µm, n=6; PUR, 4794 ± 1621 µm, n=5; Fig. 3C). Scholl analysis of dendritic arbors revealed slight differences (Fig. 3D). However, in OCM cultures, total axonal length (OCM, 6451 ± 4793 µm,

n=8) was significantly increased compared to CTRL (p=0.0148) and mid-dendritic arbors were significantly more complex at distances of 260-700 µm from the soma compared to CTRL and PUR (Fig. 3B, D). Thus, oligodendrocyte derived factors exert effects on axons and dendrites of GABAergic neurons, which were not apparent on switching from CTRL to PUR cultures.

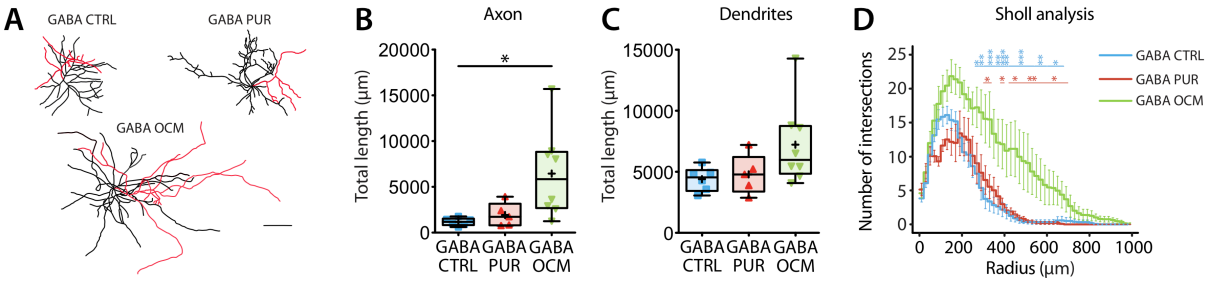

Figure 3: Axo-dendritic morphologies of biocytin filled GABAergic neurons. (A) Reconstruction of biocytin-filled GABAergic neurons at 17 DIV in different culture conditions. Axons shown in red, dendrites in black. Scale bar: 100 µm. (B) Total axonal and (C) dendritic lengths of GABAergic neurons in different conditions (Kruskal-Wallis followed by Dunn's *post hoc)*. Boxplots represent the median (middle line), the mean (+ sign), 25th and 75th percentiles (box) and the top and bottom values (whiskers). (D) Sholl analysis showing for each condition the number of dendrites intersecting increasing radii (20-1000 µm from the soma at interval 20 µm). The two segmented lines above the plot indicate significant differences between GABA OCM and CTRL (blue) and between GABA OCM and PUR (red). There were no significant differences between GABA CTRL and PUR. LMM and Type II Wald chi-square tests followed by *post-hoc* analyses using Tukey's method. Mean ± SEM is represented. (*$p < 0.05$, **$p < 0.01$, ***$p < 0.001$).

Single-cell transcriptomic analysis of electrophysiologically characterized neurons

We used single cell RNA-sequencing (scRNA-seq) of the cytoplasmic contents of GABAergic neurons to pursue the identity of protein targets underlying changes in their phenotype induced by OCM. When patch-clamp recordings were completed, the same pipette was used to harvest neuronal cytosolic contents (n=64). Sup. Fig. 3A, B illustrates the experimental workflow and bioinformatics pipeline. We noted a strong correlation (R=0.79) between the number of expressed genes and the number of aligned reads suggesting that increasing reads could improve transcript detection (Fig. 4-1C). RNA-seq data was filtered to exclude samples of poor RNA quality where fewer than 2000 transcripts were detected. We also excluded samples which expressed glial cell specific genes, such as *Mog* or *Gfap*, as likely contaminated. Samples from 21 neurons passed these two controls.

Principal component analysis (PCA) of transcriptomic profiles captured 22% of explained variance with the first two principal components, PC1 and PC2 (Fig. 4A). Pyramidal cells and GABAergic neurons were clearly segregated in this two-dimensional space. GABAergic neurons from PUR cultures were separated from GABAergic neurons in CTRL cultures. Transcriptomes of GABAergic neurons from OCM cultures overlapped with those of CTRL cultures.

We investigated transcriptomic differences between hippocampal neuron types and the transcriptional response to glial factors in GABAergic neurons. The heat map of Fig. 4B shows in red up-regulated genes and in blue genes that were down-regulated with respect to mean expression in all three conditions. High, deep sequencing detected up to 5,700 expressed genes in single neurons. Hierarchical clustering of samples from different cells in the heat map segregated 4 out of 5 pyramidal neurons from GABAergic neurons. GABAergic neurons from purified cultures (PUR) were also grouped together in the dendrogram while GABAergic neurons sampled in CTRL and OCM cultures overlapped in a large branch (Fig. 4B).

As a step towards validation of these results, we searched for the presence of known pyramidal and GABAergic neuron markers in genes from different samples. All samples expressed the neuronal marker *Snap25*. Only samples from non-fluorescent pyramidal cells expressed the vesicular glutamate transporter1 (vGlut1, *Slc17a7),* while the vesicular GABA transporter (VGAT; *Slc32a1*) and GAD67 (*Gad1*) were only detected in samples obtained from fluorescent GABAergic neurons (Fig. 4C). Subclasses of hippocampal GABAergic neurons express neuropeptides and Ca^{2+}-binding proteins. Searching for neuropeptide (Somatostatin (*Sst*), Neuropeptide Y (*Npy*), Cholecystokinin (*Cck*), Vasoactive intestinal peptide (*Vip*), Protachykinin (*Tac1*), Prepronociceptin (*Pnoc*)) and Ca^{2+}-binding protein (Parvalbumin (*Pvalb*), Calbindin-1 (*Calb1*), Calbindin-2 (*Calb2*) genes revealed a diversity of expression. Most GABAergic neurons expressed *Pnoc (87%)*, *Sst (81%)* and *Npy* (57%*)*. Samples from 56% of cells expressed both *Sst* and *Npy*, or combinations of *Sst* and *Calb1* (37%) and/or *Sst* and *Cck* (25%) and/or *Sst* and *Pvalb* (19%, Fig. 4D). GABAergic neurons expressing *Pnoc, Npy* and *Sst* neuropeptide genes were found in all culture conditions (CTRL, PUR and OCM). *Calb-1* was less frequently expressed in PUR cultures. Genes for other interneuron markers detected in GABAergic neurons included the transcription factors *Satb1* and *Nkx-2.1*, the post-synaptic protein *Elfn1*, the serotonin receptor *Htr3a*, KCC2 the potassium chloride cotransporter 2, *Slc12a5,* the kinase *Erbb4* and the protease reelin, *Reln*. We note that some molecular markers examined here are not entirely specific to GABAergic neurons, and were also detected in samples from 1 or 2 pyramidal cells (*Slc12a5*, *Calb1*, *Satb1, Reln, Sst, Npy, Elfn1 and Cck.*). Furthermore, no samples from either pyramidal or GABAergic neurons expressed *Vip, Calb2* or *Nos1* (Fig. 4D).

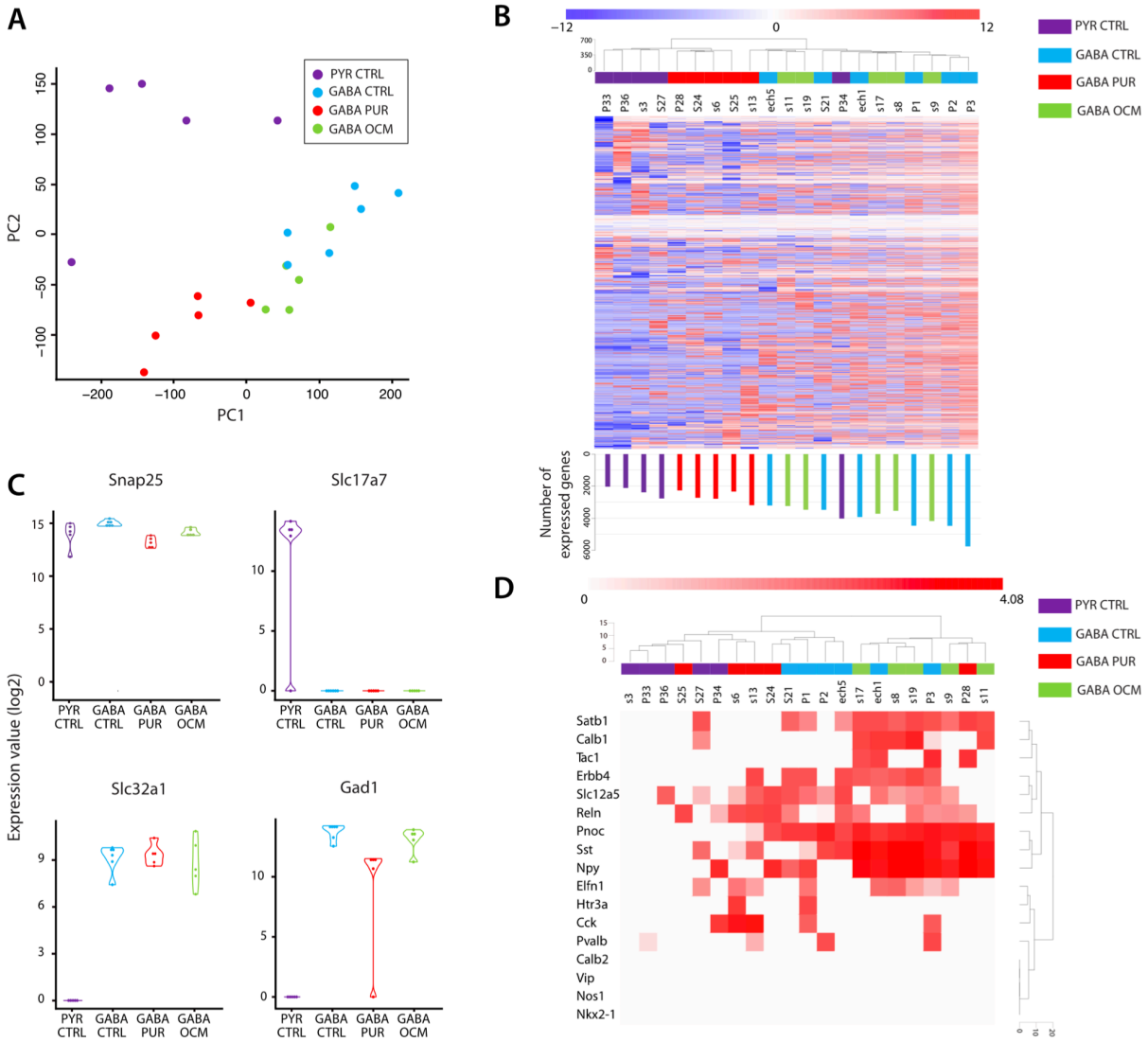

Figure 4: Gene expression analysis of the content of pyramidal or GABAergic neuron cytoplasm in the presence or absence of glial cells or oligodendrocyte secreted factors. (A) Principal component analysis showing clustering of validated neurons by culture conditions on single-cell data. PC1 and PC2 explain 14.9 % and 6.6 % of the variance, respectively. (B) Heatmap summarizing unsupervised analysis of mRNAs from validated neurons in different culture conditions. Rows represent genes and columns different neurons. Colors indicate gene expression (blue, low – red, high) normalized by row. Barplots (below) show the number of genes expressed by each neuron. 5391 genes (out of 35 152) are represented in the heatmap and only genes detected in at least 20% of neurons are included. C) Expression levels for markers for

neurons (*Snap25*), excitatory neurons (*Slc17a7*) and GABAergic neurons (*Slc32a1* and *Gad1*) in different culture conditions. (D) Differential expression of genes associated with subtypes of GABAergic neuron. Rows represent gene expression and columns represent different neurons under different culture conditions. Color intensity represents gene expression level. In A-D, data from pyramidal neurons under CTRL conditions are shown in purple, GABAergic neurons in CTRL conditions in blue, GABAergic neurons in purified neuron cultures in red and GABAergic neurons in purified cultures treated with OCM in green.

Ion channel and transmitter receptor gene expression in single hippocampal neurons

The cellular and synaptic physiology of neurons depends on the expression of genes coding for ion channels, transporters and neurotransmitter receptors. We examined quantitative expression of these genes in samples from each neuron in our RNAseq data set (Fig. 5A, B). Different neurons expressed different levels of *Atp1a, b* genes coding for Na^+/K^+-transporting ATPase subunits and *Clcn3-7* genes coding for Cl^-/H^+ exchangers, which contribute to stabilize membrane potential. The depolarization phase of action potentials is due to opening of voltage-gated sodium channels, which consist of an α-subunit forming pore (*Scn1a-9a*) and auxiliary ß subunits *(Scn1b-4b).* Almost all neurons expressed high levels of *Scn2a* (encodes Nav1.2). In contrast, only GABAergic neurons in CTRL cultures with glial cells or with oligodendroglial factors (OCM) expressed *Scn1a* (Nav1.1) and few expressed *Scn8a* (Nav1.6). The Na^+ channel modifier 1 (*Scnm1)*, which governs alternative splicing of pre-mRNAs, was detected in samples from some GABAergic neurons but not from pyramidal cells.

Various potassium channels are crucial for action potential repolarization, generate the AHP and contribute to maintenance of membrane potential. Voltage-gated K^+ channels differ in structure, biophysics and pharmacology from voltage independent, two-pore-domain (K2P) channels which support leak-type K^+ conductances. We found that distinct neurons express

specific combinations of K^+ channel $\propto$ (*Kcn a to v*) and auxiliary subunits (*Kcnab1-2*) as well as K2P channels (*Kcnk1-10*). We also examined Ca^{2+} channels, Ca^{2+}-activated K^+ channels and hyperpolarization-activated, cyclic nucleotide gated, K^+/Na^+ permeable 'h' channels (HCN).

Fig. 5B shows genes encoding ionotropic glutamate receptors, expressed at excitatory synapses, and including AMPA receptors (*Gria1-4*), NMDA receptors (*Grin1-3*) and kainate receptors (*Grik1-5*). Genes encoding $GABA_A$ receptors (*Gabra-g*), which mediate fast inhibitory neurotransmission and are assembled as heteropentameric chloride channels, are also indicated as are detected genes which code for subunits of nicotinic cholinergic receptors (*Chrna-b),* serotonin receptor *(Htr3a)* and glycine receptor *(Glra2).* Fig. 5C shows genes coding for G-protein linked receptors including metabotropic glutamate *(Grm2, 5)* and $GABA_B$ *(Gabbr1, 2)* receptors.

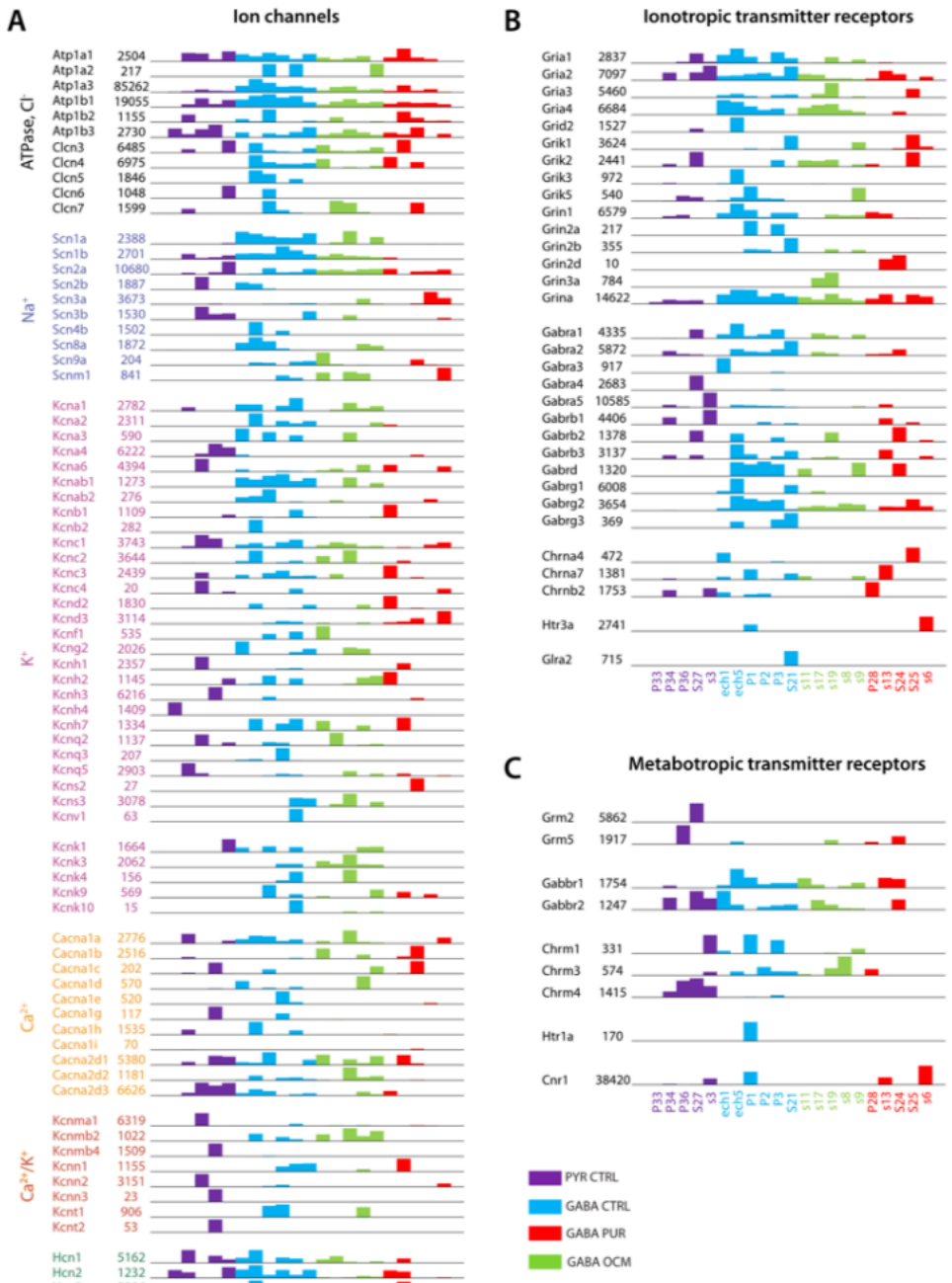

Figure 5: Cell-type specific expression of mRNAs coding for ion channel and receptors. (A) Ion channel, (B) ionotropic transmitter receptor and (C) metabotropic transmitter receptor mRNAs in different culture conditions. Maximal expression from all samples is indicated. Number of reads normalized from pyramidal neurons in CTRL conditions is shown in purple, GABAergic neurons in CTRL conditions in blue, GABAergic neurons in purified cultures in red and GABAergic neurons in purified cultures treated with OCM in green.

Correlation-based approach

These scPatch-seq data permit quantitative assays of transcriptomic features. We attempted to relate them to intrinsic neuronal electrophysiology by searching for correlations between values from transcriptomic samples and different electrophysiological parameters. Fig. 6 plots genes coding for ion channels, transporters and synaptic receptors for which a correlation (p-value <0.05) with electrophysiological parameters was detected. The analysis was based on all neurons with complete electrical and transcriptomic datasets and on cells from all culture conditions. Genes were clustered based on their relations with electrophysiological parameters. One cluster coding for α1, ß1 and α3 subunits of the Na^+, K^+ -ATPase (*Atp1a1*, *Atp1b1* and *Atp1a3*), was correlated with neuronal input resistance, *Atp1b1* was also correlated with time constant, tau and AP width. The Na^+ channel subunit *Scn2a* (coding for Nav1.2) was correlated with the time constant tau and with AP threshold, neuronal input resistance and AP width. A larger cluster, consisting of several K-channel linked genes (*Kcnc2,* coding for Kv3.2; *Kcnk3*, Task-1; *Kcnip1*, K^+ channel modulatory protein), as well as two Zn transporters (*Slc30a3,* ZnT3; *Slc30a4,* ZnT4) was strongly correlated with the Sag ratio, the AP threshold and the after-hyperpolarization amplitude (AP AHP).

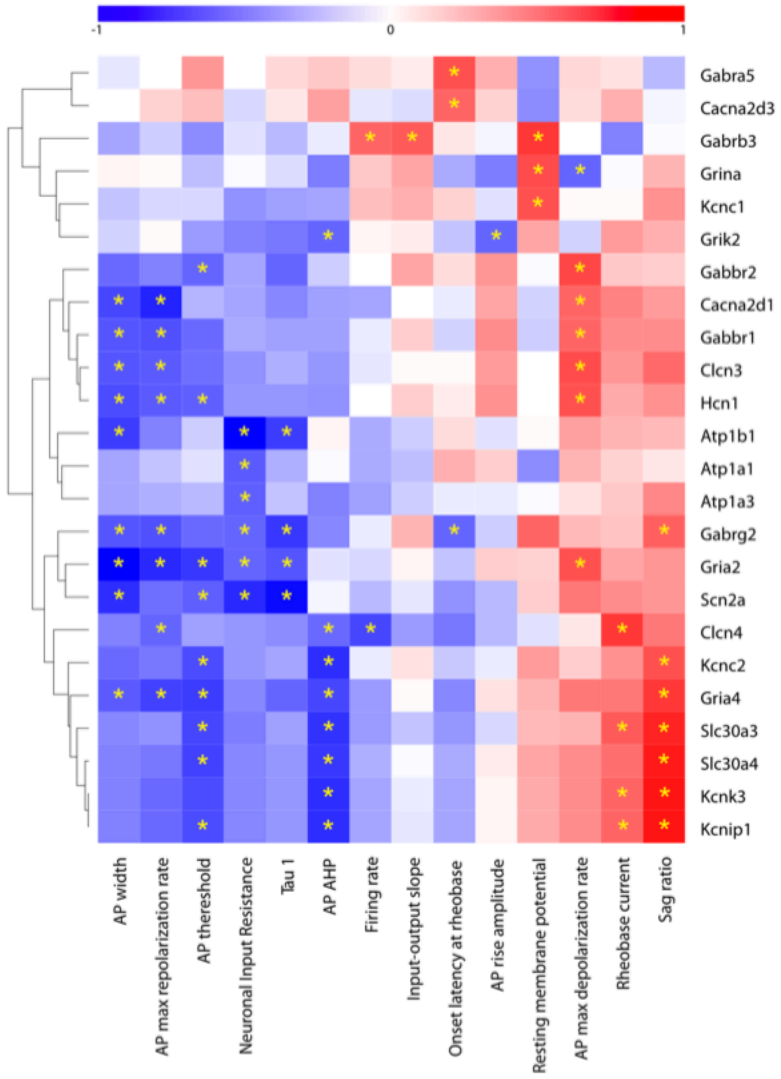

Figure 6: Pearson correlation between scRNASeq data and electrophysiological parameters. Ion channel and synapse related genes significantly correlated ($p<0.05$) with at least one parameter are shown. Color intensity represents correlation coefficient. Blue indicates negative correlation; expression decreases as the parameter increases. Red indicates positive correlation; both increase together. Significant positive or negative correlations with coefficient > 0.6 and p-value <0.05 are marked with a yellow star.

Transcriptomic patterns across groups of neurons in relation to biological processes

Gene Ontology (GO) analysis let us estimate biological processes underlying differential expression of groups of genes in different neurons or in different culture conditions. For

instance, 326 genes were differentially expressed in GABAergic neurons and pyramidal neurons in CTRL cultures (Fig. 7A, Sup. Fig5). GO process terms derived from the identity of the genes were related to synaptic transmission, organization and transmitter transport as well as cortical development. Comparing GABAergic neurons in CTRL and PUR cultures we found 219 genes were differentially expressed, mostly down-regulated in PUR conditions (Fig. 7B, Sup. Fig5). Inversely, comparing GABAergic neurons in PUR and OCM cultures, 192 genes were differentially expressed, mostly up-regulated in OCM conditions (Fig. 7C, Sup. Fig5). Many genes were down-regulated in one comparison and up-regulated in the other. GO process terms identified from their identity regulate neuronal action potential, synapse assembly, Ca^{2+}-dependent exocytosis, protein phosphorylation, kinase signaling and cell division (Fig. 7B, C). GO-analysis further suggested that genes coding for proteins involved in transmembrane transport of K^{+} were up-regulated by OCM treatment (Fig. 7C).

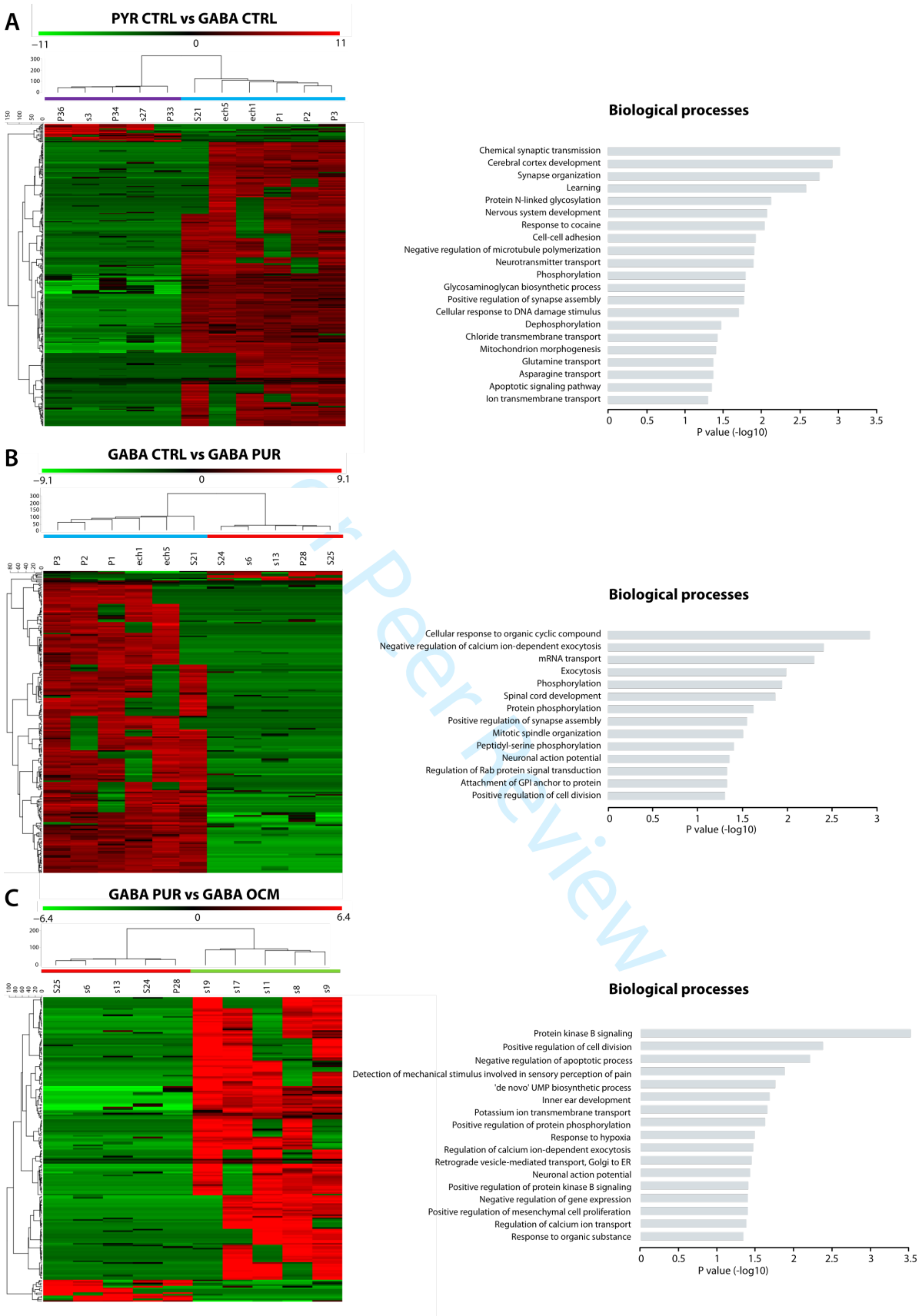

Figure 7: Heatmap of genes expressed differentially between conditions. (A) Differences between pyramidal and GABAergic neurons in CTRL culture conditions. (B) Differences between GABAergic neurons in CTRL and PUR cultures. (C) Effects of OCM on GABAergic neurons in PUR cultures. Rows represent genes and columns represent neurons in different conditions. Color intensity is mean centered expression. At the right, gene ontology analysis of biological processes for differentially expressed genes. Differences between pyramidal and GABAergic neurons in CTRL conditions (upper). Differences between GABAergic neurons in PUR cultures and CTRL. Effects of OCM on GABAergic neurons in PUR cultures (lower).

Further insights into processes affected by oligodendrocyte factors were obtained by grouping genes with similar profiles of changes. RNA-seq data from GABAergic neurons in different culture conditions was normalized with respect to expression of each gene in pyramidal cells (Fig. 8A, B and Sup. Fig6). A total of 241 genes were identified as differentially expressed between pyramidal and GABAergic neurons in CTRL cultures and were mostly insensitive to PUR or OCM culture conditions (Sup. Fig6).

We found a significant difference in the group of genes that were reduced in PUR cultures and restored in OCM cultures. For one group of these genes, expression in GABAergic and pyramidal neurons in CTRL conditions were comparable (Fig. 8A; n=137). Another second group of genes differed in that expression in GABAergic neurons was systematically higher than in pyramidal cells in CTRL cultures (Fig. 8B; n=120). GO term analysis of the identities of the first group of genes (Fig. 8a') linked them to processes including negative regulation of protein kinase activity and apoptosis signaling pathways. In contrast, the identities of the second group of genes (Fig. 8b') evoked biological processes including the membrane transport of zinc, K^+ channels, regulation of membrane potential and action potential and G-protein coupled receptor signaling pathways.

Finally, we present target genes whose expression was affected by the absence of glial cells in

PUR cultures and inversely by OCM and which are linked to GABAergic cell physiology. These target transcripts code for ion channels, transporters, synaptic markers, vesicle trafficking, cytoskeleton remodeling, cell adhesion molecules, growth factors and signaling (Fig. 8C) and were mostly up-regulated in CTRL and OCM neurons. They included Na^+ channels, *Scn1a* (Nav1.1) and *Scn1b* (ß1Nav) and K^+ channels, *Kcna1* (Kv1.1), *Kcnab1* (ß1Kv), *Kcnk3* (Task-1), *Kcnip1* (KChip-1, a K^+ channel modulatory protein). Genes encoding zinc transporters (*Slc39a11, Slc30a4* and *Slc30a3*), were upregulated by OCM, while a $Na^+/K^+/Ca^{2+}$ exchanger (*Slc24a2*) was one of the few transcripts downregulated by OCM. Among genes coding for signaling molecules, growth factors and receptors, the kinases *Nek7, Pak1* and *Akt1,* and growth factors *Vegfb, Pdfga, Fgf9 and Rara* were up-regulated in OCM culture conditions. Only the protein kinase C binding protein *Nell2* and the neuropeptide hormone Proenkephalin (*Penk*) were downregulated by OCM. To address possible coordinated changes, we also analyzed pathways of regulated genes between OCM and PUR, or CTRL and PUR. We found that the MAPK, AMPc and PI3K-Akt signal transduction pathways are significantly up-regulated by glial cells and OCM, respectively (Fig. 8D, E).

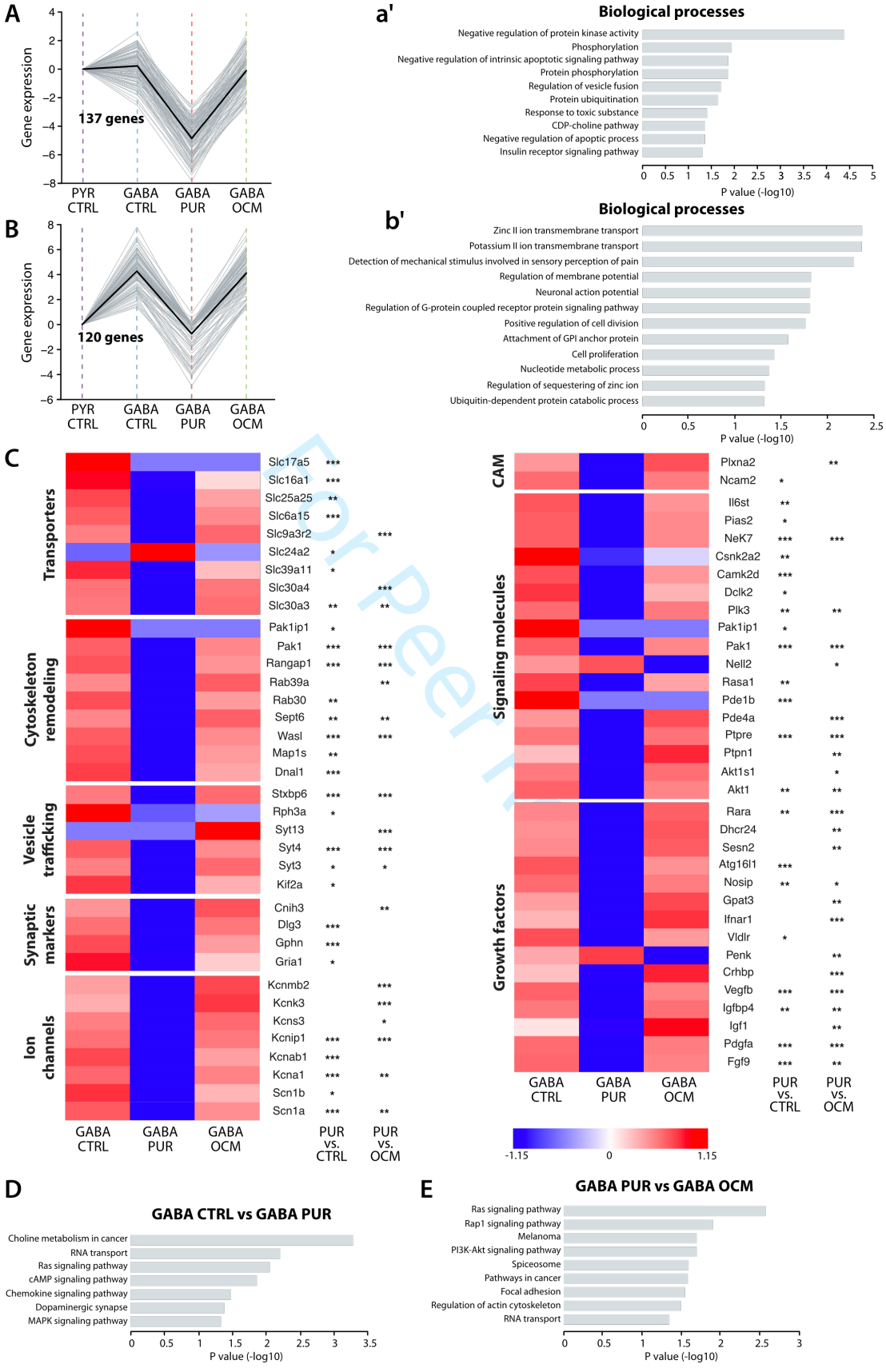

Figure 8: Gene ontology analysis of regulated genes. (A, B) Expression within clusters with a

similar expression pattern in different culture conditions. Gene expression was normalized to that of pyramidal cells in control conditions. Cluster A and B comprise 137 and 120 genes, respectively. The continuous black line shows the mean of mRNA expression in different conditions. (a', b') Gene ontology analysis of biological processes for genes of clusters A and B. (C) Heatmap of mRNAs expressed differentially in different conditions for different classes of coded protein. (*$p < 0.05$, **$p < 0.01$, ***$p < 0.001$). Color intensity shows the Z-score for differential expression. (D, E) KEGG pathway analysis on regulated genes between GABA PUR versus GABA CTRL (D), and GABA PUR versus GABA OCM (E).

DISCUSSION

Data presented here suggests that factors released by oligodendrocytes modulate the transcriptome, electrical phenotype and morphology of GABAergic neurons. The absence of glial cells from purified neuron cultures reduced synaptic activity and action potential firing of GABAergic neurons and many genes were downregulated. Processes linked to these changes included synapse assembly, action potential generation and transmembrane ion transport. Our results should help identify some of the molecular targets by which oligodendrocytes modulate GABAergic neuron excitability and synaptic function.

A hippocampal culture model permits investigation of regulation of interneuron morphology, excitability and firing properties by oligodendroglial factors

This study was based on dissociated hippocampal cell cultures. Recordings were made from (i) glutamatergic and GABAergic neurons in the presence of glial cells (CTRL), (ii) GABAergic neurons in the absence of glial cells (PUR) and (iii), GABAergic neurons in cultures without glial cells but with added oligodendrocyte conditioned medium (OCM). Our data

showed (Fig. 2) GABAergic neurons in culture conserved properties, including a relatively depolarized resting potential, and action potentials of short duration followed by a prominent AHP, which distinguish them from hippocampal pyramidal cells (Spruston and Johnston 1992; Fricker et al. 1999; Staff et al. 2000; Hu et al. 2014; Prestigio et al. 2019).

The frequency of excitatory synaptic events impinging on hippocampal GABAergic neurons was strongly reduced in the absence of glial cells. This is consistent with data showing that glutamatergic synaptic transmission is enhanced by factors secreted by glia (Turko et al. 2019) including astrocytes (Baldwin and Eroglu 2017). Here we demonstrate that oligodendrocytes regulate synaptic excitation of GABAergic interneurons. Adding OCM to PUR cultures partly restored EPSC frequencies. Additional effects of OPC or astrocyte - released factors, as well as cell-cell contacts in CTRL culture may explain differences with OCM effect.

Anatomical analysis revealed that oligodendrocyte secreted factors (OCM) enhanced the complexity of dendritic arbors, although dendritic length differed little between cultures that did (CTRL) or did not (PUR) contain glial cells. Novel synapses formed on more complex dendrites in OCM cultures may contribute to the increased EPSC frequency in these conditions.

We found similar electrophysiological properties for GABAergic neurons grown in CTRL and OCM cultures, notably a low input resistance and high rheobase. Rheobase was reduced and AP firing frequency significantly depressed in PUR cultures. The PUR condition may be similar to a lack of maturation in some respect (Okaty et al., 2009) and our study may suggest that the maturation process depend on oligodendrocyte secreted factors. The phenotype of low intrinsic excitability corresponds to mature neurons expressing a large array of voltage dependent or independent ion channels. We show (see Figure 8C-E) that numerous transcripts coding for ion channels (notably Kv1.1, Nav1.1, Task-1) and also signaling factors belonging to the PI3K-Akt signaling pathway are up-regulated by oligodendrocyte released factors. Underlying molecular

mechanisms may rely on an indirect effect through glutamatergic neurotransmission via downstream signaling pathways (Sakry et al. 2014; Birey et al. 2015, Jang et al. 2019), and/or a cell autonomous mechanism (Favuzzi et al. 2017). Oligodendroglial factors may operate homeostatically so that neurons adapt their intrinsic excitability and spontaneous firing activity in cultures with dense synaptic connections (Desai et al. 1999).

We did not attempt to identify factors released by oligodendrocytes, and their precursor cells, which mediated the effects of OCM on GABAergic neurons. Candidate molecules may include the proteoglycan NG2 (Sakry et al. 2014), FGF2 (Birey et al. 2015), or BDNF (Jang et al. 2019) which modulate glutamatergic neurotransmission on pyramidal cells but their effects on GABAergic neurons are not known. Multiple glial factors could affect optimal survival and maturation of CNS neurons, although the precise identity and combination of factors may differ depending on neuronal type and age (Meyer-Franke et al., 1995; Goldberg and Barres, 2000; Wilkins et al., 2003). We previously showed that Contactin-1 together with Phosphacan or Tenascin-R secreted by oligodendrocytes mediate early formation of prenodal clusters along hippocampal GABAergic axons likely through a direct clustering effect (Dubessy et al., 2019). In addition to its role in prenodal clustering, Contactin-1 also plays important role in the hippocampus, in synaptic plasticity, neurogenesis, and memory in adult mice (Murai et al., 2002; Puzzo D et al., 2013). It would be worth examining the role of Contactin-1 in regulating specific gene expression in GABAergic neurons. Cell adhesion molecules and extracellular matrix proteins secreted by oligodendrocytes also form perinodal and perineuronal complexes that transmit signals to neurons which could influence their physiology and connectivity (Favuzzi et al. 2017; Fawcett, Oohashi and Pizzorusso 2019).

Technical points

This work combined patch clamp recordings with single neuron RNA-seq analysis. Relatively few studies have demonstrated strong correlations between single-neuron transcriptomic profiles and electrophysiological phenotypes (Cadwell et al. 2016; Földy et al. 2016; Fuzik et al. 2016; Muñoz-Manchado et al. 2018; Scala et al. 2019). We took several steps to ensure and verify the validity of our results. The duration of patch electrode recordings was deliberately limited to ~10 min in order to minimize perturbation of the transcriptome (Fuzik et al. 2016). When possible, patch electrodes targeted isolated neuronal somata to reduce possible mRNA contamination from adjacent cells (Tripathy et al. 2017).

As for previously published single-cell RNAseq datasets, the number of sequenced reads per cell was found to be positively correlated with detected transcript counts and did not reach a plateau (Cadwell et al. 2016; Tasic et al. 2016; Tripathy et al. 2017). We attempted to validate our data by cross-correlating transcripts detected for recorded pyramidal and inhibitory neurons with expected profiles for these cell types. Most GABAergic neurons expressed molecular markers, including peptides and Ca-binding proteins, specific to known subclasses of these cells (Zeisel et al. 2015; Gouwens et al. 2020). Larger numbers of sequenced cells would have permitted enhanced statistics to assure data quality even if links between specific transcripts and identified cell types tends to support our approach.

Single neuron transcriptomes obtained in this way helped us define a global view of processes initiated by oligodendrocyte conditioned medium. They showed glial factors modify the transcriptome of GABAergic neurons to change intrinsic electrophysiological properties, AP generation, EPSC frequencies and dendritic anatomy.

Gene expression in hippocampal neuron types

Transcriptomic data are defining the classification of cortical neurons (Zeisel et al. 2015; Cembrowski et al. 2016; Harris et al. 2018; Sugino et al. 2019; Yuste et al. 2020). A recent study based on Patch-seq data from several 1000s of cells may offer the best current correspondence between transcriptomic, anatomical and electrophysiological data for GABAergic mouse cortical neurons (Gouwens et al. 2020). Our data can be interpreted in the light of those studies. Most GABAergic neurons studied in the hippocampal cultures studied here expressed Somatostatin (SST) associated with other peptide markers. Several subtypes of hippocampal inhibitory cells express SST including long-range inhibitory neurons which possess myelinated axons (and also express *Calbindin* and *Npy*), oriens-lacunosum moleculare (O-LM) interneurons (also *Elfn1* and *Pnoc*), or oriens-bistratified neurons (also *Tac1*, *Npy*, *Satb1* and *Erbb4*) (Somogyi and Klausberger 2005; Jinno 2009; Harris et al. 2018). We found some cells expressed genes for *Sst*, *Pnoc* and *Pvalb* (Jinno and Kosaka 2000; Jinno 2009; Harris et al. 2018). A minority of GABAergic neurons expressed genes for *Reelin* and *NPY* as do neurogliaform cells (Pelkey et al., 2017).

GABAergic neuron data revealed genes coding for proteins relevant to specific aspects of inhibitory cell physiology. They included Nav1.1 (*Scn1a*), Kv3.2 (*Kcnc2*) and Task-1(*Kcnk3*) in neurons with PV and/or SST genes (Chow et al. 1999; Torborg et al. 2006; Lorincz and Nusser 2008). Kv3 channels with fast kinetics curtail action potentials permitting sustained firing at high frequencies (Rudy and McBain 2001; Gu et al. 2018; Hu et al. 2018). Task-1 forms K^+ permeable leak channels which contribute to resting potential and membrane resistance (Okaty et al. 2009). We found high levels of genes for the zinc transporters, ZnT3 (*Slc30a3*) and ZnT4 (*Slc30a4*), which are found in SST-containing interneurons (Paul et al. 2017). ZnT3 is a vesicular transporter which may contribute to the co-release of zinc in synaptic vesicles with GABA (McAllister and Dyck 2017).

Correlation between gene expression and electrophysiological parameters

We attempted to link expression of genes for ion channels and neurotransmitter receptors with elements of electrophysiological phenotypes using a correlation-based analysis on data from different cell types and culture conditions. The analysis suggests genes for α1, ß1 and α3 subunits of the Na^+, K^+ -ATPase, *Atp1a1*, *Atp1b1* and *Atp1a3,* are linked to neuronal input resistance. The Na^+/K^+-ATPase maintains transmembrane ionic gradients and resting membrane thus affecting neuronal excitability (Larsen et al. 2016). The Na-channel subunit *Scn2a* (Nav1.2) was found to be correlated with action potential width, neuronal input resistance, and the membrane time constant, tau. A cluster including several K^+ channels (*Kcnc2*, *Kcnk3* and *Kcnip-1*) and two Zinc transporters (*Slc30a3 and Slc30a*), was expressed selectively in GABAergic neurons, and correlated with AP threshold, sag ratio and the after-hyperpolarization amplitude. We should note that these correlations do not imply causality and caution that class-driven correlations are an important confound in our dataset. Some within-cell-type correlations may have been missed (Bomkamp et al. 2019).

Biological processes affected by glial cells and oligodendroglial secreted factors

Clustering genes with similar patterns of altered expression revealed GO process terms regulated by factors in OCM. Processes identified in this way matched quite efficiently with changes in GABAergic neuron phenotype inferred from electrophysiological and anatomical observations. Enriched processes included synapse assembly, action potential generation, transmembrane transport of ions specifically zinc, and kinase signaling. They derived from differential expression of K^+ channel genes, including *Kcna1* (Kv1.1), *Kcnab1* (Kv ß1chain), *Kcnip1* (KChIP) and *Kcnk3* (Task-1), and Na^+ channel genes, including *Scn1a* (Nav1.1) and *Scn1b* (Nav ß1chain). We found two kinases which were upregulated in OCM. Nek7 is involved in microtubule polymerization during the formation of PV+ interneuron connections (Hinojosa et

al. 2018). In addition, we found that the PI3K-Akt, MAPK and AMPc signal transduction pathways are significantly up-regulated by OCM and glial cells. These signaling pathways control gene expression by phosphorylating a number of transcription factors and thus regulating their transcriptional activity. Previous studies have shown that these pathways are activated by oligodendrocytes secreted factors to exert their neuromodulatory functions on cultured neurons (Meyer-Franke et al. 1995; Wilkins et al. 2003). PIP3-Akt1-mTOR activation is critical for neuronal development, and notably for hippocampal function (Wang et al. 2003; Lai et al. 2006; Goebbels et al. 2017; Balu et al. 2012). It increases the caliber of axons and the expression of numerous genes encoding regulatory proteins, which might be sufficient to trigger all steps of myelination (Goebbels et al. 2017).

In conclusion, our study provides new insights into communication between glial cells and neurons showing that factors secreted by oligodendrocytes induce transcriptomic changes which may modulate the physiology and anatomy of hippocampal GABAergic neurons. Further study analyzing OCM effect on purified GABAergic neurons would allow to discriminate indirect effect via glutamatergic neurotransmission and cell-autonomous effect. In addition, it is now established that PV^+ neurons as well as some Sst^+ neurons with long range projections through the hippocampus and more distant regions are frequently myelinated (Jinno et al. 2007; Micheva et al. 2016; Stedehouder et al. 2017). It is fundamental to understand how OPCs and oligodendrocytes feedback to neurons and contribute to the assembly, maturation and myelination of cortical circuits during post-natal development. Moreover, CNS demyelination likely results in altered neuron-oligodendrocyte interactions, and this disruption might influence neuronal function and myelin repair capacity in demyelinating diseases such as multiple sclerosis. »

Acknowledgements

We thank Marie-Stéphane Aigrot and Loane Wallon, Claire Lovo from ICM Quant, Yannick Marie and Emeline Mundwiller from iGenSeq, and François-Xavier Lejeune from iCONICS, for technical support. We thank Bernard Zalc, Richard Miles and Anne Desmazieres for discussion and critical reading of the manuscript. This work was supported by the French MS research foundation ARSEP (Aide à la Recherche sur la Sclérose en Plaques), Bouvet-Labruyère prize to NSF, and Biogen funding to EM.

REFERENCES

Arancibia-Cárcamo IL, Ford MC, Cossell L, Ishida K, Tohyama K, Attwell D. 2017. Node of Ranvier length as a potential regulator of myelinated axon conduction speed. Elife. 6.

Baldwin KT, Eroglu C. 2017. Molecular mechanisms of astrocyte-induced synaptogenesis. Curr Opin Neurobiol. 45:113–120.

Balu DT, Carlson GC, Talbot K, Kazi H, Hill-Smith TE, Easton RM, Birnbaum MJ, Lucki I. 2012. Akt1 deficiency in schizophrenia and impairment of hippocampal plasticity and function. Hippocampus. 22:230-40.

Bates D, Mächler M, Bolker B, Walker S. 2015. Fitting Linear Mixed-Effects Models Using lme4. Journal of Statistical Software 67, 1–48.

Barres BA, Raff MC. 1993. Proliferation of oligodendrocyte precursor cells depends on electrical activity in axons. Nature. 361(6409):258–260.

Battefeld A, Klooster J, Kole MHP. 2016. Myelinating satellite oligodendrocytes are integrated in a glial syncytium constraining neuronal high-frequency activity. Nat Commun. 7:11298.

Bechler ME, Swire M, Ffrench-Constant C. 2018. Intrinsic and adaptive myelination-A sequential mechanism for smart wiring in the brain. Dev Neurobiol. 78:68–79.

Birey F, Kloc M, Chavali M, Hussein I, Wilson M, Christoffel DJ, Chen T, Frohman MA, Robinson JK, Russo SJ, Maffei A, Aguirre A. 2015. Genetic and Stress-Induced Loss of NG2 Glia Triggers Emergence of Depressive-like Behaviors through Reduced Secretion of FGF2. Neuron. 88:941–956.

Bomkamp C, Tripathy SJ, Bengtsson Gonzales C, Hjerling-Leffler J, Craig AM, Pavlidis P. 2019. Transcriptomic correlates of electrophysiological and morphological diversity within and across excitatory and inhibitory neuron classes. PLoS Comput Biol. 15:e1007113.

Bonetto G, Hivert B, Goutebroze L, Karagogeos D, Crépel V, Faivre-Sarrailh C. 2019. Selective Axonal Expression of the Kv1 Channel Complex in Pre-myelinated GABAergic Hippocampal Neurons. Front Cell Neurosci. 13:222.

Cadwell CR, Palasantza A, Jiang X, Berens P, Deng Q, Yilmaz M, Reimer J, Shen S, Bethge M, Tolias KF, Sandberg R, Tolias AS. 2016. Electrophysiological, transcriptomic and morphologic profiling of single neurons using Patch-seq. Nat Biotechnol. 34:199–203.

Cembrowski MS, Wang L, Sugino K, Shields BC, Spruston N. 2016. Hipposeq: a comprehensive RNA-seq database of gene expression in hippocampal principal neurons. Elife. 5:e14997.

Chow A, Erisir A, Farb C, Nadal MS, Ozaita A, Lau D, Welker E, Rudy B. 1999. K(+) channel expression distinguishes subpopulations of parvalbumin- and somatostatin-containing neocortical interneurons. J Neurosci. 19:9332–9345.

Demerens C, Stankoff B, Logak M, Anglade P, Allinquant B, Couraud F, Zalc B, Lubetzki C. 1996. Induction of myelination in the central nervous system by electrical activity. Proc Natl Acad Sci USA. 93(18):9887–9892.

Desai NJ, Rutherford LC and Turrigiano GG. 1999. Plasticity in the intrinsic excitability of cortical pyramidal neurons. Nat Neurosci. 2(6):515-520.

Dobin A, Davis CA, Schlesinger F, Drenkow J, Zaleski C, Jha S, Batut P, Chaisson M, Gingeras TR. 2013. STAR: ultrafast universal RNA-seq aligner. Bioinformatics. 29:15–21.

Dubessy A-L, Mazuir E, Rappeneau Q, Ou S, Abi Ghanem C, Piquand K, Aigrot M-S, Thétiot M, Desmazières A, Chan E, Fitzgibbon M, Fleming M, Krauss R, Zalc B, Ranscht B, Lubetzki C, Sol-Foulon N. 2019. Role of a Contactin multi-molecular complex secreted by oligodendrocytes in nodal protein clustering in the CNS. Glia. 67:2248–2263.

Favuzzi E, Marques-Smith A, Deogracias R, Winterflood CM, Sanchez-Aguilera A, Mantoan L, Maeso P, Fernandes C, Ewers H, Rico B. 2017. Activity-dependent gating of parvalbumin interneuron function by the perineuronal net protein brevican. Neuron. 95(3):639-655.

Fawcett JW, Oohashi T and Pizzorusso T 2019. The roles of perineuronal nets and the perinodal extracellular matrix in neuronal function. Nat Rev Neurosci. 20: 451-465.

Földy C, Darmanis S, Aoto J, Malenka RC, Quake SR, Südhof TC. 2016. Single-cell RNAseq reveals cell adhesion molecule profiles in electrophysiologically defined neurons. Proc Natl Acad Sci USA. 113:E5222-5231.

Freeman SA, Desmazières A, Fricker D, Lubetzki C, Sol-Foulon N. 2016. Mechanisms of sodium channel clustering and its influence on axonal impulse conduction. Cell Mol Life Sci. 73:723–735.

Freeman SA, Desmazières A, Simonnet J, Gatta M, Pfeiffer F, Aigrot MS, Rappeneau Q, Guerreiro S, Michel PP, Yanagawa Y, Barbin G, Brophy PJ, Fricker D, Lubetzki C, Sol-Foulon N. 2015. Acceleration of conduction velocity linked to clustering of nodal components precedes myelination. Proc Natl Acad Sci USA. 112:E321-328.

Fricker D, Verheugen JA, Miles R. 1999. Cell-attached measurements of the firing threshold of rat hippocampal neurones. J Physiol. 517:791–804.

Frühbeis C, Fröhlich D, Kuo WP, Amphornrat J, Thilemann S, Saab AS, Kirchhoff F, Möbius W, Goebbels S, Nave K-A, Schneider A, Simons M, Klugmann M, Trotter J, Krämer-Albers EM. 2013. Neurotransmitter-triggered transfer of exosomes mediates oligodendrocyte-neuron communication. PLoS Biol. 11:e1001604.

Fünfschilling U, Supplie LM, Mahad D, Boretius S, Saab AS, Edgar J, Brinkmann BG, Kassmann CM, Tzvetanova ID, Möbius W, Diaz F, Meijer D, Suter U, Hamprecht B, Sereda MW, Moraes CT, Frahm J, Goebbels S, Nave KA. 2012. Glycolytic oligodendrocytes maintain myelin and long-term axonal integrity. Nature. 485:517–521.

Fuzik J, Zeisel A, Máté Z, Calvigioni D, Yanagawa Y, Szabó G, Linnarsson S, Harkany T. 2016. Integration of electrophysiological recordings with single-cell RNA-seq data identifies neuronal subtypes. Nat Biotechnol. 34:175–183.

Goebbels S, Wieser GL, Pieper A, Spitzer S, Weege B, Yan K, Edgar JM, Yagensky O, Wichert SP, Agarwal A, Karram K, Renier N, Tessier-Lavigne M, Rossner MJ, Káradóttir RT, Nave KA. 2017. A neuronal PI(3,4,5)P3-dependent program of oligodendrocyte precursor recruitment and myelination. Nat Neurosci. 20:10–15.

Goldberg JL and Barres BA. 2000. The relationship between neuronal survival and regeneration. Annu Rev Neurosci. 23: 579-612.

Gouwens NW, Sorensen SA, Baftizadeh F, Budzillo A, Lee BR, Jarsky T, Alfiler L, Arkhipov A, Baker K, Barkan E, et al. 2020. Integrated morphoelectric and transcriptomic classification of cortical GABAergic cells. Cell. 183(4):935-953.e19.

Gu Y, Servello D, Han Z, Lalchandani RR, Ding JB, Huang K, Gu C. 2018. Balanced Activity

between Kv3 and Nav Channels Determines Fast-Spiking in Mammalian Central Neurons. iScience. 9:120–137.

Hu H, Gan J, Jonas P 2014. Interneurons. Fast-spiking, parvalbumin^{+} GABAergic interneurons: from cellular design to microcircuit function. Science. 345: 1255263.

Harris KD, Hochgerner H, Skene NG, Magno L, Katona L, Bengtsson Gonzales C, Somogyi P, Kessaris N, Linnarsson S, Hjerling-Leffler J. 2018. Classes and continua of hippocampal CA1 inhibitory neurons revealed by single-cell transcriptomics. PLoS Biol. 16:e2006387.

Hinojosa AJ, Deogracias R, Rico B. 2018. The Microtubule Regulator NEK7 Coordinates the Wiring of Cortical Parvalbumin Interneurons. Cell Rep. 24:1231–1242.

Hu H, Roth FC, Vandael D, Jonas P. 2018. Complementary Tuning of Na+ and K+ Channel Gating Underlies Fast and Energy-Efficient Action Potentials in GABAergic Interneuron Axons. Neuron. 98:156-165.e6.

Huang DW, Sherman BT, Tan Q, Collins JR, Alvord WG, Roayaei J, Stephens R, Baseler MW, Lane HC, Lempicki RA. 2007. The DAVID Gene Functional Classification Tool: a novel biological module-centric algorithm to functionally analyze large gene lists. Genome Biol. 8: R183.

Huang L-W, Simonnet J, Nassar M, Richevaux L, Lofredi R, Fricker D. 2017. Laminar Localization and Projection-Specific Properties of Presubicular Neurons Targeting the Lateral Mammillary Nucleus, Thalamus, or Medial Entorhinal Cortex. eNeuro. 4:0370-16 .

Jang M, Gould E, Xu J, Kim EJ, Kim JH. 2019. Oligodendrocytes regulate presynaptic properties and neurotransmission through BDNF signaling in the mouse brainstem. Elife. 8:e42156.

Jinno S, Kosaka T. 2000. Colocalization of parvalbumin and somatostatin-like immunoreactivity in the mouse hippocampus: Quantitative analysis with optical disector. The J Comp Neurol. 428:377–388.

Jinno S, Klausberger T, Marton LF, Dalezios Y, Roberts JD, Fuentealba P, Bushong EA, Henze D, Buzsaki G, Somogyi P. 2007. Neuronal diversity in GABAergic long-range projections from the hippocampus. J Neurosci. 27:8790-804.

Jinno S. 2009. Structural organization of long-range GABAergic projection system of the hippocampus. Front Neuroanat. 3:13.

Kaplan MR, Meyer-Franke A, Lambert S, Bennett V, Duncan ID, Levinson SR, Barres BA. 1997. Induction of sodium channel clustering by oligodendrocytes. Nature. 386:724–728.

Lai W-S, Xu B, Westphal KGC, Paterlini M, Olivier B, Pavlidis P, Karayiorgou M, Gogos JA. 2006. Akt1 deficiency affects neuronal morphology and predisposes to abnormalities in prefrontal cortex functioning. Proc Natl Acad Sci USA. 103:16906–16911.

Larsen BR, Stoica A, MacAulay N. 2016. Managing Brain Extracellular K(+) during Neuronal Activity: The Physiological Role of the Na(+)/K(+)-ATPase Subunit Isoforms. Front Physiol. 7:141.

Lee Y, Morrison BM, Li Y, Lengacher S, Farah MH, Hoffman PN, Liu Y, Tsingalia A, Jin L, Zhang P-W, Pellerin L, Magistretti PJ, Rothstein JD. 2012. Oligodendroglia metabolically support axons and contribute to neurodegeneration. Nature. 487:443–448.

Lorincz A, Nusser Z. 2008. Cell-type-dependent molecular composition of the axon initial segment. J Neurosci. 28:14329–14340.

Love MI, Huber W, Anders S. 2014. Moderated estimation of fold change and dispersion for RNA-seq data with DESeq2. Genome Biol. 15:550.

Mazuir E, Dubessy A-L, Wallon L, Aigrot M-S, Lubetzki C, Sol-Foulon N. 2020. Generation of Oligodendrocytes and Oligodendrocyte-Conditioned Medium for Co-Culture Experiments. J Vis Exp. (156).

McAllister BB, Dyck RH. 2017. Zinc transporter 3 (ZnT3) and vesicular zinc in central nervous system function. Neurosci Biobehav Rev. 80:329–350.

McCarthy KD, de Vellis J. 1980. Preparation of separate astroglial and oligodendroglial cell cultures from rat cerebral tissue. J Cell Biol. 85:890–902.

McKenzie IA, Ohayon D, Li H, de Faria JP, Emery B, Tohyama K, Richardson WD. 2014. Motor skill learning requires active central myelination. Science. 346:318–322.

Meyer-Franke A, Kaplan MR, Pfrieger FW, Barres BA. 1995. Characterization of the signaling interactions that promote the survival and growth of developing retinal ganglion cells in culture. Neuron. 15:805-819.

Micheva KD, Wolman D, Mensh BD, Pax E, Buchanan J, Smith SJ, Bock DD. 2016. A large fraction of neocortical myelin ensheathes axons of local inhibitory neurons. eLife. 5:e15784.

Monje M. 2018. Myelin Plasticity and Nervous System Function. Annu Rev Neurosci. 41:61–76.

Muñoz-Manchado AB, Bengtsson Gonzales C, Zeisel A, Munguba H, Bekkouche B, Skene NG, Lönnerberg P, Ryge J, Harris KD, Linnarsson S, Leffler JH. 2018. Diversity of Interneurons in the Dorsal Striatum Revealed by Single-Cell RNA Sequencing and PatchSeq. Cell Rep. 24:2179-2190.e7.

Murai KK, Misner D, Ranscht B. 2002. Contactin supports synaptic plasticity associated with hippocampal long-term depression but not potentiation. Curr Biol. 12(3):181-191.

Noli L, Capalbo A, Ogilvie C, Khalaf Y, Ilic D. 2015. Discordant Growth of Monozygotic Twins Starts at the Blastocyst Stage: A Case Study. Stem Cell Reports. 5:946–953.

Okaty BW, Miller MN, Sugino K, Hempel CM, Nelson SB. 2009. Transcriptional and electrophysiological maturation of neocortical fast-spiking GABAergic interneurons. J Neurosci.

29:7040–7052.

Paul A, Crow M, Raudales R, He M, Gillis J, Huang ZJ. 2017. Transcriptional Architecture of Synaptic Communication Delineates GABAergic Neuron Identity. Cell. 171:522-539.e20.

Pelkey KA, Chittajallu R, Craig MT, Tricoire L, Wester JC, McBain CJ. 2017. Hippocampal GABAergic Inhibitory Interneurons. Physiol Rev. 97:1619–1747.

Prestigio C, Ferrante D, Valente P, Casagrande S, Albanesi E, Yanagawa Y, Benfenati F, Baldelli P. 2019. Spike-related electrophysiological identification of cultured hippocampal excitatory and inhibitory neurons. Mol. Neurobiol. 56(9):6276-6292.

Puzzo D, Bizzoca A, Privitera L, Furnari D, Giunta S, Girolamo F, Pinto M, Gennarini G, Palmeri A. 2013. F3/Contactin promotes hippocampal neurogenesis, synaptic plasticity, and memory in adult mice. Hippocampus. 23(12):1367-82.

Qiu S, Luo S, Evgrafov O, Li R, Schroth GP, Levitt P, Knowles JA, Wang K. 2012. Single-neuron RNA-Seq: technical feasibility and reproducibility. Front Genet. 3:124.

Rudy B, McBain CJ. 2001. Kv3 channels: voltage-gated K+ channels designed for high-frequency repetitive firing. Trends Neurosci. 24:517–526.

Saab AS, Tzvetavona ID, Trevisiol A, Baltan S, Dibaj P, Kusch K, Möbius W, Goetze B, Jahn HM, Huang W, Steffens H, Schomburg ED, Pérez-Samartín A, Pérez-Cerdá F, Bakhtiari D, Matute C, Löwel S, Griesinger C, Hirrlinger J, Kirchhoff F, Nave KA. 2016. Oligodendroglial NMDA Receptors Regulate Glucose Import and Axonal Energy Metabolism. Neuron. 91:119–132.

Sakry D, Neitz A, Singh J, Frischknecht R, Marongiu D, Binamé F, Perera SS, Endres K, Lutz B, Radyushkin K, Trotter J, Mittmann T. 2014. Oligodendrocyte precursor cells modulate the neuronal network by activity-dependent ectodomain cleavage of glial NG2. PLoS Biol. 12(11):e1001993.

Sakry D, Yigit H, Dimou L, Trotter J. 2015. Oligodendrocyte precursor cells synthesize neuromodulatory factors. PLoS ONE. 10:e0127222.

Scala F, Kobak D, Shan S, Bernaerts Y, Laturnus S, Cadwell CR, Hartmanis L, Froudarakis E, Castro JR, Tan ZH, Papadopoulos S, Patel SS, Sandberg R, Berens P, Jiang X, Tolias AS. 2019. Layer 4 of mouse neocortex differs in cell types and circuit organization between sensory areas. Nat Commun. 10:4174.

Seidl AH. 2014. Regulation of conduction time along axons. Neuroscience. 276:126–134.

Sherman DL, Brophy PJ. 2005. Mechanisms of axon ensheathment and myelin growth. Nat Rev Neurosci. 6:683–690.

Somogyi P, Klausberger T. 2005. Defined types of cortical interneurone structure space and spike timing in the hippocampus. J Physiol. 562:9–26.

Spruston N, Johnston D. 1992. Perforated patch-clamp analysis of the passive membrane properties of three classes of hippocampal neurons. J Neurophysiol. 67:508–529.

Staff NP, Jung HY, Thiagarajan T, Yao M, Spruston N. 2000. Resting and active properties of pyramidal neurons in subiculum and CA1 of rat hippocampus. J Neurophysiol. 84: 2398-2408.

Stedehouder J, Couey JJ, Brizee D, Hosseini B, Slotman JA, Dirven CMF, Shpak G, Houtsmuller AB, Kushner SA. 2017. Fast-spiking parvalbumin interneurons are frequently myelinated in the cerebral cortex of mice and humans. Cereb. Cortex. 27: 5001-5013.

Stedehouder J, Brizee D, Shpak G, Kushner SA. 2018. Activity-Dependent Myelination of Parvalbumin Interneurons Mediated by Axonal Morphological Plasticity. J Neurosci. 38:3631–3642.

Sugino K, Clark E, Schulmann A, Shima Y, Wang L, Hunt DL, Hooks BM, Tränkner D, Chandrashekar J, Picard S, Lemire AL, Spruston N, Hantman AW Nelson SB. 2019. Mapping the

transcriptional diversity of genetically and anatomically defined cell populations in the mouse brain. Elife. 8:e38619.

Tasic B, Menon V, Nguyen TN, Kim TK, Jarsky T, Yao Z, Levi B, Gray LT, Sorensen SA, Dolbeare T, Bertagnolli D, Goldy J, Shapovalova N, Parry S, Lee C, Smith K, Bernard A, Madisen L, Sunkin SM, Hawrylycz M, Koch C, Zeng H. 2016. Adult mouse cortical cell taxonomy revealed by single cell transcriptomics. Nat Neurosci. 19:335–346.

Torborg CL, Berg AP, Jeffries BW, Bayliss DA, McBain CJ. 2006. TASK-like conductances are present within hippocampal CA1 stratum oriens interneuron subpopulations. J Neurosci. 26:7362–7367.

Tripathy SJ, Toker L, Li B, Crichlow C-L, Tebaykin D, Mancarci BO, Pavlidis P. 2017. Transcriptomic correlates of neuron electrophysiological diversity. PLoS Comput Biol. 13:e1005814.

Turko P, Groberman K, Browa F, Cobb S, Vida I. 2019. Differential Dependence of GABAergic and Glutamatergic Neurons on Glia for the Establishment of Synaptic Transmission. Cereb Cortex. 29:1230–1243.

Uematsu M, Hirai Y, Karube F, Ebihara S, Kato M, Abe K, Obata K, Yoshida S, Hirabayashi M, Yanagawa Y, Kawaguchi Y. 2008. Quantitative chemical composition of cortical GABAergic neurons revealed in transgenic venus-expressing rats. Cereb Cortex. 18(2):315–330.

Wang Q, Liu L, Pei L, Ju W, Ahmadian G, Lu J, Wang Y, Liu F, Wang YT. 2003. Control of synaptic strength, a novel function of Akt. Neuron. 38:915–928.

Wickham H. 2016. Ggplot2: Elegant Graphics for Data Analysis. Springer-Verlag New York. ISBN 978-3-319-24277-4

Wilkins A, Chandran S, Compston A. 2003. Oligodendrocytes promote neuronal survival and axonal length by distinct intracellular mechanisms: a novel role for oligodendrocyte-derived glial cell line-derived neurotrophic factor. J Neurosci. 23(12):4967-74.

Wilson MD, Sethi S, Lein PJ, Keil KP. 2017. Valid statistical approaches for analyzing sholl data: Mixed effects versus simple linear models. J Neurosci Methods. 279:33–43.

Xin W, Mironova YA, Shen H, Marino RAM, Waisman A, Lamers WH, Bergles DE, Bonci A. 2019. Oligodendrocytes Support Neuronal Glutamatergic Transmission via Expression of Glutamine Synthetase. Cell Rep. 27:2262-2271.e5.

Yuste R, Hawrylycz M, Aalling N, Aguilar-Valles A, Arendt D, Arnedillo RA, Ascoli GA, Bielza C, Bokharaie V, Bergmann TB, et al. 2020. A community-based transcriptomics classification and nomenclature of neocortical cell types. Nat Neurosci. PMID: 32839617.

Zeisel A, Muñoz-Manchado AB, Codeluppi S, Lönnerberg P, La Manno G, Juréus A, Marques S, Munguba H, He L, Betsholtz C, Rolny C, Castelo-Branco G, Hjerling-Leffler J, Linnarsson S. 2015. Brain structure. Cell types in the mouse cortex and hippocampus revealed by single-cell RNA-seq. Science. 347:1138–1142.

Supplementary material

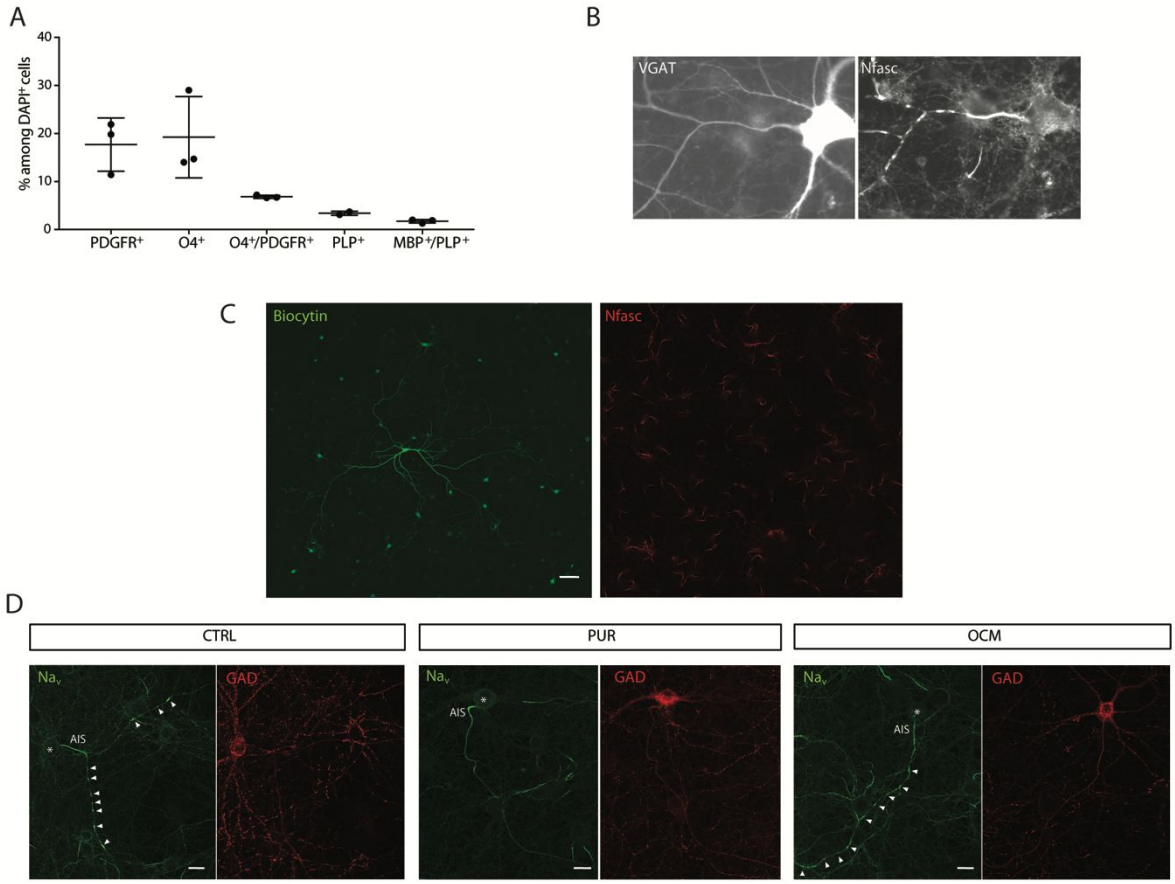

Sup. Figure 1: (A) Quantification of oligodendroglial cell phenotype in CTRL hippocampal cultures depending on positivity of PDGFR, O4, PLP and MBP. n=3 different cultures; mean ± SEM; between 1,500 to 2,000 cells were counted on acquired images for each staining and in each experiment. (**B**) Image from OCM culture, incubated with Nfasc Ab directly coupled with Alexa594, before patch-clamp recordings. Fluorescent GABAergic neuron (VGAT-venus) with Nfasc staining showing axon initial segment and prenodal clusters along axon. (**C**) Nfasc staining (in red) on fixed OCM culture, corresponding to reconstruction of neuronal morphology of a biocytin injected neuron (in green). Scale bar: 100 µm (**D**) Immunostainings of mixed hippocampal neurons (CTRL) and purified neurons in the absence (PUR) or presence of OCM (OCM), at 17 DIV. Na_v is in green and GAD67 in red. Nav clusters (indicated by

arrows) are formed along hippocampal GABAergic axons (identified by the presence of the axon initial segment (AIS)) in CTRL and OCM cultures. Scale bar: 20 µm

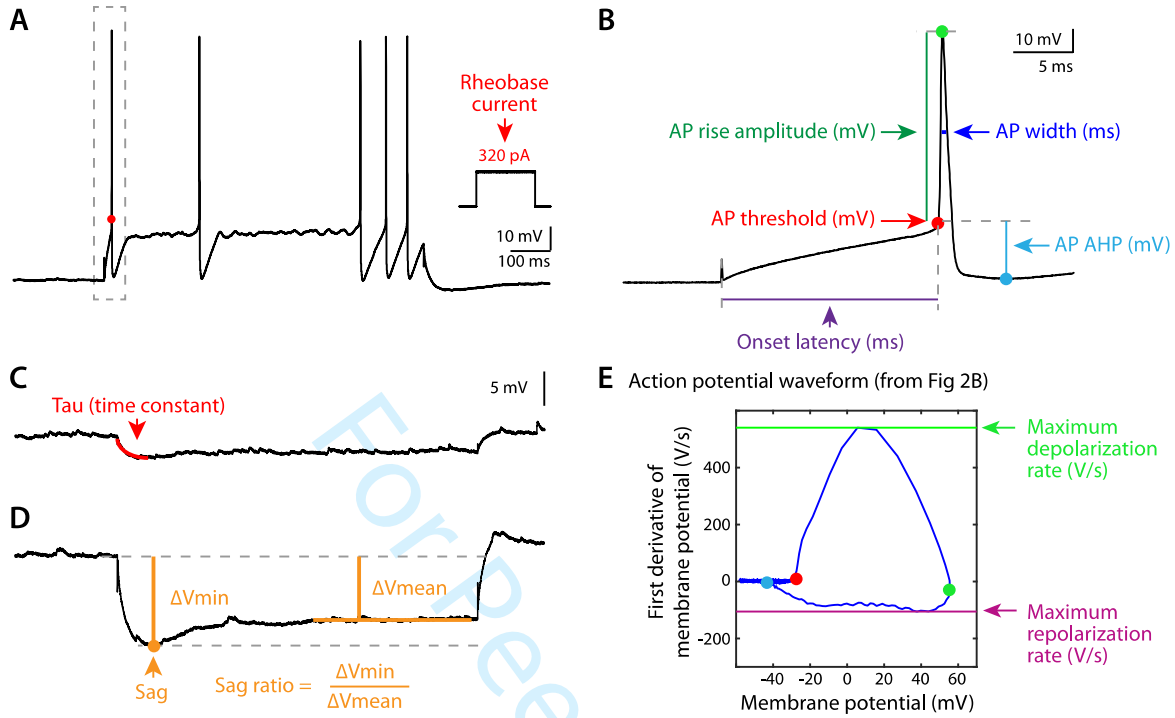

Sup. Figure 2: (A) Voltage response of an inhibitory cell to rheobase injected current, the minimal intensity needed to initiate an action potential (AP). In this example, rheobase is 320 pA. The AP voltage threshold is defined as the point at the foot of the first AP where dV/dt exceeds 30 mV/ms, indicated by a red dot. **(B)** The first AP at rheobase (dashed grey area from **A)**. The following measures of active neuronal properties presented in **Fig. 1** and **2** are derived from analysis of this waveform: Onset latency (purple line), AP threshold (red dot), AP rise amplitude (green line), AP width (dark blue line), AP afterhyperpolarization (AHP, light blue dot and line). Green point represents AP peak. **(C)** The membrane time constant (Tau) is the shorter time constant determined by fitting a double exponential function to a membrane response (-10 mV frombaseline) to a small hyperpolarizing current. **(D)** Sag ratio is related to the I_h current. Measures of the ratio between ΔVmin and ΔVmean were made on three consecutive traces where the steady state voltage during the second half of the hyperpolarizing

pulse was close to -100mV. ΔVmin is the difference between the minimal potential reached during of the first part of the hyperpolarizing step and the baseline (ΔVmin). ΔVmean is the difference between the mean potential during the second part of the step and the baseline (ΔVmean). **(E)** Phase plot representation of the first action potential at rheobase, as the first derivative of membrane potential against membrane potential. Dots indicate membrane potential parameters as in **(B):** the derivative increases from the threshold (red dot) to maximum depolarization rate (maximum slope of AP depolarization, green line) and then decreases to the AP peak (green dot). After peak, the derivative decreases to reach the maximum repolarization rate (maximum slope of AP repolarization) and then further to AP AHP (blue dot), the most negative voltage point of the AP waveform.

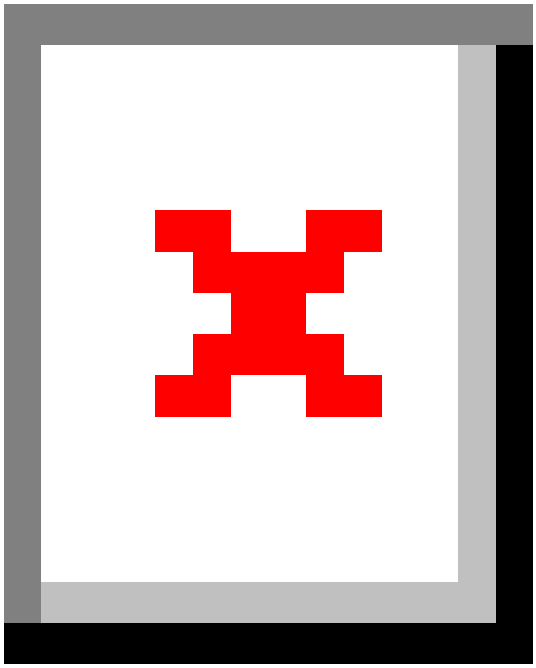

Sup. Figure 3: (A) Overview of transcript library preparation. Cytosol content was extracted from hippocampal neurons by a patch pipette. SMART-Seq v4 technology was used for mRNA capture, reverse transcription and cDNA amplification. Full-length cDNA was processed with the Nextera XT DNA Library Preparation Kit from Illumina to generate multiplex sequencing libraries. Next-generation sequencing was used to produce libraries with the Illumina NextSeq500 after a 2x75bp paired end sequencing. **(B)** Bioinformatic pipeline of scRNASeq data treatment. Each step is shown (left column) together with the tool used (right column). **(C)**

Number of expressed genes plotted against the number of uniquely mapped reads. (R^2=0.79 all samples, R^2= 0.57, selected samples). Black symbols represent cells that passed quality control and grey symbols cells which failed quality control. Circles represent pyramidal neurons under CTRL conditions, squares GABAergic neurons under CTRL conditions. GABAergic neurons in purified neuron cultures are shown in red and in purified neuron cultures treated with OCM in green. **(D)** Mapping statistics of reads for each sample (top, quality control passed, bottom, quality control failed). **(E)** Distribution of reads of transcripts with different origins for each sample (top, quality control passed, bottom, quality control failed).

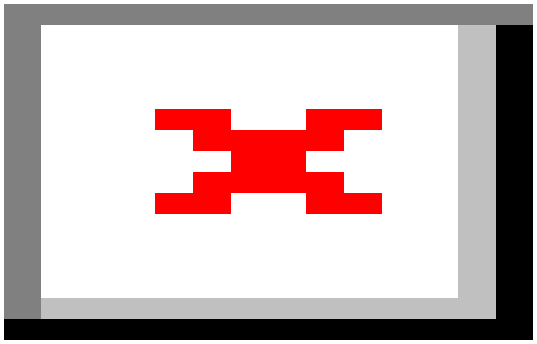

Sup. Figure 4: Comparison of distributions for genes expressed (representative example, sample 34, PYR) within noncoding regions (intergenic, black) and coding regions. Genes were not detected when their expression fell within 98% of intergenic regions. In this case, *Scn1b* and *Kcnc1* were considered to be expressed while *Bsn* was not.

Sup. Figure 5: Lists of regulated genes in the different comparisons, PYR vs GABA CTRL (1), GABA PUR vs GABA CTRL (2), GABA PUR vs GABA OCM (3), GABA OCM vs GABA CTRL (4)

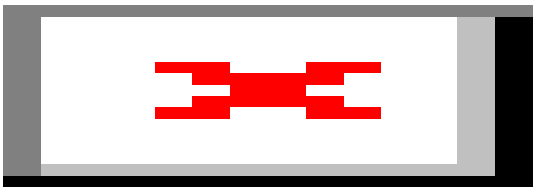

Sup. Figure 6: Expression of genes in a cluster with similar expression pattern in different culture conditions. Gene expression was normalized to that of pyramidal cells in control conditions. The number of genes for each cluster is indicated. The continuous black line shows the mean gene expression in different culture conditions.

List of the 326 Regulated Genes (Fold-change ≥ 1,

FAST DB STABLE ID	Gene Symbol	Regulation	Fold-Change
GSRG0000560	Slc17a7	up	16918.32
GSRG0002948	Prkcg	up	4642.46
GSRG0026715	Nfkbia	up	2981.33
GSRG0002531	Sgk1	up	922.89
GSRG0013623	Spry4	up	423.62
GSRG0015016	Spata2L	up	203.79
GSRG0017766	Cd24	up	138.50
GSRG0022848	Neurod6	up	97.83
GSRG0025424	Nasp	up	86.28
GSRG0012842	Hist1h4b	up	75.27
GSRG0024955	Slc24a2	up	52.13
GSRG0013303	--	up	51.72
GSRG0009687	Zfp238	up	44.96
GSRG0019546	--	up	41.11
GSRG0022863	Snca	up	40.84
GSRG0015022	Ccsap	up	35.58
GSRG0024940	--	up	28.64
GSRG0009994	Rgs4	up	21.49
GSRG0013681	Rbm22	up	20.40
GSRG0023849	Rpl7	up	4.92
GSRG0018804	Gad1	down	16727.68
GSRG0033108	Dner	down	5724.64
GSRG0034492	Uba1	down	4160.43
GSRG0015557	Sv2a	down	3253.04
GSRG0012231	Spock3	down	3071.60
GSRG0022680	--	down	2324.87
GSRG0006308	Kcnip1	down	2234.85
GSRG0007991	Pom121	down	2018.75
GSRG0020026	Slc32a1	down	1852.63
GSRG0036252	Brix1	down	1841.54
GSRG0032304	Nabp1	down	1658.96
GSRG0013772	Neto1	down	1625.89
GSRG0011717	Pnoc	down	1609.67
GSRG0021375	Nxph1	down	1478.22
GSRG0036488	Deaf1	down	1396.69
GSRG0015089	Ankrd34b	down	1394.61
GSRG0020659	Pdhx	down	1319.10
GSRG0004821	Vegfb	down	1306.99
GSRG0023056	Sfxn5	down	1283.91
GSRG0015402	Kcnab1	down	1270.91
GSRG0005815	Igfbp4	down	1057.25

GSRG0015667	Extl2	down	987.69
GSRG0028182	Csdc2	down	973.27
GSRG0029722	Slc38a1	down	968.97
GSRG0031867	Slc17a5	down	953.13
GSRG0002264	Smc3	down	936.04
GSRG0000412	Atp5sl	down	922.17
GSRG0026695	Stxbp6	down	877.20
GSRG0009858	Nek7	down	870.48
GSRG0010407	Vstm2a	down	839.95
GSRG0029946	--	down	821.59
GSRG0006796	Ormdl3	down	818.47
GSRG0015289	Usp13	down	806.73
GSRG0030658	Gria4	down	791.02
GSRG0024321	Meaf6	down	746.53
GSRG0024467	Casp9	down	746.17
GSRG0023359	Wnt7a	down	723.15
GSRG0023969	Nfx1	down	710.03
GSRG0014272	Fam210a	down	694.05
GSRG0012763	Sirt5	down	629.95
GSRG0024969	Elavl2	down	617.75
GSRG0015701	Camk2d	down	609.79
GSRG0028286	Letmd1	down	580.97
GSRG0034591	Ap1s2	down	574.99
GSRG0022888	Tgoln2	down	569.64
GSRG0029330	Lynx1	down	550.47
GSRG0011067	Med4	down	543.22
GSRG0021798	Slc6a1	down	522.99
GSRG0009613	Creg1	down	518.93
GSRG0033044	Lancl1	down	518.67
GSRG0011989	Tenm3	down	503.97
GSRG0006834	Nt5c3b	down	495.39
GSRG0010011	Pcp4l1	down	485.28
GSRG0011506	Zfp385d	down	457.15
GSRG0006857	Aarsd1	down	446.91
GSRG0001759	Ubfd1	down	431.53
GSRG0032453	Neu2	down	418.98
GSRG0029596	Rps19bp1	down	411.93
GSRG0014616	Cntnap4	down	406.45
GSRG0005831	Tubg2	down	406.34
GSRG0024218	Rab3b	down	399.77
GSRG0000359	Pnmal2	down	391.86
GSRG0016396	Glrb	down	388.02
GSRG0024704	Tstd3	down	383.90
GSRG0015615	Slc16a1	down	368.12
GSRG0024749	--	down	357.24
GSRG0010809	Pno1	down	353.48

GSRG0025990	Ap4s1	down	352.86
GSRG0008103	Rnf10	down	352.55
GSRG0029606	Rangap1	down	350.02
GSRG0021638	LRRTM1	down	347.45
GSRG0020416	--	down	347.38
GSRG0012470	Lman2	down	345.79
GSRG0029369	MGC94207	down	343.91
GSRG0023833	Amn1	down	339.41
GSRG0025855	Lbh	down	326.88
GSRG0027460	Mbd3	down	325.80
GSRG0000256	Tfpt	down	325.69
GSRG0002201	--	down	323.84
GSRG0003572	--	down	319.24
GSRG0004950	Ranbp6	down	316.28
GSRG0020147	Zgpat	down	313.15
GSRG0010749	Drg1	down	305.45
GSRG0007852	Mcoln1	down	305.15
GSRG0012440	Agtpbp1	down	305.05
GSRG0032457	Dgkd	down	297.20
GSRG0004958	Sgms1	down	274.55
GSRG0034043	Arx	down	273.79
GSRG0008042	Abcb9	down	272.04
GSRG0032237	Ccdc115	down	268.62
GSRG0013915	Cep120	down	266.68
GSRG0014676	Cdk10	down	265.50
GSRG0034650	Eif2s3	down	253.31
GSRG0023848	Stau2	down	247.94
GSRG0030119	Bace1	down	245.66
GSRG0004927	Fam189a2	down	245.13
GSRG0029709	Slc2a13	down	241.64
GSRG0036721	Tes	down	230.92
GSRG0031432	RGD1309779	down	222.68
GSRG0030208	Rpp25	down	219.90
GSRG0035015	--	down	215.07
GSRG0025896	--	down	212.86
GSRG0034875	Zdhhc9	down	209.94
GSRG0022886	Elmod3	down	208.22
GSRG0012951	Plxdc2	down	207.09
GSRG0032869	--	down	199.78
GSRG0015813	Rasa1	down	197.87
GSRG0031919	Pxylp1	down	197.81
GSRG0013521	RGD1311805	down	195.11
GSRG0033974	Clcn4	down	194.41
GSRG0011557	Ttc5	down	191.17
GSRG0000476	Dpf1	down	189.93
GSRG0020273	Slc25a25	down	189.76

GSRG0029609	Phf5a	down	188.98
GSRG0016022	Zc2hc1a	down	183.74
GSRG0030501	Tmem115	down	181.28
GSRG0007362	Pi4ka	down	180.47
GSRG0028688	Actr6	down	177.91
GSRG0030674	Endod1	down	175.88
GSRG0036082	Fam13b	down	174.11
GSRG0015955	Mrps30	down	170.52
GSRG0025787	Cptp	down	170.26
GSRG0034878	Aifm1	down	169.88
GSRG0006168	Nubp1	down	166.62
GSRG0036211	Zfp148	down	166.42
GSRG0002170	Hectd2	down	162.89
GSRG0020281	Slc2a8	down	162.64
GSRG0000549	Nup62	down	160.38
GSRG0012893	Pitrm1	down	160.02
GSRG0032105	--	down	159.76
GSRG0022959	Mrpl19	down	158.59
GSRG0036591	Akap2	down	152.88
GSRG0006992	Acox1	down	152.41
GSRG0009710	Cnih4	down	151.46
GSRG0021258	Samd10	down	149.25
GSRG0024488	Dffa	down	144.68
GSRG0013012	B4galt7	down	143.26
GSRG0024281	Foxj3	down	140.02
GSRG0016443	Hcn3	down	139.28
GSRG0022691	Bmt2	down	136.95
GSRG0031938	Slc35g2	down	134.69
GSRG0015143	Il6st	down	132.58
GSRG0007589	Ccdc50	down	129.26
GSRG0002006	Rasgrp2	down	128.07
GSRG0020342	Ppp6c	down	127.75
GSRG0013719	Prelid3a	down	125.53
GSRG0018533	Fam229b	down	124.61
GSRG0022878	Ptcd3	down	121.96
GSRG0006325	Gabrg2	down	121.50
GSRG0032163	Ppp2r5d	down	115.86
GSRG0006071	Mrps7	down	112.91
GSRG0030101	Slc37a4	down	112.80
GSRG0008075	Rph3a	down	110.97
GSRG0021118	Ahcy	down	110.76
GSRG0015217	Ctnnd2	down	109.57
GSRG0037062	--	down	109.41
GSRG0015248	Pex2	down	108.50
GSRG0036688	Ift52	down	108.41
GSRG0004218	Man2a2	down	106.12

GSRG0028415	Matk	down	103.47
GSRG0032367	Atic	down	101.21
GSRG0010329	LOC680039	down	100.90
GSRG0011981	Galntl6	down	100.29
GSRG0004243	Arnt2	down	99.74
GSRG0022835	Hibadh	down	96.86
GSRG0011901	Fam213a	down	96.06
GSRG0006957	Slc39a11	down	95.70
GSRG0001710	Ipo7	down	95.56
GSRG0028151	Mgat3	down	95.47
GSRG0004194	Slco3a1	down	95.41
GSRG0032455	Atg16l1	down	95.36
GSRG0019759	Cds2	down	93.84
GSRG0027443	Gng7	down	93.10
GSRG0010385	Dbnl	down	92.42
GSRG0034674	Slc7a3	down	92.08
GSRG0016839	Atf6b	down	91.97
GSRG0036603	Elavl4	down	91.86
GSRG0014809	Rad23a	down	91.42
GSRG0001503	Hddc3	down	90.39
GSRG0014694	Gnpat	down	90.38
GSRG0010962	Thtpa	down	88.71
GSRG0012881	--	down	87.57
GSRG0026745	Vcpkmt	down	85.59
GSRG0010288	Lgi2	down	85.51
GSRG0009616	Tada1	down	84.89
GSRG0024362	Pef1	down	82.43
GSRG0012481	Thoc3	down	82.21
GSRG0021352	Cldn12	down	81.70
GSRG0012237	Mfap3l	down	81.51
GSRG0028788	Cpsf6	down	80.75
GSRG0033071	Abcb6	down	79.77
GSRG0003204	Fam98c	down	79.50
GSRG0007942	Zfp68	down	78.65
GSRG0006141	Tbcd	down	77.32
GSRG0036538	Tigar	down	76.54
GSRG0011694	Nefm	down	73.74
GSRG0010307	Fbxl5	down	73.71
GSRG0005641	Poldip2	down	72.91
GSRG0026364	Golga5	down	71.80
GSRG0014644	Mlycd	down	70.33
GSRG0014332	Slc38a7	down	70.27
GSRG0007023	Aatk	down	66.75
GSRG0005828	Coasy	down	65.78
GSRG0015633	Kcna2	down	65.06
GSRG0023361	Xpc	down	64.11

GSRG0029746	Ddx23	down	63.76
GSRG0007430	Gart	down	63.68
GSRG0018818	Rapgef4	down	63.22
GSRG0005300	Rnf145	down	62.79
GSRG0032295	Asnsd1	down	62.09
GSRG0013699	St8sia3	down	59.77
GSRG0032472	Ube2f	down	59.69
GSRG0015568	Pex11b	down	59.18
GSRG0012252	Aga	down	59.08
GSRG0024240	Atpaf1	down	58.97
GSRG0015476	Rit1	down	58.66
GSRG0034325	--	down	58.33
GSRG0010671	Smim20	down	56.64
GSRG0023923	Ccnc	down	56.29
GSRG0020103	Cstf1	down	56.01
GSRG0010760	Mtfp1	down	55.81
GSRG0012821	Nrsn1	down	55.12
GSRG0009744	Lpgat1	down	54.92
GSRG0033045	Erbb4	down	53.73
GSRG0034459	Naa10	down	53.00
GSRG0026671	Bcap29	down	52.23
GSRG0015121	Sgtb	down	51.77
GSRG0037008	LOC317456	down	51.43
GSRG0023726	Chtop	down	51.10
GSRG0019739	Ptpra	down	49.63
GSRG0023914	Mmp16	down	49.38
GSRG0032551	Ppip5k2	down	49.08
GSRG0021152	Mafb	down	48.92
GSRG0007034	Alyref	down	48.83
GSRG0025892	Adcy3	down	48.58
GSRG0013593	Slc35a4	down	48.40
GSRG0003080	Bckdha	down	46.49
GSRG0023441	Erc1	down	45.02
GSRG0020405	Stk39	down	42.85
GSRG0005277	--	down	42.78
GSRG0008980	--	down	42.77
GSRG0022727	Impdh1	down	42.42
GSRG0004240	Cemip	down	42.30
GSRG0032964	Rnf149	down	41.80
GSRG0003380	Bax	down	40.71
GSRG0025741	--	down	40.12
GSRG0024724	RGD1359108	down	39.32
GSRG0036716	Sdhaf3	down	37.94
GSRG0022895	Ctnna2	down	37.62
GSRG0014508	Farsa	down	37.41
GSRG0026023	Mgat2	down	37.19

GSRG0021713	Tpra1	down	37.11
GSRG0030373	Ccpg1	down	36.72
GSRG0006092	Mgat5b	down	36.70
GSRG0030404	Irak1bp1	down	35.29
GSRG0033905	RGD1565685	down	35.19
GSRG0006292	Mpg	down	34.11
GSRG0008961	Tpst1	down	33.96
GSRG0034071	Nlgn3	down	33.55
GSRG0030592	Glb1	down	33.27
GSRG0009332	Chfr	down	32.72
GSRG0012257	Rwdd4	down	32.61
GSRG0020043	Gdap1l1	down	32.49
GSRG0022971	Dguok	down	31.45
GSRG0001760	--	down	31.35
GSRG0022860	Nap1l5	down	31.03
GSRG0027274	Itpk1	down	30.88
GSRG0010446	Pnpt1	down	30.13
GSRG0026166	Nrxn3	down	29.89
GSRG0020851	--	down	29.71
GSRG0019760	--	down	29.55
GSRG0012962	Gad2	down	29.41
GSRG0025780	Gabrd	down	29.38
GSRG0015761	Ddah1	down	29.12
GSRG0024731	Topors	down	28.92
GSRG0030754	Herpud2	down	28.45
GSRG0016680	Ap1ar	down	28.29
GSRG0010470	Rpl5	down	28.28
GSRG0020402	Scn1a	down	27.06
GSRG0037033	--	down	24.95
GSRG0016679	--	down	24.65
GSRG0019734	Nop56	down	24.47
GSRG0006408	Anxa6	down	23.95
GSRG0028835	Lrp1	down	23.54
GSRG0025742	--	down	23.40
GSRG0036181	Sst	down	23.13
GSRG0001513	Tm6sf1	down	22.57
GSRG0006876	Hdac5	down	22.53
GSRG0014269	Spire1	down	22.04
GSRG0008871	--	down	21.58
GSRG0015487	--	down	21.25
GSRG0006976	Gga3	down	21.14
GSRG0018613	Fam69b	down	19.11
GSRG0021660	Bola3	down	17.10
GSRG0010144	Fam69a	down	17.00
GSRG0009573	Astn1	down	16.08
GSRG0029871	Dcun1d5	down	14.98

GSRG0032125	--	down	13.65
GSRG0036853	--	down	11.11
GSRG0034667	--	down	10.93
GSRG0019586	Disp2	down	10.62
GSRG0010140	Cplx1	down	9.95
GSRG0008872	Vgf	down	9.34
GSRG0013844	Reep5	down	8.57
GSRG0004774	Klc2	down	7.79
GSRG0003068	Atp1a3	down	4.87

,5; P-Value ≤ 0,05) - P\

P-Value	Adjusted P-Value
4.36E-09	3.21E-06
1.22E-06	2.72E-04
2.53E-06	5.04E-04
1.04E-05	1.39E-03
1.97E-04	1.04E-02
1.28E-03	3.40E-02
3.05E-03	5.74E-02
5.64E-03	7.88E-02
9.19E-03	1.05E-01
1.22E-02	1.25E-01
7.09E-03	9.02E-02
2.30E-02	1.87E-01
1.81E-02	1.60E-01
1.26E-02	1.28E-01
2.91E-02	2.16E-01
3.40E-02	2.39E-01
2.92E-02	2.16E-01
4.32E-02	2.76E-01
4.42E-02	2.80E-01
4.10E-02	2.67E-01
9.44E-18	6.95E-14
7.67E-14	2.82E-10
6.67E-12	9.83E-09
1.56E-10	1.44E-07
1.63E-12	3.01E-09
9.87E-12	1.21E-08
1.36E-08	7.14E-06
1.21E-08	7.14E-06
1.51E-11	1.59E-08
6.34E-06	1.02E-03
6.76E-06	1.04E-03
9.47E-13	2.32E-09
1.51E-08	7.41E-06
3.63E-08	1.57E-05
7.85E-09	5.25E-06
6.08E-07	1.72E-04
1.33E-08	7.14E-06
3.75E-07	1.26E-04
8.24E-07	2.09E-04
1.07E-06	2.54E-04
9.52E-07	2.34E-04

1.99E-07	7.00E-05
3.54E-08	1.57E-05
7.79E-08	3.19E-05
6.54E-05	4.92E-03
7.06E-05	5.20E-03
3.64E-06	6.87E-04
3.63E-06	6.87E-04
4.38E-06	7.68E-04
4.42E-07	1.41E-04
3.89E-05	3.58E-03
5.29E-05	4.38E-03
2.74E-05	2.92E-03
1.93E-06	4.19E-04
1.50E-07	5.82E-05
1.20E-04	7.41E-03
1.13E-06	2.59E-04
1.33E-05	1.66E-03
1.48E-04	8.57E-03
8.03E-07	2.09E-04
2.51E-06	5.04E-04
3.47E-05	3.32E-03
2.85E-05	2.95E-03
4.05E-06	7.31E-04
4.07E-06	7.31E-04
1.23E-05	1.57E-03
2.07E-06	4.35E-04
1.22E-09	1.00E-06
7.10E-06	1.07E-03
8.68E-06	1.19E-03
1.21E-05	1.56E-03
5.06E-05	4.24E-03
4.83E-05	4.09E-03
1.52E-05	1.83E-03
1.09E-05	1.44E-03
1.51E-05	1.83E-03
1.29E-04	7.74E-03
5.75E-07	1.69E-04
4.17E-05	3.78E-03
2.23E-05	2.52E-03
7.91E-06	1.16E-03
8.55E-06	1.19E-03
5.77E-05	4.57E-03
2.88E-05	2.95E-03
3.58E-04	1.53E-02
5.91E-06	9.79E-04
3.13E-04	1.42E-02

2.65E-05	2.87E-03
8.17E-06	1.18E-03
7.42E-07	2.02E-04
6.06E-05	4.70E-03
1.75E-05	2.04E-03
2.81E-04	1.35E-02
4.57E-05	3.99E-03
2.82E-05	2.95E-03
3.10E-05	3.05E-03
3.45E-05	3.32E-03
1.55E-04	8.78E-03
6.81E-05	5.07E-03
2.21E-04	1.13E-02
8.83E-05	5.86E-03
6.75E-04	2.23E-02
6.35E-05	4.87E-03
5.42E-05	4.41E-03
7.83E-05	5.55E-03
7.44E-05	5.32E-03
7.79E-04	2.46E-02
5.35E-07	1.64E-04
8.03E-05	5.63E-03
5.80E-04	2.00E-02
5.55E-04	1.96E-02
3.23E-04	1.45E-02
3.54E-04	1.53E-02
8.50E-05	5.75E-03
6.48E-04	2.15E-02
5.97E-04	2.02E-02
3.15E-04	1.42E-02
5.20E-04	1.87E-02
8.17E-04	2.52E-02
6.32E-04	2.11E-02
1.36E-03	3.52E-02
1.21E-04	7.42E-03
3.66E-04	1.54E-02
1.23E-03	3.29E-02
1.13E-03	3.14E-02
1.65E-04	9.23E-03
1.60E-03	3.92E-02
2.04E-03	4.52E-02
1.20E-03	3.24E-02
4.36E-04	1.68E-02
3.93E-04	1.61E-02
1.84E-04	1.00E-02
1.73E-03	4.12E-02

1.09E-03	3.05E-02
3.77E-04	1.58E-02
4.30E-04	1.67E-02
5.98E-06	9.79E-04
4.19E-04	1.65E-02
1.53E-04	8.72E-03
2.04E-03	4.52E-02
5.75E-04	1.99E-02
8.85E-04	2.67E-02
1.46E-03	3.70E-02
4.94E-04	1.86E-02
5.12E-04	1.87E-02
9.31E-04	2.78E-02
5.58E-04	1.96E-02
2.01E-03	4.50E-02
5.73E-04	1.99E-02
1.06E-03	3.01E-02
1.58E-03	3.91E-02
2.90E-03	5.63E-02
2.69E-03	5.36E-02
1.14E-03	3.14E-02
5.46E-04	1.94E-02
1.18E-03	3.22E-02
8.48E-04	2.60E-02
3.25E-03	5.93E-02
2.40E-04	1.20E-02
3.48E-03	6.08E-02
1.32E-03	3.46E-02
3.39E-03	5.99E-02
8.67E-04	2.63E-02
7.92E-04	2.48E-02
9.32E-04	2.78E-02
1.02E-03	2.96E-02
3.80E-03	6.43E-02
1.77E-03	4.19E-02
3.07E-05	3.05E-03
4.81E-06	8.24E-04
1.90E-03	4.36E-02
2.17E-03	4.73E-02
2.98E-04	1.40E-02
5.15E-03	7.53E-02
3.77E-03	6.42E-02
2.16E-03	4.73E-02
6.46E-03	8.47E-02
4.39E-03	6.77E-02
3.42E-03	6.00E-02

4.96E-03	7.34E-02
4.13E-03	6.58E-02
4.77E-03	7.21E-02
4.03E-03	6.54E-02
3.98E-03	6.53E-02
3.39E-03	5.99E-02
4.08E-03	6.55E-02
7.45E-03	9.30E-02
4.97E-03	7.34E-02
2.19E-03	4.75E-02
5.47E-03	7.76E-02
3.29E-03	5.93E-02
8.39E-03	9.96E-02
6.06E-03	8.19E-02
3.27E-03	5.93E-02
3.12E-03	5.81E-02
3.40E-03	5.99E-02
3.49E-03	6.08E-02
3.19E-03	5.90E-02
6.70E-03	8.71E-02
3.89E-03	6.51E-02
5.86E-03	8.06E-02
7.07E-03	9.02E-02
5.70E-03	7.91E-02
2.76E-03	5.44E-02
1.02E-02	1.10E-01
4.10E-03	6.55E-02
1.06E-02	1.13E-01
6.21E-03	8.33E-02
1.09E-02	1.16E-01
2.21E-03	4.75E-02
4.29E-03	6.69E-02
4.15E-03	6.59E-02
7.19E-03	9.10E-02
8.09E-03	9.82E-02
5.86E-03	8.06E-02
6.02E-05	4.70E-03
6.40E-03	8.44E-02
5.93E-04	2.01E-02
8.21E-03	9.90E-02
9.78E-03	1.07E-01
6.41E-03	8.44E-02
1.13E-02	1.19E-01
8.97E-03	1.03E-01
1.41E-02	1.37E-01
1.65E-02	1.52E-01

9.04E-03	1.04E-01
1.63E-02	1.51E-01
8.50E-03	1.00E-01
4.27E-03	6.69E-02
8.86E-03	1.03E-01
1.78E-02	1.59E-01
1.10E-02	1.16E-01
1.08E-02	1.15E-01
1.46E-02	1.40E-01
1.60E-02	1.49E-01
1.15E-02	1.20E-01
1.74E-05	2.04E-03
1.20E-02	1.24E-01
1.24E-02	1.26E-01
1.58E-02	1.49E-01
9.82E-03	1.08E-01
1.60E-02	1.49E-01
5.68E-03	7.91E-02
1.38E-02	1.35E-01
1.61E-02	1.50E-01
1.10E-02	1.17E-01
1.29E-02	1.30E-01
1.72E-02	1.55E-01
2.29E-03	4.86E-02
1.38E-03	3.56E-02
1.60E-02	1.49E-01
1.99E-02	1.71E-01
1.96E-02	1.69E-01
7.27E-03	9.15E-02
1.66E-02	1.52E-01
1.83E-02	1.61E-01
2.10E-02	1.76E-01
2.56E-02	1.99E-01
2.06E-02	1.75E-01
8.94E-03	--
1.89E-02	1.65E-01
2.51E-02	1.96E-01
2.07E-02	1.75E-01
2.58E-02	2.00E-01
2.45E-02	1.94E-01
8.81E-03	1.03E-01
1.81E-02	1.60E-01
2.15E-02	1.79E-01
1.82E-02	1.60E-01
2.46E-02	1.94E-01
2.53E-02	1.97E-01

3.09E-02	2.25E-01
2.83E-02	2.12E-01
3.17E-02	2.30E-01
3.44E-02	2.41E-01
3.26E-02	2.34E-01
3.54E-02	2.45E-01
3.18E-02	2.30E-01
1.69E-02	1.54E-01
3.69E-02	2.51E-01
3.24E-02	2.33E-01
4.07E-02	2.66E-01
8.90E-03	1.03E-01
3.57E-02	2.47E-01
2.76E-02	2.09E-01
3.06E-03	5.74E-02
3.68E-02	2.51E-01
4.13E-02	2.68E-01
2.57E-03	5.24E-02
4.81E-02	2.96E-01
3.00E-02	--
2.57E-03	5.24E-02
4.96E-02	3.02E-01
1.35E-02	1.33E-01
3.15E-02	2.29E-01
4.46E-02	2.82E-01
1.68E-02	1.53E-01
1.11E-03	3.08E-02
1.75E-02	1.56E-01
4.55E-02	2.85E-01
4.70E-02	2.92E-01
2.85E-03	5.56E-02
2.42E-02	1.92E-01
3.32E-02	2.36E-01
2.38E-02	1.90E-01
4.34E-02	2.77E-01
1.22E-02	1.25E-01
3.59E-02	2.47E-01
4.12E-02	2.67E-01
1.17E-02	1.22E-01
4.79E-02	2.96E-01
3.32E-02	2.36E-01
1.72E-02	1.55E-01
3.31E-03	5.93E-02
4.29E-02	2.76E-01
2.57E-02	2.00E-01
4.79E-02	2.96E-01

3.59E-02	2.47E-01
4.08E-02	2.66E-01
2.35E-02	1.89E-01
2.87E-02	2.14E-01
2.46E-02	1.94E-01
2.96E-02	2.18E-01
2.61E-02	2.02E-01
5.00E-02	3.03E-01
3.29E-02	2.35E-01

YR CTRL vs GABA CTRL

Gene Name
solute carrier family 17 member 7
protein kinase C, gamma
NFKB inhibitor alpha
serum/glucocorticoid regulated kinase 1
sprouty RTK signaling antagonist 4
spermatogenesis associated 2-like
CD24 molecule
neuronal differentiation 6
nuclear autoantigenic sperm protein
histone cluster 1, H4b
solute carrier family 24 member 2
--
zinc finger protein 238
--
synuclein alpha
centriole, cilia and spindle-associated protein
--
regulator of G-protein signaling 4
RNA binding motif protein 22
ribosomal protein L7
glutamate decarboxylase 1
delta/notch-like EGF repeat containing
ubiquitin-like modifier activating enzyme 1
synaptic vesicle glycoprotein 2a
SPARC/osteonectin, cwcv and kazal like domains proteoglycan 3
--
potassium voltage-gated channel interacting protein 1
POM121 transmembrane nucleoporin
solute carrier family 32 member 1
BRX1, biogenesis of ribosomes
nucleic acid binding protein 1
neuropilin and tolloid like 1
prepronociceptin
neurexophilin 1
DEAF1 transcription factor
ankyrin repeat domain 34B
pyruvate dehydrogenase complex, component X
vascular endothelial growth factor B
sideroflexin 5
potassium voltage-gated channel subfamily A member regulatory beta subunit 1
insulin-like growth factor binding protein 4

exostosin-like glycosyltransferase 2
cold shock domain containing C2
solute carrier family 38, member 1
solute carrier family 17 member 5
structural maintenance of chromosomes 3
ATP5S-like
syntaxin binding protein 6
NIMA-related kinase 7
V-set and transmembrane domain containing 2A
--
ORMDL sphingolipid biosynthesis regulator 3
ubiquitin specific peptidase 13
glutamate ionotropic receptor AMPA type subunit 4
MYST/Esa1-associated factor 6
caspase 9
wingless-type MMTV integration site family, member 7A
nuclear transcription factor, X-box binding 1
family with sequence similarity 210, member A
sirtuin 5
ELAV like RNA binding protein 2
calcium/calmodulin-dependent protein kinase II delta
LETM1 domain containing 1
adaptor-related protein complex 1, sigma 2 subunit
trans-golgi network protein 2
Ly6/neurotoxin 1
mediator complex subunit 4
solute carrier family 6 member 1
cellular repressor of E1A-stimulated genes 1
LanC like 1
teneurin transmembrane protein 3
5'-nucleotidase, cytosolic IIIB
Purkinje cell protein 4-like 1
zinc finger protein 385D
alanyl-tRNA synthetase domain containing 1
ubiquitin family domain containing 1
neuraminidase 2
ribosomal protein S19 binding protein 1
contactin associated protein-like 4
tubulin, gamma 2
RAB3B, member RAS oncogene family
paraneoplastic Ma antigen family-like 2
glycine receptor, beta
thiosulfate sulfurtransferase (rhodanese)-like domain containing 3
solute carrier family 16 member 1
--
partner of NOB1 homolog

adaptor-related protein complex 4, sigma 1 subunit
ring finger protein 10
RAN GTPase activating protein 1
leucine rich repeat transmembrane neuronal 1
--
lectin, mannose-binding 2
similar to RIKEN cDNA C030006K11
antagonist of mitotic exit network 1 homolog
limb bud and heart development
methyl-CpG binding domain protein 3
TCF3 (E2A) fusion partner
--
--
RAN binding protein 6
zinc finger CCCH-type and G-patch domain containing
developmentally regulated GTP binding protein 1
mucolipin 1
ATP/GTP binding protein 1
diacylglycerol kinase, delta
sphingomyelin synthase 1
aristaless related homeobox
ATP binding cassette subfamily B member 9
coiled-coil domain containing 115
centrosomal protein 120
cyclin-dependent kinase 10
eukaryotic translation initiation factor 2 subunit gamma
staufen double-stranded RNA binding protein 2
beta-secretase 1
family with sequence similarity 189, member A2
solute carrier family 2 member 13
testin LIM domain protein
similar to ENSANGP00000021391
ribonuclease P/MRP 25 subunit
--
--
zinc finger, DHHC-type containing 9
ELMO domain containing 3
plexin domain containing 2
--
RAS p21 protein activator 1
2-phosphoxylose phosphatase 1
similar to RIKEN cDNA 2400010D15
chloride voltage-gated channel 4
tetratricopeptide repeat domain 5
double PHD fingers 1
solute carrier family 25 member 25

PHD finger protein 5A
zinc finger, C2HC-type containing 1A
transmembrane protein 115
phosphatidylinositol 4-kinase alpha
ARP6 actin-related protein 6 homolog
endonuclease domain containing 1
family with sequence similarity 13, member B
mitochondrial ribosomal protein S30
ceramide-1-phosphate transfer protein
apoptosis inducing factor, mitochondria associated 1
nucleotide binding protein 1
zinc finger protein 148
HECT domain E3 ubiquitin protein ligase 2
solute carrier family 2 member 8
nucleoporin 62
pitrilysin metallopeptidase 1
--
mitochondrial ribosomal protein L19
A-kinase anchoring protein 2
acyl-CoA oxidase 1
cornichon family AMPA receptor auxiliary protein 4
sterile alpha motif domain containing 10
DNA fragmentation factor subunit alpha
beta-1, 4-galactosyltransferase 7
forkhead box J3
hyperpolarization-activated cyclic nucleotide-gated potassium channel 3
base methyltransferase of 25S rRNA 2 homolog
solute carrier family 35, member G2
interleukin 6 signal transducer
coiled-coil domain containing 50
RAS guanyl releasing protein 2
protein phosphatase 6, catalytic subunit
PRELI domain containing 3A
family with sequence similarity 229, member B
Pentatricopeptide repeat domain 3
gamma-aminobutyric acid type A receptor gamma 2 subunit
protein phosphatase 2, regulatory subunit B', delta
mitochondrial ribosomal protein S7
solute carrier family 37 member 4
rabphilin 3A
adenosylhomocysteinase
catenin delta 2
--
peroxisomal biogenesis factor 2
intraflagellar transport 52
mannosidase, alpha, class 2A, member 2

megakaryocyte-associated tyrosine kinase
5-aminoimidazole-4-carboxamide ribonucleotide formyltransferase/IMP cyclohydrolase
hypothetical protein LOC680039
polypeptide N-acetylgalactosaminyltransferase-like 6
aryl hydrocarbon receptor nuclear translocator 2
3-hydroxyisobutyrate dehydrogenase
family with sequence similarity 213, member A
solute carrier family 39, member 11
importin 7
mannosyl (beta-1, 4-)-glycoprotein beta-1, 4-N-acetylglucosaminyltransferase
solute carrier organic anion transporter family, member 3a1
autophagy related 16-like 1
CDP-diacylglycerol synthase 2
G protein subunit gamma 7
drebrin-like
solute carrier family 7 member 3
activating transcription factor 6 beta
ELAV like RNA binding protein 4
RAD23 homolog A, nucleotide excision repair protein
HD domain containing 3
glyceronephosphate O-acyltransferase
thiamine triphosphatase
--
valosin containing protein lysine methyltransferase
leucine-rich repeat LGI family, member 2
transcriptional adaptor 1
penta-EF hand domain containing 1
THO complex 3
claudin 12
microfibrillar-associated protein 3-like
cleavage and polyadenylation specific factor 6
ATP-binding cassette, subfamily B (MDR/TAP), member 6
family with sequence similarity 98, member C
zinc finger protein 68
tubulin folding cofactor D
TP53 induced glycolysis regulatory phosphatase
neurofilament, medium polypeptide
F-box and leucine-rich repeat protein 5
DNA polymerase delta interacting protein 2
golgin A5
malonyl-CoA decarboxylase
solute carrier family 38, member 7
apoptosis-associated tyrosine kinase
Coenzyme A synthase
potassium voltage-gated channel subfamily A member 2
XPC complex subunit, DNA damage recognition and repair factor

DEAD-box helicase 23
phosphoribosylglycinamide formyltransferase
Rap guanine nucleotide exchange factor 4
ring finger protein 145
asparagine synthetase domain containing 1
ST8 alpha-N-acetyl-neuraminide alpha-2, 8-sialyltransferase 3
ubiquitin-conjugating enzyme E2F (putative)
peroxisomal biogenesis factor 11 beta
aspartylglucosaminidase
ATP synthase mitochondrial F1 complex assembly factor 1
Ras-like without CAAX 1
--
small integral membrane protein 20
cyclin C
cleavage stimulation factor subunit 1
mitochondrial fission process 1
neurensin 1
lysophosphatidylglycerol acyltransferase 1
erb-b2 receptor tyrosine kinase 4
N(alpha)-acetyltransferase 10, NatA catalytic subunit
B-cell receptor-associated protein 29
small glutamine rich tetratricopeptide repeat containing beta
hypothetical LOC317456
chromatin target of PRMT1
protein tyrosine phosphatase, receptor type, A
matrix metallopeptidase 16
diphosphoinositol pentakisphosphate kinase 2
MAF bZIP transcription factor B
Aly/REF export factor
adenylate cyclase 3
solute carrier family 35, member A4
branched chain ketoacid dehydrogenase E1, alpha polypeptide
ELKS/RAB6-interacting/CAST family member 1
serine threonine kinase 39
--
--
inosine monophosphate dehydrogenase 1
cell migration-inducing hyaluronan binding protein
ring finger protein 149
BCL2 associated X, apoptosis regulator
--
similar to RIKEN cDNA 3110043O21
succinate dehydrogenase complex assembly factor 3
catenin alpha 2
phenylalanyl-tRNA synthetase, alpha subunit
mannosyl (alpha-1, 6-)-glycoprotein beta-1, 2-N-acetylglucosaminyltransferase

transmembrane protein adipocyte associated 1
cell cycle progression 1
mannosyl (alpha-1, 6-)-glycoprotein beta-1, 6-N-acetyl-glucosaminyltransferase, isozyme B
interleukin-1 receptor-associated kinase 1 binding protein 1
similar to RIKEN cDNA 1810030O07
N-methylpurine-DNA glycosylase
tyrosylprotein sulfotransferase 1
neuroligin 3
galactosidase, beta 1
checkpoint with forkhead and ring finger domains
RWD domain containing 4
ganglioside-induced differentiation-associated protein 1-like 1
deoxyguanosine kinase
--
nucleosome assembly protein 1-like 5
inositol-tetrakisphosphate 1-kinase
polyribonucleotide nucleotidyltransferase 1
neurexin 3
--
--
glutamate decarboxylase 2
gamma-aminobutyric acid type A receptor delta subunit
dimethylarginine dimethylaminohydrolase 1
TOP1 binding arginine/serine rich protein
HERPUD family member 2
adaptor-related protein complex 1 associated regulatory protein
ribosomal protein L5
sodium voltage-gated channel alpha subunit 1
--
--
NOP56 ribonucleoprotein
annexin A6
LDL receptor related protein 1
--
somatostatin
transmembrane 6 superfamily member 1
histone deacetylase 5
spire-type actin nucleation factor 1
--
--
golgi associated, gamma adaptin ear containing, ARF binding protein 3
family with sequence similarity 69, member B
bolA family member 3
family with sequence similarity 69, member A
astrotactin 1
defective in cullin neddylation 1 domain containing 5

--
--
--
dispatched RND transporter family member 2
complexin 1
VGF nerve growth factor inducible
receptor accessory protein 5
kinesin light chain 2
ATPase Na+/K+ transporting subunit alpha 3

List of the 219 Regulated Genes (Fold-change ≥ 1,

FAST DB STABLE ID	Gene Symbol	Regulation	Fold-Change
GSRG0021091	Nrsn2	up	1022.12
GSRG0025694	Igsf21	up	40.67
GSRG0016369	Lxn	up	39.79
GSRG0006002	Arf2	up	37.47
GSRG0024955	Slc24a2	up	24.11
GSRG0024695	Maged2	up	22.83
GSRG0003565	--	up	11.61
GSRG0008871	--	down	2563.68
GSRG0006308	Kcnip1	down	2147.92
GSRG0036252	Brix1	down	1735.13
GSRG0032304	Nabp1	down	1532.74
GSRG0013907	Tmed7	down	1420.91
GSRG0023056	Sfxn5	down	1281.68
GSRG0015402	Kcnab1	down	1273.14
GSRG0029606	Rangap1	down	1223.71
GSRG0026087	Gphn	down	1005.02
GSRG0000412	Atp5sl	down	924.05
GSRG0031867	Slc17a5	down	921.18
GSRG0002264	Smc3	down	907.22
GSRG0026695	Stxbp6	down	877.43
GSRG0009858	Nek7	down	874.10
GSRG0015289	Usp13	down	827.85
GSRG0006796	Ormdl3	down	747.37
GSRG0024467	Casp9	down	713.66
GSRG0001557	Pak1	down	669.55
GSRG0023378	Tmf1	down	667.03
GSRG0014272	Fam210a	down	664.42
GSRG0015089	Ankrd34b	down	637.92
GSRG0013826	Syt4	down	636.29
GSRG0006408	Anxa6	down	623.90
GSRG0015701	Camk2d	down	617.64
GSRG0020611	Madd	down	602.83
GSRG0019603	Rtf1	down	598.47
GSRG0028286	Letmd1	down	591.24
GSRG0026756	Trim9	down	571.23
GSRG0034068	Dlg3	down	541.81
GSRG0006834	Nt5c3b	down	500.57
GSRG0006333	Ublcp1	down	496.12
GSRG0002210	Cnnm1	down	418.62
GSRG0029946	--	down	415.29
GSRG0003193	Mrps12	down	393.42

GSRG0007941	Pdgfa	down	385.80
GSRG0015615	Slc16a1	down	376.89
GSRG0010809	Pno1	down	362.70
GSRG0032455	Atg16l1	down	360.38
GSRG0012470	Lman2	down	354.73
GSRG0018406	LOC294154	down	354.12
GSRG0021713	Tpra1	down	349.96
GSRG0022714	Wasl	down	341.04
GSRG0003572	--	down	323.93
GSRG0020828	Pcna	down	302.49
GSRG0010144	Fam69a	down	292.68
GSRG0026692	Lrrn3	down	292.38
GSRG0026548	Fbxo11	down	289.98
GSRG0028324	Pde1b	down	285.84
GSRG0005300	Rnf145	down	284.77
GSRG0026127	Dnal1	down	282.98
GSRG0005807	Casc3	down	282.65
GSRG0004958	Sgms1	down	281.14
GSRG0024716	Pnrc1	down	278.81
GSRG0032237	Ccdc115	down	275.44
GSRG0013915	Cep120	down	273.05
GSRG0005434	Gid4	down	267.63
GSRG0030255	Pdcd7	down	261.25
GSRG0004821	Vegfb	down	258.33
GSRG0034650	Eif2s3	down	256.91
GSRG0012479	Nop16	down	254.91
GSRG0004927	Fam189a2	down	251.86
GSRG0026146	Eif2b2	down	251.26
GSRG0030119	Bace1	down	250.51
GSRG0024519	Cep104	down	244.42
GSRG0005298	Pwwp2a	down	242.45
GSRG0013170	Gadd45g	down	236.92
GSRG0004850	Asrgl1	down	235.95
GSRG0001855	Ptpre	down	235.52
GSRG0014470	Brd7	down	235.43
GSRG0027665	Slc6a15	down	233.04
GSRG0010351	Slbp	down	229.80
GSRG0004860	Dagla	down	227.58
GSRG0008011	Sbds	down	227.44
GSRG0031432	RGD1309779	down	227.29
GSRG0008817	Kdelr2	down	226.12
GSRG0010061	Adss	down	223.40
GSRG0035015	--	down	219.17
GSRG0032126	--	down	209.91
GSRG0015813	Rasa1	down	202.09
GSRG0013521	RGD1311805	down	200.19

GSRG0024724	RGD1359108	down	195.18
GSRG0026028	Atl1	down	194.67
GSRG0011004	Fgf9	down	194.30
GSRG0020273	Slc25a25	down	194.00
GSRG0026364	Golga5	down	192.29
GSRG0029609	Phf5a	down	192.09
GSRG0019511	Chst1	down	190.79
GSRG0025971	Dgkb	down	188.90
GSRG0000549	Nup62	down	187.53
GSRG0023498	Kcna1	down	185.65
GSRG0018780	Slc4a10	down	184.78
GSRG0021290	Actr3b	down	178.53
GSRG0013015	Prr7	down	178.51
GSRG0036082	Fam13b	down	178.06
GSRG0020402	Scn1a	down	178.03
GSRG0015143	Il6st	down	177.77
GSRG0013016	Grk6	down	177.47
GSRG0001944	Chka	down	174.57
GSRG0034878	Aifm1	down	174.32
GSRG0029295	Fam49b	down	167.07
GSRG0018818	Rapgef4	down	166.62
GSRG0014335	Csnk2a2	down	165.63
GSRG0004194	Slco3a1	down	165.07
GSRG0009020	--	down	163.99
GSRG0022959	Mrpl19	down	162.48
GSRG0009785	Insig2	down	160.15
GSRG0005047	Slit1	down	157.60
GSRG0006992	Acox1	down	155.77
GSRG0036591	Akap2	down	154.70
GSRG0020103	Cstf1	down	152.08
GSRG0020147	Zgpat	down	151.97
GSRG0012186	Map1s	down	151.54
GSRG0004212	Ap3s2	down	142.31
GSRG0022691	Bmt2	down	140.13
GSRG0034712	Taf9b	down	137.16
GSRG0029711	Yaf2	down	135.13
GSRG0012252	Aga	down	132.61
GSRG0027340	Akt1	down	129.95
GSRG0001542	Rab30	down	129.84
GSRG0028164	Sgsm3	down	129.60
GSRG0029703	Chkb	down	125.36
GSRG0011756	Gtf2f2	down	122.78
GSRG0007154	Cmss1	down	116.84
GSRG0015802	Nr2f1	down	116.33
GSRG0031919	Pxylp1	down	112.54
GSRG0011159	Pcca	down	111.90

GSRG0034673	Pdzd11	down	109.42
GSRG0005814	Rara	down	105.12
GSRG0005237	Gng13	down	102.58
GSRG0006464	Tom1l2	down	101.53
GSRG0001964	mrpl11	down	99.93
GSRG0006465	Atpaf2	down	98.56
GSRG0029944	Icam5	down	96.81
GSRG0012881	--	down	92.98
GSRG0003583	--	down	91.01
GSRG0032238	Bend6	down	90.99
GSRG0005137	--	down	90.49
GSRG0017318	Pdxk	down	90.44
GSRG0009616	Tada1	down	86.62
GSRG0009893	Smg7	down	79.67
GSRG0008780	Rasl11a	down	77.64
GSRG0005815	Igfbp4	down	74.00
GSRG0036647	Nosip	down	73.65
GSRG0034327	Bhlhb9	down	72.67
GSRG0025396	Prpf38a	down	72.15
GSRG0013285	Pak1ip1	down	71.70
GSRG0021769	Thumpd3	down	70.38
GSRG0016414	Dclk2	down	69.13
GSRG0025430	Plk3	down	68.09
GSRG0022886	Elmod3	down	66.80
GSRG0034842	Sept6	down	66.00
GSRG0012489	--	down	64.35
GSRG0032175	Polr1c	down	63.12
GSRG0002132	Vldlr	down	61.87
GSRG0024721	Smim8	down	61.56
GSRG0009488	Ivns1abp	down	61.03
GSRG0021376	Phf14	down	61.00
GSRG0008927	Bcl7b	down	60.65
GSRG0006229	Pdpk1	down	58.94
GSRG0025868	Slc30a3	down	56.58
GSRG0032334	Abi2	down	55.42
GSRG0011056	Lgi3	down	55.22
GSRG0012042	Brf2	down	54.53
GSRG0006957	Slc39a11	down	52.76
GSRG0026573	Galnt14	down	52.55
GSRG0002105	--	down	50.44
GSRG0025906	Pum2	down	50.09
GSRG0002539	Ccdc127	down	48.96
GSRG0013947	Fech	down	48.66
GSRG0024731	Topors	down	48.46
GSRG0021119	Pigu	down	48.26
GSRG0010906	Fbxo34	down	46.96

GSRG0028792	Rap1b	down	43.78
GSRG0000541	Syt3	down	43.16
GSRG0001487	Aen	down	42.54
GSRG0028309	Pcbp2	down	41.90
GSRG0004453	Btbd10	down	41.75
GSRG0000414	Exosc5	down	41.61
GSRG0020224	Fam163b	down	41.27
GSRG0013662	Csnk1g3	down	40.80
GSRG0021118	Ahcy	down	39.94
GSRG0005277	--	down	39.61
GSRG0026808	Dhrs7	down	39.57
GSRG0032934	Fam168b	down	37.19
GSRG0030373	Ccpg1	down	37.02
GSRG0026659	Trappc12	down	36.28
GSRG0020063	Dnttip1	down	35.11
GSRG0025607	--	down	34.58
GSRG0021286	Ube3c	down	33.34
GSRG0028144	Cby1	down	31.86
GSRG0017401	Lrrtm3	down	31.37
GSRG0031993	--	down	30.61
GSRG0013749	Pias2	down	30.38
GSRG0003276	Uri1	down	29.78
GSRG0029611	Polr3h	down	29.76
GSRG0008019	Psph	down	29.54
GSRG0036721	Tes	down	29.18
GSRG0031922	Clstn2	down	29.18
GSRG0019760	--	down	28.83
GSRG0030208	Rpp25	down	26.98
GSRG0012951	Plxdc2	down	26.15
GSRG0007991	Pom121	down	25.35
GSRG0023827	Pthlh	down	24.98
GSRG0010011	Pcp4l1	down	21.85
GSRG0008075	Rph3a	down	21.10
GSRG0005383	Gria1	down	20.98
GSRG0005636	Pigs	down	19.72
GSRG0015889	Kif2a	down	17.61
GSRG0003245	Scn1b	down	14.98
GSRG0000359	Pnmal2	down	14.82
GSRG0036149	Ncam2	down	14.75
GSRG0028182	Csdc2	down	13.52

,5; P-Value ≤ 0,05) - G/

P-Value	Adjusted P-Value
7.94E-05	1.21E-02
3.62E-02	2.71E-01
3.83E-02	2.79E-01
1.90E-02	1.90E-01
3.02E-02	2.46E-01
3.36E-02	2.61E-01
2.11E-02	2.00E-01
1.39E-09	1.03E-05
2.58E-08	4.79E-05
9.29E-06	3.45E-03
1.10E-05	3.87E-03
1.80E-08	4.45E-05
9.55E-07	1.01E-03
1.25E-06	1.16E-03
5.56E-09	2.06E-05
2.79E-07	4.15E-04
3.61E-06	1.93E-03
8.06E-05	1.21E-02
8.59E-05	1.23E-02
3.85E-06	1.93E-03
4.95E-06	2.30E-03
2.49E-05	6.84E-03
8.29E-05	1.21E-02
1.49E-04	1.68E-02
3.91E-06	1.93E-03
2.57E-06	1.91E-03
1.83E-04	1.86E-02
5.51E-06	2.41E-03
7.58E-07	9.38E-04
7.20E-06	2.81E-03
3.31E-05	7.92E-03
1.36E-05	4.60E-03
2.28E-06	1.88E-03
3.11E-05	7.92E-03
3.91E-06	1.93E-03
6.75E-06	2.78E-03
4.87E-05	9.27E-03
3.80E-06	1.93E-03
7.41E-05	1.20E-02
1.85E-04	1.86E-02
2.33E-05	6.65E-03

1.97E-05	6.10E-03
3.34E-04	2.56E-02
2.90E-04	2.46E-02
1.68E-04	1.80E-02
2.60E-04	2.27E-02
3.92E-05	8.09E-03
6.20E-04	3.13E-02
3.88E-05	8.09E-03
2.11E-04	2.01E-02
4.10E-05	8.22E-03
5.94E-05	1.00E-02
6.68E-05	1.10E-02
4.77E-05	9.27E-03
6.42E-04	3.20E-02
1.20E-04	1.50E-02
2.47E-04	2.21E-02
1.84E-04	1.86E-02
7.29E-04	3.43E-02
5.60E-05	9.66E-03
5.39E-04	3.01E-02
5.18E-04	2.93E-02
5.15E-04	2.93E-02
2.42E-04	2.21E-02
3.77E-05	8.09E-03
3.38E-04	2.56E-02
2.09E-05	6.21E-03
5.52E-04	3.03E-02
4.59E-04	2.79E-02
6.12E-04	3.13E-02
1.83E-04	1.86E-02
7.81E-04	3.51E-02
5.18E-05	9.61E-03
3.27E-04	2.56E-02
1.20E-04	1.50E-02
3.00E-04	2.46E-02
1.44E-04	1.65E-02
1.21E-04	1.50E-02
2.47E-04	2.21E-02
2.33E-04	2.16E-02
7.70E-04	3.50E-02
1.42E-04	1.64E-02
2.50E-04	2.21E-02
1.29E-03	4.52E-02
3.96E-04	2.63E-02
1.51E-03	4.81E-02
1.12E-03	4.16E-02

7.16E-04	3.41E-02
6.04E-04	3.13E-02
5.93E-04	3.13E-02
1.63E-03	5.00E-02
1.20E-03	4.31E-02
1.04E-03	4.12E-02
3.53E-04	2.62E-02
2.98E-04	2.46E-02
1.46E-03	4.76E-02
6.33E-04	3.18E-02
4.07E-04	2.63E-02
6.56E-04	3.25E-02
2.77E-04	2.39E-02
1.93E-03	5.50E-02
2.01E-04	1.96E-02
1.90E-03	5.50E-02
6.08E-04	3.13E-02
3.85E-04	2.63E-02
1.36E-03	4.59E-02
4.97E-04	2.88E-02
1.32E-03	4.57E-02
1.25E-03	4.42E-02
1.93E-03	5.50E-02
1.35E-03	4.57E-02
1.48E-03	4.79E-02
7.67E-04	3.50E-02
1.35E-03	4.57E-02
2.55E-03	6.05E-02
2.82E-03	6.36E-02
2.64E-03	6.14E-02
2.68E-03	6.18E-02
1.12E-03	4.16E-02
1.08E-03	4.16E-02
3.30E-03	6.95E-02
1.09E-03	4.16E-02
1.34E-03	4.57E-02
3.50E-03	7.14E-02
1.16E-03	4.27E-02
1.94E-03	5.50E-02
1.18E-03	4.29E-02
2.31E-03	5.82E-02
4.99E-03	8.63E-02
4.51E-03	8.13E-02
3.17E-03	6.77E-02
5.71E-03	9.16E-02
1.97E-03	5.50E-02

3.09E-03	6.68E-02
1.39E-03	4.61E-02
2.43E-03	5.92E-02
3.48E-03	7.13E-02
2.73E-03	6.22E-02
3.82E-03	7.53E-02
3.35E-03	6.98E-02
6.87E-03	1.04E-01
4.52E-03	8.13E-02
1.62E-03	5.00E-02
3.75E-03	7.47E-02
4.68E-03	8.28E-02
9.75E-03	1.28E-01
1.00E-02	1.30E-01
4.51E-03	8.13E-02
1.98E-03	5.50E-02
5.74E-03	9.19E-02
7.47E-03	1.09E-01
7.07E-03	1.06E-01
1.36E-02	1.54E-01
4.46E-03	8.11E-02
1.08E-02	1.36E-01
5.52E-03	9.04E-02
9.95E-03	1.30E-01
6.22E-03	9.76E-02
2.54E-03	6.05E-02
1.67E-02	1.75E-01
1.14E-02	1.42E-01
8.57E-03	1.20E-01
7.51E-03	1.10E-01
5.39E-03	9.00E-02
1.07E-02	1.36E-01
1.28E-02	1.52E-01
5.45E-03	9.01E-02
1.80E-02	1.85E-01
1.77E-02	1.83E-01
2.17E-02	2.02E-01
1.92E-02	1.90E-01
1.46E-02	1.62E-01
1.57E-02	1.70E-01
1.19E-02	1.46E-01
1.60E-02	1.71E-01
2.14E-02	2.01E-01
1.32E-02	1.53E-01
2.29E-02	2.07E-01
1.34E-02	1.54E-01

2.03E-02	1.95E-01
1.89E-02	1.90E-01
2.69E-02	2.29E-01
2.05E-02	1.97E-01
2.12E-02	2.01E-01
2.40E-02	2.12E-01
2.55E-02	2.22E-01
1.31E-02	1.53E-01
2.77E-02	2.34E-01
1.33E-02	1.54E-01
2.32E-02	2.08E-01
3.51E-02	2.67E-01
2.79E-02	2.35E-01
3.33E-02	2.60E-01
3.34E-02	2.60E-01
3.38E-02	2.62E-01
3.53E-02	2.67E-01
4.22E-02	2.91E-01
3.65E-02	2.72E-01
2.45E-02	2.16E-01
3.71E-02	2.74E-01
4.35E-02	2.97E-01
3.86E-02	2.80E-01
4.13E-02	2.88E-01
3.03E-02	2.46E-01
3.91E-02	2.80E-01
3.52E-02	2.67E-01
3.44E-02	2.64E-01
4.58E-02	3.06E-01
9.82E-03	1.29E-01
3.49E-02	2.66E-01
4.14E-02	2.88E-01
1.75E-02	1.82E-01
2.20E-02	2.03E-01
3.53E-02	2.67E-01
4.74E-02	3.12E-01
2.44E-02	2.15E-01
4.15E-02	2.88E-01
4.96E-02	3.21E-01
3.52E-02	2.67E-01

ABA PUR vs GABA CTRL

Gene Name
neurensin 2
immunoglobin superfamily, member 21
latexin
ADP-ribosylation factor 2
solute carrier family 24 member 2
MAGE family member D2
--
--
potassium voltage-gated channel interacting protein 1
BRX1, biogenesis of ribosomes
nucleic acid binding protein 1
transmembrane p24 trafficking protein 7
sideroflexin 5
potassium voltage-gated channel subfamily A member regulatory beta subunit 1
RAN GTPase activating protein 1
gephyrin
ATP5S-like
solute carrier family 17 member 5
structural maintenance of chromosomes 3
syntaxin binding protein 6
NIMA-related kinase 7
ubiquitin specific peptidase 13
ORMDL sphingolipid biosynthesis regulator 3
caspase 9
p21 (RAC1) activated kinase 1
TATA element modulatory factor 1
family with sequence similarity 210, member A
ankyrin repeat domain 34B
synaptotagmin 4
annexin A6
calcium/calmodulin-dependent protein kinase II delta
MAP-kinase activating death domain
Rtf1, Paf1/RNA polymerase II complex component, homolog (S. cerevisiae)
LETM1 domain containing 1
tripartite motif-containing 9
discs large MAGUK scaffold protein 3
5'-nucleotidase, cytosolic IIIB
ubiquitin-like domain containing CTD phosphatase 1
cyclin and CBS domain divalent metal cation transport mediator 1
--
mitochondrial ribosomal protein S12

platelet derived growth factor subunit A
solute carrier family 16 member 1
partner of NOB1 homolog
autophagy related 16-like 1
lectin, mannose-binding 2
similar to chromosome 6 open reading frame 106 isoform a
transmembrane protein adipocyte associated 1
Wiskott-Aldrich syndrome-like
--
proliferating cell nuclear antigen
family with sequence similarity 69, member A
leucine rich repeat neuronal 3
F-box protein 11
phosphodiesterase 1B
ring finger protein 145
dynein, axonemal, light chain 1
cancer susceptibility candidate 3
sphingomyelin synthase 1
proline-rich nuclear receptor coactivator 1
coiled-coil domain containing 115
centrosomal protein 120
GID complex subunit 4
programmed cell death 7
vascular endothelial growth factor B
eukaryotic translation initiation factor 2 subunit gamma
NOP16 nucleolar protein
family with sequence similarity 189, member A2
eukaryotic translation initiation factor 2B subunit beta
beta-secretase 1
centrosomal protein 104
PWWP domain containing 2A
growth arrest and DNA-damage-inducible, gamma
asparaginase like 1
protein tyrosine phosphatase, receptor type, E
bromodomain containing 7
solute carrier family 6 member 15
stem-loop binding protein
diacylglycerol lipase, alpha
SBDS ribosome assembly guanine nucleotide exchange factor
similar to ENSANGP00000021391
KDEL endoplasmic reticulum protein retention receptor 2
adenylosuccinate synthase
--
--
RAS p21 protein activator 1
similar to RIKEN cDNA 2400010D15

similar to RIKEN cDNA 3110043O21
atlastin GTPase 1
fibroblast growth factor 9
solute carrier family 25 member 25
golgin A5
PHD finger protein 5A
carbohydrate sulfotransferase 1
diacylglycerol kinase, beta
nucleoporin 62
potassium voltage-gated channel subfamily A member 1
solute carrier family 4 member 10
ARP3 actin related protein 3 homolog B
proline rich 7 (synaptic)
family with sequence similarity 13, member B
sodium voltage-gated channel alpha subunit 1
interleukin 6 signal transducer
G protein-coupled receptor kinase 6
choline kinase alpha
apoptosis inducing factor, mitochondria associated 1
family with sequence similarity 49, member B
Rap guanine nucleotide exchange factor 4
casein kinase 2 alpha 2
solute carrier organic anion transporter family, member 3a1
--
mitochondrial ribosomal protein L19
insulin induced gene 2
slit guidance ligand 1
acyl-CoA oxidase 1
A-kinase anchoring protein 2
cleavage stimulation factor subunit 1
zinc finger CCCH-type and G-patch domain containing
microtubule-associated protein 1S
adaptor-related protein complex 3, sigma 2 subunit
base methyltransferase of 25S rRNA 2 homolog
TATA-box binding protein associated factor 9b
YY1 associated factor 2
aspartylglucosaminidase
AKT serine/threonine kinase 1
RAB30, member RAS oncogene family
small G protein signaling modulator 3
choline kinase beta
general transcription factor IIF subunit 2
cms1 ribosomal small subunit homolog (yeast)
nuclear receptor subfamily 2, group F, member 1
2-phosphoxylose phosphatase 1
propionyl-CoA carboxylase alpha subunit

PDZ domain containing 11
retinoic acid receptor, alpha
G protein subunit gamma 13
target of myb1 like 2 membrane trafficking protein
mitochondrial ribosomal protein L11
ATP synthase mitochondrial F1 complex assembly factor 2
intercellular adhesion molecule 5
--
--
BEN domain containing 6
--
pyridoxal (pyridoxine, vitamin B6) kinase
transcriptional adaptor 1
SMG7 nonsense mediated mRNA decay factor
RAS-like family 11 member A
insulin-like growth factor binding protein 4
nitric oxide synthase interacting protein
basic helix-loop-helix domain containing, class B, 9
pre-mRNA processing factor 38A
PAK1 interacting protein 1
THUMP domain containing 3
doublecortin-like kinase 2
polo-like kinase 3
ELMO domain containing 3
septin 6
--
RNA polymerase I subunit C
very low density lipoprotein receptor
small integral membrane protein 8
influenza virus NS1A binding protein
PHD finger protein 14
BCL tumor suppressor 7B
3-phosphoinositide dependent protein kinase-1
solute carrier family 30 member 3
abl-interactor 2
leucine-rich repeat LGI family, member 3
BRF2, RNA polymerase III transcription initiation factor 50 subunit
solute carrier family 39, member 11
polypeptide N-acetylgalactosaminyltransferase 14
--
pumilio RNA-binding family member 2
coiled-coil domain containing 127
ferrochelatase
TOP1 binding arginine/serine rich protein
phosphatidylinositol glycan anchor biosynthesis, class U
F-box protein 34

RAP1B, member of RAS oncogene family
synaptotagmin 3
apoptosis enhancing nuclease
poly(rC) binding protein 2
BTB domain containing 10
exosome component 5
family with sequence similarity 163, member B
casein kinase 1, gamma 3
adenosylhomocysteinase
--
dehydrogenase/reductase 7
family with sequence similarity 168, member B
cell cycle progression 1
trafficking protein particle complex 12
deoxynucleotidyltransferase, terminal, interacting protein 1
--
ubiquitin protein ligase E3C
chibby family member 1, beta catenin antagonist
leucine rich repeat transmembrane neuronal 3
--
protein inhibitor of activated STAT, 2
URI1, prefoldin-like chaperone
RNA polymerase III subunit H
phosphoserine phosphatase
testin LIM domain protein
calsyntenin 2
--
ribonuclease P/MRP 25 subunit
plexin domain containing 2
POM121 transmembrane nucleoporin
parathyroid hormone-like hormone
Purkinje cell protein 4-like 1
rabphilin 3A
glutamate ionotropic receptor AMPA type subunit 1
phosphatidylinositol glycan anchor biosynthesis, class S
kinesin family member 2A
sodium voltage-gated channel beta subunit 1
paraneoplastic Ma antigen family-like 2
neural cell adhesion molecule 2
cold shock domain containing C2

List of the 192 Regulated Genes (Fold-change ≥ 1,

FAST DB STABLE ID	Gene Symbol	Regulation	Fold-Change
GSRG0000256	Tfpt	up	782.96
GSRG0021091	Nrsn2	up	776.48
GSRG0022737	Zc3hc1	up	284.58
GSRG0031980	Gnai2	up	260.06
GSRG0024597	Penk	up	237.43
GSRG0009861	RGD1566099	up	123.61
GSRG0015292	Sox2	up	84.59
GSRG0023366	Rbsn	up	75.16
GSRG0015759	Znhit6	up	51.74
GSRG0013452	Ankrd16	up	49.20
GSRG0002031	Stx5	up	48.74
GSRG0028880	Rad21	up	45.27
GSRG0027470	Med16	up	28.23
GSRG0029718	Nell2	up	21.86
GSRG0006308	Kcnip1	down	1791.25
GSRG0008871	--	down	1715.09
GSRG0000412	Atp5sl	down	1057.61
GSRG0026695	Stxbp6	down	1005.73
GSRG0013907	Tmed7	down	937.91
GSRG0019514	Syt13	down	823.69
GSRG0023056	Sfxn5	down	633.01
GSRG0013170	Gadd45g	down	555.62
GSRG0015282	Kcnmb2	down	550.92
GSRG0006333	Ublcp1	down	537.82
GSRG0026603	Kcnk3	down	488.98
GSRG0023378	Tmf1	down	481.94
GSRG0007094	Ifnar1	down	480.88
GSRG0009858	Nek7	down	475.02
GSRG0029606	Rangap1	down	468.15
GSRG0006834	Nt5c3b	down	461.79
GSRG0015089	Ankrd34b	down	428.12
GSRG0026020	Fancm	down	417.05
GSRG0013258	Iars	down	401.60
GSRG0002284	Fam160b1	down	394.67
GSRG0010351	Slbp	down	381.96
GSRG0020767	Slc30a4	down	380.31
GSRG0010144	Fam69a	down	379.33
GSRG0026692	Lrrn3	down	378.07
GSRG0001557	Pak1	down	368.09
GSRG0015833	Crhbp	down	361.58
GSRG0008817	Kdelr2	down	360.12

GSRG0022959	Mrpl19	down	332.49
GSRG0026756	Trim9	down	318.30
GSRG0013826	Syt4	down	315.98
GSRG0007941	Pdgfa	down	301.72
GSRG0008011	Sbds	down	297.43
GSRG0020657	Fjx1	down	289.60
GSRG0004927	Fam189a2	down	269.01
GSRG0006244	Slc9a3r2	down	254.74
GSRG0003390	Sult2b1	down	253.09
GSRG0003193	Mrps12	down	247.47
GSRG0029945	Pde4a	down	244.94
GSRG0013566	Apc	down	243.03
GSRG0001855	Ptpre	down	238.09
GSRG0007979	Prkrip1	down	221.80
GSRG0012479	Nop16	down	215.81
GSRG0029609	Phf5a	down	207.82
GSRG0006093	Sec14l1	down	206.08
GSRG0027609	Igf1	down	200.12
GSRG0013015	Prr7	down	200.04
GSRG0032466	Ackr3	down	193.94
GSRG0004212	Ap3s2	down	187.88
GSRG0010509	Gpat3	down	187.41
GSRG0024716	Pnrc1	down	182.26
GSRG0022714	Wasl	down	180.47
GSRG0014684	--	down	175.74
GSRG0007041	Myadml2	down	175.40
GSRG0015365	Trpc4	down	171.84
GSRG0024434	Eif4g3	down	169.02
GSRG0028697	Snrpf	down	168.93
GSRG0011159	Pcca	down	164.14
GSRG0020828	Pcna	down	163.81
GSRG0004821	Vegfb	down	162.67
GSRG0028103	Mfsd3	down	161.91
GSRG0019546	--	down	157.63
GSRG0028796	Lemd3	down	156.94
GSRG0025610	Sesn2	down	154.60
GSRG0031432	RGD1309779	down	154.45
GSRG0032308	Coq10b	down	149.67
GSRG0024196	Dhcr24	down	149.28
GSRG0017769	Rtn4ip1	down	147.39
GSRG0005814	Rara	down	147.20
GSRG0021260	Rgs19	down	142.93
GSRG0031845	Tex9	down	142.23
GSRG0012470	Lman2	down	141.93
GSRG0010061	Adss	down	140.33
GSRG0025995	Akap6	down	138.94

GSRG0009785	Insig2	down	134.66
GSRG0001551	Alg8	down	132.63
GSRG0030976	Rab39a	down	131.89
GSRG0014604	Dhodh	down	129.45
GSRG0011004	Fgf9	down	125.03
GSRG0023498	Kcna1	down	124.16
GSRG0009711	Cnih3	down	121.46
GSRG0020093	Ptpn1	down	120.18
GSRG0012489	--	down	116.61
GSRG0030402	Senp6	down	116.58
GSRG0005807	Casc3	down	108.06
GSRG0029295	Fam49b	down	106.79
GSRG0023977	Phf24	down	105.30
GSRG0032998	Tyw5	down	104.01
GSRG0009488	Ivns1abp	down	101.91
GSRG0021544	Mpp6	down	101.46
GSRG0034842	Sept6	down	100.51
GSRG0009754	Plxna2	down	98.57
GSRG0005239	Narfl	down	97.69
GSRG0010843	Chac2	down	93.76
GSRG0004850	Asrgl1	down	93.03
GSRG0020402	Scn1a	down	90.53
GSRG0026589	Snx17	down	88.81
GSRG0025396	Prpf38a	down	88.01
GSRG0005137	--	down	87.77
GSRG0027340	Akt1	down	84.54
GSRG0029711	Yaf2	down	83.17
GSRG0021769	Thumpd3	down	77.71
GSRG0036155	Gfm1	down	75.70
GSRG0005815	Igfbp4	down	74.81
GSRG0014547	Nol3	down	74.01
GSRG0025999	Srp54a	down	72.14
GSRG0001964	mrpl11	down	72.02
GSRG0006506	Rangrf	down	71.73
GSRG0032315	Spats2l	down	71.64
GSRG0005237	Gng13	down	71.49
GSRG0022586	Ccdc91	down	70.86
GSRG0015523	Them4	down	70.60
GSRG0021290	Actr3b	down	69.06
GSRG0020088	Ddx27	down	65.44
GSRG0026736	Mdga2	down	63.18
GSRG0025353	Caap1	down	62.82
GSRG0003253	Lsm14a	down	61.41
GSRG0026565	Clip4	down	60.83
GSRG0018780	Slc4a10	down	60.66
GSRG0025868	Slc30a3	down	60.55

GSRG0007885	Rnf6	down	59.48
GSRG0024306	Mycbp	down	58.18
GSRG0036839	Arhgap5	down	57.66
GSRG0028164	Sgsm3	down	57.56
GSRG0036647	Nosip	down	57.29
GSRG0013400	Mplkip	down	57.16
GSRG0023059	Egr4	down	57.06
GSRG0004287	Uvrag	down	55.94
GSRG0025430	Plk3	down	55.60
GSRG0002105	--	down	55.51
GSRG0025810	Morn2	down	55.44
GSRG0036313	--	down	55.25
GSRG0036814	Kcns3	down	55.18
GSRG0032238	Bend6	down	53.38
GSRG0000541	Syt3	down	53.25
GSRG0011737	Fam160b2	down	52.22
GSRG0024580	Rb1cc1	down	50.68
GSRG0007220	Umps	down	50.33
GSRG0006659	Wsb1	down	49.76
GSRG0000551	Akt1s1	down	48.78
GSRG0026076	Mthfd1	down	47.86
GSRG0006193	Naa60	down	47.55
GSRG0010956	Bcl2l2	down	47.25
GSRG0021593	Ppm1k	down	45.89
GSRG0029819	--	down	45.66
GSRG0013466	Phyh	down	44.86
GSRG0008398	N4bp2l2	down	44.75
GSRG0034565	Tspyl2	down	43.77
GSRG0024721	Smim8	down	43.50
GSRG0005692	Ptrh2	down	43.27
GSRG0027325	Cinp	down	42.88
GSRG0022729	Tnpo3	down	42.27
GSRG0008019	Psph	down	40.84
GSRG0030416	Mrap2	down	40.74
GSRG0031930	Mras	down	40.57
GSRG0007986	Tmem120a	down	39.83
GSRG0025945	Fam150b	down	38.86
GSRG0032822	--	down	38.22
GSRG0021184	Acot8	down	36.29
GSRG0014672	Spg7	down	36.24
GSRG0013662	Csnk1g3	down	35.37
GSRG0017921	Ppil1	down	35.22
GSRG0011525	Rpp14	down	34.00
GSRG0010557	Utp3	down	33.56
GSRG0029818	--	down	33.46
GSRG0023398	Crbn	down	31.92

GSRG0010246	Lnx1	down	31.12
GSRG0015013	--	down	30.36
GSRG0028271	Spats2	down	28.44
GSRG0011976	Tll1	down	27.80
GSRG0000492	U2af1l4	down	27.47
GSRG0004453	Btbd10	down	27.37
GSRG0005277	--	down	24.23
GSRG0024007	Nans	down	22.85
GSRG0021895	Mrpl51	down	19.43
GSRG0024183	Sgip1	down	19.31
GSRG0005636	Pigs	down	18.31
GSRG0015202	Golph3	down	15.35
GSRG0021248	Eef1a2	down	11.54

,5; P-Value ≤ 0,05) - G/

P-Value	Adjusted P-Value
1.67E-05	9.27E-03
1.86E-04	3.30E-02
8.06E-04	6.86E-02
3.02E-04	4.11E-02
1.46E-03	9.48E-02
3.84E-03	1.51E-01
1.71E-03	1.00E-01
1.20E-02	2.64E-01
2.29E-02	3.56E-01
2.50E-02	3.62E-01
2.42E-02	3.60E-01
6.55E-03	1.92E-01
3.04E-02	3.93E-01
2.98E-02	3.90E-01
1.10E-07	3.99E-04
2.31E-08	1.67E-04
4.04E-06	4.91E-03
4.24E-06	4.91E-03
2.55E-07	6.14E-04
1.87E-04	3.30E-02
1.61E-05	9.27E-03
5.44E-06	4.91E-03
6.79E-05	1.76E-02
5.35E-06	4.91E-03
1.48E-04	2.97E-02
1.40E-05	9.27E-03
1.64E-04	3.21E-02
4.93E-05	1.60E-02
1.00E-06	1.81E-03
9.01E-05	2.10E-02
3.36E-05	1.60E-02
7.94E-04	6.83E-02
1.37E-04	2.90E-02
2.57E-04	3.95E-02
4.38E-05	1.60E-02
1.01E-04	2.28E-02
4.46E-05	1.60E-02
5.07E-05	1.60E-02
4.58E-05	1.60E-02
5.75E-04	6.02E-02
5.86E-05	1.69E-02

3.90E-04	4.77E-02
4.67E-05	1.60E-02
1.89E-05	9.75E-03
6.80E-05	1.76E-02
1.69E-04	3.21E-02
5.09E-04	5.59E-02
6.29E-04	6.23E-02
7.12E-04	6.76E-02
8.40E-04	6.90E-02
1.47E-04	2.97E-02
5.38E-04	5.71E-02
6.21E-04	6.23E-02
1.78E-04	3.30E-02
4.28E-04	4.99E-02
6.29E-05	1.75E-02
1.12E-03	7.88E-02
2.81E-04	4.11E-02
2.56E-03	1.19E-01
2.98E-04	4.11E-02
2.31E-03	1.14E-01
7.63E-04	6.76E-02
2.12E-03	1.11E-01
2.93E-04	4.11E-02
3.63E-04	4.68E-02
3.83E-03	1.51E-01
2.41E-03	1.17E-01
3.28E-03	1.38E-01
3.15E-04	4.22E-02
4.05E-04	4.79E-02
1.10E-03	7.88E-02
3.69E-04	4.68E-02
2.44E-04	3.84E-02
1.59E-03	9.71E-02
1.05E-03	7.74E-02
2.82E-03	1.25E-01
2.59E-03	1.19E-01
2.23E-03	1.12E-01
3.46E-03	1.42E-01
3.48E-03	1.42E-01
3.31E-03	1.39E-01
8.30E-04	6.90E-02
2.25E-03	1.12E-01
4.47E-03	1.60E-01
2.56E-03	1.19E-01
1.12E-03	7.88E-02
2.22E-03	1.12E-01

1.53E-03	9.65E-02
5.56E-03	1.78E-01
4.27E-03	1.59E-01
5.66E-03	1.78E-01
2.14E-03	1.11E-01
2.10E-03	1.11E-01
5.05E-03	1.65E-01
1.93E-03	1.10E-01
7.47E-04	6.76E-02
2.60E-03	1.19E-01
2.49E-03	1.19E-01
1.98E-03	1.11E-01
4.50E-03	1.60E-01
8.35E-03	2.14E-01
3.36E-03	1.39E-01
1.79E-03	1.04E-01
3.32E-03	1.39E-01
7.63E-03	2.04E-01
7.31E-03	2.02E-01
1.15E-02	2.57E-01
3.65E-03	1.47E-01
1.69E-03	9.99E-02
4.50E-03	1.60E-01
5.89E-03	1.79E-01
4.96E-03	1.65E-01
3.90E-03	1.51E-01
4.83E-03	1.65E-01
4.59E-03	1.61E-01
1.05E-02	2.44E-01
2.59E-03	1.19E-01
8.54E-03	2.17E-01
1.57E-02	2.97E-01
6.63E-03	1.92E-01
1.51E-02	2.91E-01
7.12E-03	1.98E-01
6.40E-03	1.90E-01
9.90E-03	2.38E-01
9.96E-03	2.38E-01
6.63E-03	1.92E-01
1.23E-02	2.67E-01
1.37E-02	2.82E-01
2.16E-02	3.45E-01
2.12E-02	3.41E-01
1.42E-02	2.87E-01
6.77E-03	1.95E-01
5.97E-03	1.81E-01

1.11E-03	7.88E-02
1.22E-02	2.66E-01
1.13E-02	2.54E-01
8.48E-03	2.16E-01
1.11E-02	2.52E-01
2.40E-02	3.58E-01
1.04E-02	2.44E-01
2.36E-02	3.57E-01
1.00E-02	2.38E-01
1.55E-02	2.96E-01
2.18E-02	3.45E-01
1.40E-02	2.84E-01
2.42E-02	3.60E-01
6.90E-03	1.97E-01
1.54E-02	2.96E-01
1.98E-02	3.32E-01
2.12E-02	3.41E-01
2.38E-02	3.57E-01
1.92E-02	3.26E-01
1.86E-02	3.23E-01
2.87E-02	3.82E-01
1.76E-02	3.14E-01
2.34E-02	3.57E-01
3.11E-02	3.96E-01
2.40E-02	3.58E-01
3.15E-02	3.96E-01
2.01E-02	3.34E-01
1.20E-02	2.65E-01
1.88E-02	3.25E-01
2.87E-02	3.82E-01
2.68E-02	3.76E-01
2.32E-02	3.56E-01
2.85E-02	3.82E-01
3.05E-02	3.93E-01
2.81E-02	3.80E-01
3.88E-02	4.41E-01
3.82E-02	4.39E-01
4.38E-02	4.60E-01
3.10E-02	3.96E-01
3.49E-02	4.19E-01
2.01E-02	3.34E-01
3.49E-02	4.19E-01
3.04E-02	3.93E-01
5.00E-02	4.93E-01
3.84E-02	--
2.26E-02	3.53E-01

4.43E-02	4.64E-01
2.67E-02	3.76E-01
2.68E-02	3.76E-01
4.88E-02	4.89E-01
2.87E-02	3.82E-01
4.56E-02	4.71E-01
3.56E-02	--
4.02E-02	4.44E-01
3.95E-02	4.42E-01
4.06E-02	4.45E-01
4.61E-02	4.75E-01
3.09E-02	3.96E-01
3.53E-02	4.21E-01

ABA PUR vs GABA OCM

Gene Name
TCF3 (E2A) fusion partner
neurensin 2
zinc finger, C3HC-type containing 1
G protein subunit alpha i2
proenkephalin
similar to novel protein
SRY box 2
rabenosyn, RAB effector
zinc finger, HIT-type containing 6
ankyrin repeat domain 16
syntaxin 5
RAD21 cohesin complex component
mediator complex subunit 16
neural EGFL like 2
potassium voltage-gated channel interacting protein 1
--
ATP5S-like
syntaxin binding protein 6
transmembrane p24 trafficking protein 7
synaptotagmin 13
sideroflexin 5
growth arrest and DNA-damage-inducible, gamma
potassium calcium-activated channel subfamily M regulatory beta subunit 2
ubiquitin-like domain containing CTD phosphatase 1
potassium two pore domain channel subfamily K member 3
TATA element modulatory factor 1
interferon alpha and beta receptor subunit 1
NIMA-related kinase 7
RAN GTPase activating protein 1
5'-nucleotidase, cytosolic IIIB
ankyrin repeat domain 34B
Fanconi anemia, complementation group M
isoleucyl-tRNA synthetase
family with sequence similarity 160, member B1
stem-loop binding protein
solute carrier family 30 member 4
family with sequence similarity 69, member A
leucine rich repeat neuronal 3
p21 (RAC1) activated kinase 1
corticotropin releasing hormone binding protein
KDEL endoplasmic reticulum protein retention receptor 2

mitochondrial ribosomal protein L19
tripartite motif-containing 9
synaptotagmin 4
platelet derived growth factor subunit A
SBDS ribosome assembly guanine nucleotide exchange factor
four jointed box 1
family with sequence similarity 189, member A2
SLC9A3 regulator 2
sulfotransferase family 2B member 1
mitochondrial ribosomal protein S12
phosphodiesterase 4A
APC, WNT signaling pathway regulator
protein tyrosine phosphatase, receptor type, E
Prkr interacting protein 1 (IL11 inducible)
NOP16 nucleolar protein
PHD finger protein 5A
SEC14-like lipid binding 1
insulin-like growth factor 1
proline rich 7 (synaptic)
atypical chemokine receptor 3
adaptor-related protein complex 3, sigma 2 subunit
glycerol-3-phosphate acyltransferase 3
proline-rich nuclear receptor coactivator 1
Wiskott-Aldrich syndrome-like
--
myeloid-associated differentiation marker-like 2
transient receptor potential cation channel, subfamily C, member 4
eukaryotic translation initiation factor 4 gamma, 3
small nuclear ribonucleoprotein polypeptide F
propionyl-CoA carboxylase alpha subunit
proliferating cell nuclear antigen
vascular endothelial growth factor B
major facilitator superfamily domain containing 3
--
LEM domain containing 3
sestrin 2
similar to ENSANGP00000021391
coenzyme Q10B
24-dehydrocholesterol reductase
reticulon 4 interacting protein 1
retinoic acid receptor, alpha
regulator of G-protein signaling 19
testis expressed 9
lectin, mannose-binding 2
adenylosuccinate synthase
A-kinase anchoring protein 6

insulin induced gene 2
ALG8, alpha-1, 3-glucosyltransferase
RAB39A, member RAS oncogene family
dihydroorotate dehydrogenase (quinone)
fibroblast growth factor 9
potassium voltage-gated channel subfamily A member 1
cornichon family AMPA receptor auxiliary protein 3
protein tyrosine phosphatase, non-receptor type 1
--
SUMO1/sentrin specific peptidase 6
cancer susceptibility candidate 3
family with sequence similarity 49, member B
PHD finger protein 24
tRNA-yW synthesizing protein 5
influenza virus NS1A binding protein
membrane palmitoylated protein 6
septin 6
plexin A2
nuclear prelamin A recognition factor-like
ChaC cation transport regulator 2
asparaginase like 1
sodium voltage-gated channel alpha subunit 1
sorting nexin 17
pre-mRNA processing factor 38A
--
AKT serine/threonine kinase 1
YY1 associated factor 2
THUMP domain containing 3
G elongation factor, mitochondrial 1
insulin-like growth factor binding protein 4
nucleolar protein 3
signal recognition particle 54A
mitochondrial ribosomal protein L11
RAN guanine nucleotide release factor
spermatogenesis associated, serine-rich 2-like
G protein subunit gamma 13
coiled-coil domain containing 91
thioesterase superfamily member 4
ARP3 actin related protein 3 homolog B
DEAD-box helicase 27
MAM domain containing glycosylphosphatidylinositol anchor 2
caspase activity and apoptosis inhibitor 1
LSM14A mRNA processing body assembly factor
CAP-GLY domain containing linker protein family, member 4
solute carrier family 4 member 10
solute carrier family 30 member 3

ring finger protein 6
Myc binding protein
Rho GTPase activating protein 5
small G protein signaling modulator 3
nitric oxide synthase interacting protein
M-phase specific PLK1 interacting protein
early growth response 4
UV radiation resistance associated
polo-like kinase 3
--
MORN repeat containing 2
--
potassium voltage-gated channel, modifier subfamily S, member 3
BEN domain containing 6
synaptotagmin 3
family with sequence similarity 160, member B2
RB1-inducible coiled-coil 1
uridine monophosphate synthetase
WD repeat and SOCS box-containing 1
AKT1 substrate 1
methylenetetrahydrofolate dehydrogenase, cyclohydrolase and formyltetrahydrofolate synthetase 1
N(alpha)-acetyltransferase 60, NatF catalytic subunit
Bcl2-like 2
protein phosphatase, Mg2+/Mn2+ dependent, 1K
--
phytanoyl-CoA 2-hydroxylase
NEDD4 binding protein 2-like 2
TSPY-like 2
small integral membrane protein 8
peptidyl-tRNA hydrolase 2
cyclin-dependent kinase 2-interacting protein
transportin 3
phosphoserine phosphatase
melanocortin 2 receptor accessory protein 2
muscle RAS oncogene homolog
transmembrane protein 120A
family with sequence similarity 150, member B
--
acyl-CoA thioesterase 8
SPG7, paraplegin matrix AAA peptidase subunit
casein kinase 1, gamma 3
peptidylprolyl isomerase like 1
ribonuclease P/MRP 14 subunit
UTP3, small subunit processome component homolog (S. cerevisiae)
--
cereblon

ligand of numb-protein X 1
--
spermatogenesis associated, serine-rich 2
tolloid-like 1
U2 small nuclear RNA auxiliary factor 1-like 4
BTB domain containing 10
--
N-acetylneuraminate synthase
mitochondrial ribosomal protein L51
SH3-domain GRB2-like (endophilin) interacting protein 1
phosphatidylinositol glycan anchor biosynthesis, class S
golgi phosphoprotein 3
eukaryotic translation elongation factor 1 alpha 2

List of the 68 Regulated Genes (Fold-change ≥ 1,5

FAST DB STABLE ID	Gene Symbol	Regulation	Fold-Change
GSRG0019514	Syt13	up	1354.01
GSRG0026020	Fancm	up	697.69
GSRG0014684	--	up	269.65
GSRG0032466	Ackr3	up	260.39
GSRG0018539	Rpf2	up	246.51
GSRG0008967	Sumf2	up	171.63
GSRG0006423	Zfp672	up	140.68
GSRG0013466	Phyh	up	123.50
GSRG0032824	--	up	101.57
GSRG0025810	Morn2	up	86.95
GSRG0013400	Mplkip	up	85.10
GSRG0005486	Ctc1	up	80.08
GSRG0020417	Dlx2	up	67.45
GSRG0005145	Zc3h7a	up	65.77
GSRG0027614	Igf1	up	50.77
GSRG0016423	Rrnad1	up	24.49
GSRG0036252	Brix1	down	2378.19
GSRG0032304	Nabp1	down	2147.97
GSRG0031867	Slc17a5	down	1200.98
GSRG0002264	Smc3	down	1177.14
GSRG0006796	Ormdl3	down	1045.74
GSRG0024467	Casp9	down	941.28
GSRG0014272	Fam210a	down	872.64
GSRG0000256	Tfpt	down	447.27
GSRG0021713	Tpra1	down	420.12
GSRG0032453	Neu2	down	405.72
GSRG0005434	Gid4	down	319.67
GSRG0028324	Pde1b	down	310.69
GSRG0023969	Nfx1	down	278.21
GSRG0026146	Eif2b2	down	226.38
GSRG0005298	Pwwp2a	down	212.66
GSRG0015283	Pik3ca	down	157.31
GSRG0018533	Fam229b	down	141.26
GSRG0011756	Gtf2f2	down	140.97
GSRG0007154	Cmss1	down	123.22
GSRG0015248	Pex2	down	117.17
GSRG0019759	Cds2	down	102.19
GSRG0036688	Ift52	down	92.76
GSRG0012481	Thoc3	down	89.71
GSRG0013699	St8sia3	down	88.57
GSRG0015952	Pelo	down	87.03

GSRG0012237	Mfap3l	down	86.89
GSRG0024281	Foxj3	down	82.16
GSRG0002210	Cnnm1	down	78.40
GSRG0034928	Slitrk4	down	74.64
GSRG0006754	Pdk2	down	74.57
GSRG0013285	Pak1ip1	down	74.42
GSRG0007430	Gart	down	66.47
GSRG0023361	Xpc	down	65.78
GSRG0032175	Polr1c	down	65.14
GSRG0001503	Hddc3	down	64.52
GSRG0020830	Gpcpd1	down	61.82
GSRG0029946	--	down	56.27
GSRG0012042	Brf2	down	55.74
GSRG0028761	Ppp1r12a	down	48.75
GSRG0024746	Ubap2	down	47.89
GSRG0011023	Stmn4	down	42.19
GSRG0020147	Zgpat	down	35.00
GSRG0010043	Cadm3	down	31.66
GSRG0005300	Rnf145	down	31.08
GSRG0002156	Pten	down	30.19
GSRG0021308	Tmub1	down	30.09
GSRG0014335	Csnk2a2	down	23.80
GSRG0020611	Madd	down	21.49
GSRG0027470	Med16	down	20.20
GSRG0008075	Rph3a	down	12.96
GSRG0032016	Arpp19	down	11.17
GSRG0006987	Wbp2	down	9.65

; P-Value ≤ 0,05) - GA

P-Value	Adjusted P-Value
4.13E-05	2.98E-02
1.96E-04	6.12E-02
1.44E-03	9.70E-02
1.03E-03	8.90E-02
7.86E-04	8.36E-02
2.81E-03	1.27E-01
4.98E-03	1.61E-01
5.65E-03	1.70E-01
8.61E-03	2.12E-01
9.36E-03	2.23E-01
1.18E-02	2.57E-01
1.23E-02	2.64E-01
1.67E-02	3.24E-01
1.73E-02	3.32E-01
2.66E-02	4.33E-01
3.50E-02	5.09E-01
2.63E-06	1.15E-02
2.88E-06	1.15E-02
3.34E-05	2.98E-02
3.65E-05	2.98E-02
2.78E-05	2.98E-02
6.22E-05	2.98E-02
7.84E-05	3.29E-02
5.34E-05	2.98E-02
3.66E-04	6.69E-02
1.22E-04	4.47E-02
3.00E-04	6.12E-02
5.05E-04	7.45E-02
1.23E-04	4.47E-02
5.21E-04	7.45E-02
9.31E-04	8.63E-02
2.16E-03	1.16E-01
2.81E-03	1.27E-01
3.63E-03	1.41E-01
3.99E-03	1.47E-01
5.46E-03	1.67E-01
7.01E-03	1.92E-01
5.56E-03	1.69E-01
8.86E-03	2.16E-01
9.35E-03	2.23E-01
4.55E-03	1.54E-01

9.54E-03	2.26E-01
8.52E-03	2.12E-01
3.27E-03	1.34E-01
7.49E-03	1.99E-01
8.89E-03	2.16E-01
1.26E-02	2.67E-01
1.50E-02	3.04E-01
1.58E-02	3.13E-01
1.57E-02	3.13E-01
1.18E-02	2.57E-01
1.15E-02	2.55E-01
1.15E-02	2.55E-01
2.09E-02	3.79E-01
1.42E-02	2.92E-01
1.62E-02	3.19E-01
2.48E-02	4.20E-01
3.22E-02	4.87E-01
2.05E-02	3.75E-01
1.72E-02	3.31E-01
1.60E-02	3.16E-01
2.48E-02	4.20E-01
4.31E-02	5.75E-01
3.51E-02	5.09E-01
4.55E-02	5.99E-01
4.54E-02	5.98E-01
2.20E-02	3.89E-01
2.97E-03	1.29E-01

BA OCM vs GABA CTRL

Gene Name
synaptotagmin 13
Fanconi anemia, complementation group M
--
atypical chemokine receptor 3
ribosome production factor 2 homolog
sulfatase modifying factor 2
zinc finger protein 672
phytanoyl-CoA 2-hydroxylase
--
MORN repeat containing 2
M-phase specific PLK1 interacting protein
CST telomere replication complex component 1
distal-less homeobox 2
zinc finger CCCH type containing 7 A
insulin-like growth factor 1
ribosomal RNA adenine dimethylase domain containing 1
BRX1, biogenesis of ribosomes
nucleic acid binding protein 1
solute carrier family 17 member 5
structural maintenance of chromosomes 3
ORMDL sphingolipid biosynthesis regulator 3
caspase 9
family with sequence similarity 210, member A
TCF3 (E2A) fusion partner
transmembrane protein adipocyte associated 1
neuraminidase 2
GID complex subunit 4
phosphodiesterase 1B
nuclear transcription factor, X-box binding 1
eukaryotic translation initiation factor 2B subunit beta
PWWP domain containing 2A
phosphatidylinositol-4, 5-bisphosphate 3-kinase, catalytic subunit alpha
family with sequence similarity 229, member B
general transcription factor IIF subunit 2
cms1 ribosomal small subunit homolog (yeast)
peroxisomal biogenesis factor 2
CDP-diacylglycerol synthase 2
intraflagellar transport 52
THO complex 3
ST8 alpha-N-acetyl-neuraminide alpha-2, 8-sialyltransferase 3
pelota homolog (Drosophila)

microfibrillar-associated protein 3-like
forkhead box J3
cyclin and CBS domain divalent metal cation transport mediator 1
SLIT and NTRK-like family, member 4
pyruvate dehydrogenase kinase 2
PAK1 interacting protein 1
phosphoribosylglycinamide formyltransferase
XPC complex subunit, DNA damage recognition and repair factor
RNA polymerase I subunit C
HD domain containing 3
glycerophosphocholine phosphodiesterase 1
--
BRF2, RNA polymerase III transcription initiation factor 50 subunit
protein phosphatase 1, regulatory subunit 12A
ubiquitin-associated protein 2
stathmin 4
zinc finger CCCH-type and G-patch domain containing
cell adhesion molecule 3
ring finger protein 145
phosphatase and tensin homolog
transmembrane and ubiquitin-like domain containing 1
casein kinase 2 alpha 2
MAP-kinase activating death domain
mediator complex subunit 16
rabphilin 3A
cAMP-regulated phosphoprotein 19
WW domain binding protein 2

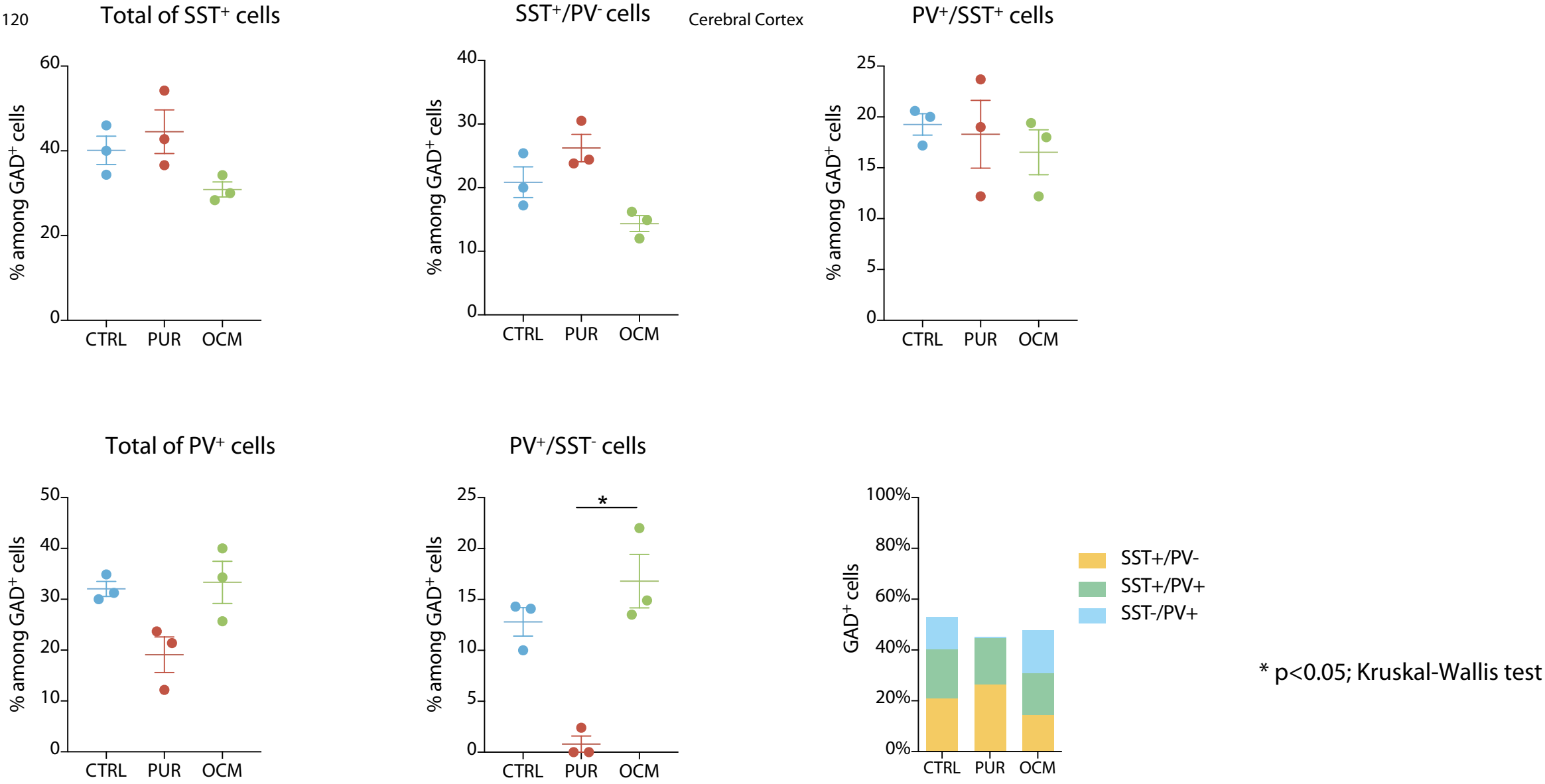

* p<0.05; Kruskal-Wallis test

Quantification of GABAergic neurons (GAD+) expressing PV, SST or both in CTRL, PUR and OCM hippocampal cultures. n=3 different cultures; mean ±SEM; about 70 to 100 GAD+ neurons were counted on acquired images in each experiment.

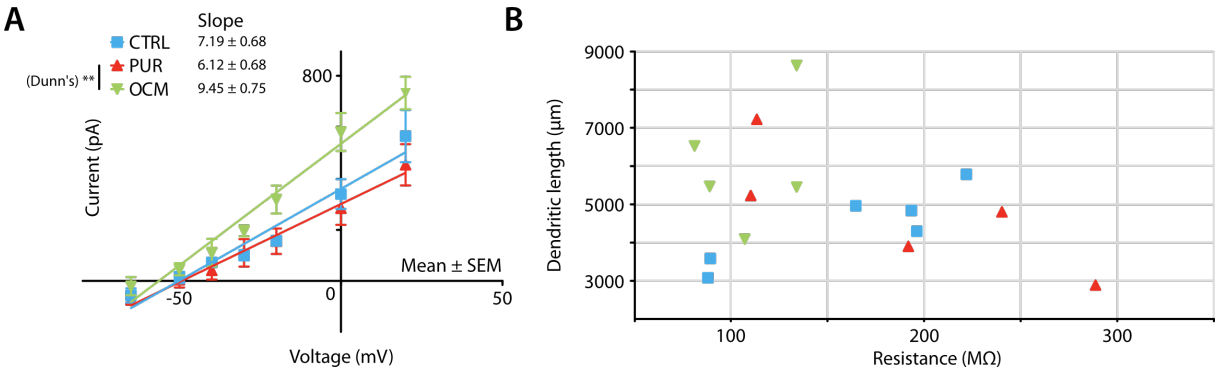

Figure for Reviewer 3. Correlating dendritic length and resistance. (A) I-V curves of GABAergic neurons for the three culture conditions: CTRL n = 5, PUR n = 6, OCM n = 5. I-V curves were obtained for a set of reconstructed neurons (from Figure 3) recorded with Cesium-based internal solution. Cs-based solution was composed of (in mM): CsGluc 125, QX-314 Cl 5, HEPES 10, MgCl2 2, EGTA 0.2, MgATP 2H2O 4, Na3-GFTP 2H2O, Na2-phosphocreatine 10. Biocytin was added to the solution as in the Materials and Methods. Cells were recorded in voltage clamp at holding potentials ranging from -65mV to +20mV. For each potential, an average on 5s of the corresponding steady-state current was measured. The graph gives the mean ± SEM of currents for each condition. The slopes of these curves were obtained from linear fits. PUR and OCM were significantly different ($p < 0.01$, Dunn's multiple comparison test) indicating that GABAergic cells from OCM cultures had lower resistance than GABAergic cells from PUR ones. **(B)** Dendritic length as a function of resistance plotted for each cell. GABAergic cells from OCM cultures tended to have lower resistance and greater dendritic length.

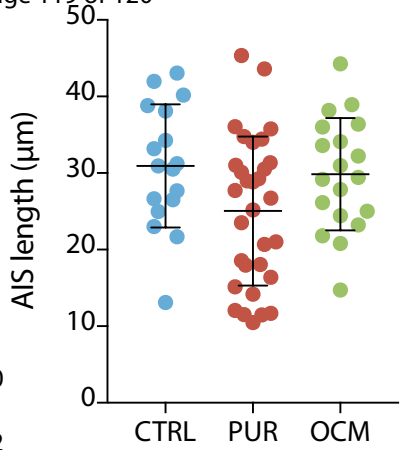

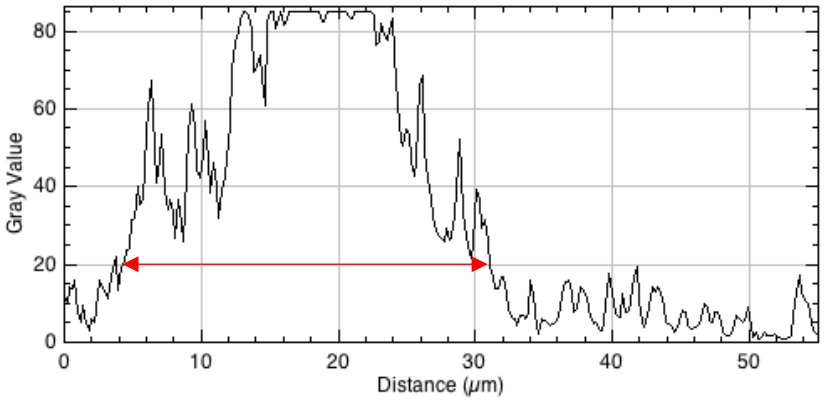

Measure of AIS lengths on plot profile of Na_v intensity from acquired images after Na_v and GAD immunostainings of mixed hippocampal neurons (CTRL) and purified neurons in the absence (PUR) or presence of OCM (OCM), at 17 DIV. Data represent mean ± SD.